WATER AND SOLIDS MOBILITY IN FOODS

SHELLY J. SCHMIDT

Department of Food Science and Human Nutrition
University of Illinois at Urbana-Champaign
Urbana, Illinois 61801

I. INTRODUCTION

"*Water—blood of the earth*"
From *Life's Matrix*, by Philip Ball (2001)

Water is the most abundant, unique, and necessary substance on the face of the earth. It is one of the earth's most precious resources and, along with oxygen, is more important for sustaining life, in the short term, than even the consumption of food.

ADVANCES IN FOOD AND NUTRITION RESEARCH VOL 48
ISSN: 1043-4526

Because of its vast and vital importance to life, water has been the focus of at least two and a half millennia of philosophical and scientific inquiry. However, there still remains much about water that we do not yet know and/or understand (Angell, 2001; Ball, 2001). The quest to identify the chemical and physical nature of water dates back at least as far as Thales, who lived from seventh to sixth century B.C. Thales, a citizen of the Greek colony of Miletus in Ionia, proposed that all of reality originated from a single material substance and that substance was water (O'Grady, 2001). The Greek philosopher Empedocles of Acragas in fifth century B.C. is credited with popularizing the classic four-element natural philosophy of Greece. Water was then considered one of four primary elements or "roots" of the universe, along with fire, air, and earth (O'Grady, 2001). Despite continuous investigation, it was not until several centuries later that the true elemental composition and proportions of water were uncovered. In 1781, the British chemist Henry Cavendish, extending the studies of others, demonstrated that the igniting of hydrogen and oxygen produces water. Two years later, the French chemist Antoine Lavoisier proved that water was not an element, but rather a compound composed of oxygen and hydrogen. In 1805,[1] the French chemist Joseph Gay-Lussac, collaborating with the German naturalist Alexander von Humboldt, determined that water consists of two volumes of hydrogen to one volume of oxygen (Green and Peterson, 1992). A few years later, Avogadro (1811) stated "...since we know that the ratio of the volumes of hydrogen and oxygen in the formation of water is 2 to 1, it follows that water results from the union of each molecule of oxygen with two molecules of hydrogen." In 1814 Berzelius proposed that compounds be described by chemical signs (which evolved into the modern-day chemical formula) based on their elemental substance—the sign for water being $2H + O$ (Berzelius, 1814), thereby approaching the modern-day chemical composition and formula for water—H_2O.

In addition to its philosophical and scientific importance, water has also been the subject of multitudinous authors, artists, and musicians. Many are familiar with the saying "Water, water everywhere and not a drop to drink"[2]

[1]Some sources give the date as 1804. Gay-Lussac read these now famous results before the Philomathic Society in 1808, which were published in 1809, in Gay Lussac, J.L., Memoir on the Combination of Gaseous Substances with Each Other. Mémoires de la Société d'Arcueil 2, 207–34. An English translation of this document, published by Henry A. Boorse and Lloyd Motz, eds., The World of the Atom, Vol. 1. New York: Basic Books, 1966 (translation: Alembic Club Reprint No. 4), can be found at http://webserver.lemoyne.edu/faculty/giunta/gaylussac.html.

[2]The exact quote from The Rime of the Ancient Mariner by Coleridge (1798) is: "Water, water, everywhere, And all the boards did shrink; Water, water, everywhere, Nor any drop to drink."

(Coleridge, 1798), the 1906 *Water Lilies*[3] painting by Claude Monet, and the 1717 work *Water Music*[4] by George Frideric Handel. Water has also served as a bridge connecting science and art, as expressed by the research and photos of Nagel studying "the cascade of structure in a drop of water falling from a faucet[5]" (Shi *et al*., 1994) and the photographs of Wick (1997) in his book entitled "*A Drop of Water*." Finally, water in substance and symbol has been profoundly woven into the theology of the world's religions. For the interested reader, a comprehensive biography of water has been published by Ball (2001), exploring the central secret of water's nature as the matrix of life. In addition, a multidisciplinary examination of the significance and role of water in the life and culture of planet earth is currently under construction on the World Wide Web by Witcombe and Hwang (2004).

The importance of water in foods begins with the hydrological cycle and concludes with the consumption of safe, wholesome, and plentiful foods. In between, water is a vital component in the various stages of food production and preservation. Water in the final food product, whether fresh or processed, profoundly influences the chemistry, microbiological safety, nutritional value, texture, appearance, and taste of the food. Because of this intimate relationship between water and food quality and safety, a more complete understanding of water and its properties, behavior, and influence, alone and in foods, is of prime importance.

The objectives of this review are to discuss the fundamental and more recently discovered properties of water alone and to critically examine the system properties and measurement methods used to measure the mobility of water and solids in foods—specifically water activity, nuclear magnetic resonance (NMR), and the glass transition.

II. WATER

A. WATER MOLECULE STRUCTURE

As traced historically in the introduction, water has the molecular formula H_2O. However, it is important to mention that the hydrogen atoms are not

[3]More about Claude Monet and his *Water Lilies* painting can be found at Pioch, N. WebMuseum, Paris. http://www.ibiblio.org/wm/paint/auth/monet 19 September 2002 (Accessed 12 January 2004).

[4]More about George Frideric Handel and his *Water Music* can be found at Boynick, M. *Classical Music Pages*. http://w3.rz-berlin.mpg.de/cmp/handel.html 10 October (Accessed 12 January 2004).

[5]For the interested reader, the image and movie of the Cascade of Structure in a Drop Falling from a Faucet, by Nagel and co-workers, can be viewed at http://mrsec.uchicago.edu/Nuggets/NagelDrop/index.html 8 July 1995 (Accessed 12 January 2004).

permanently attached to each oxygen; rather, the hydrogen atoms are constantly exchanging due to protonation–deprotonation processes (also called proton exchange) (Chaplin, 2004). This exchange process is catalyzed by both acids and bases (i.e., the exchange rate is slowest near neutral pH and faster under acidic or basic pH conditions). The influence of proton exchange on oxygen-17 (^{17}O) NMR relaxation in water and other systems has been investigated by several researchers (Glasel, 1972; Richardson, 1989). The average residence time for a hydrogen atom at pH 7 is about a millisecond (Chaplin, 2004). Despite the dynamic effects of the proton exchange process on the structure of water, water is usually regarded as having a permanent structure.

The electronic structure of an isolated water molecule is often described as being composed of four sp^3-hybridized electron pairs—two associated with the hydrogen atoms and two as lone-pair orbitals of the oxygen atom—with an overall nearly tetrahedral geometry (Figure 1). The common "two lone-pair orbitals on the oxygen atom" description of water (referred to as "rabbit ears") is actually controversial (Chaplin, 2004; Finney, 2001). Based on ultraviolet absorption or photoelectron spectra or ionization energy of water, only one lone-pair orbital is invoked, the other orbital being at a much lower energy (Laing, 1987). Nevertheless, based on the localized molecular orbital procedure, it is appropriate and useful to describe water as having two equivalent lone-pair orbitals on the oxygen atoms; however, Martin (1988) suggested that they may be better described as "squirrel ears."

Regardless of which orbital description is selected, the four localized regions of excess charge appearing in a tetrahedral arrangement around

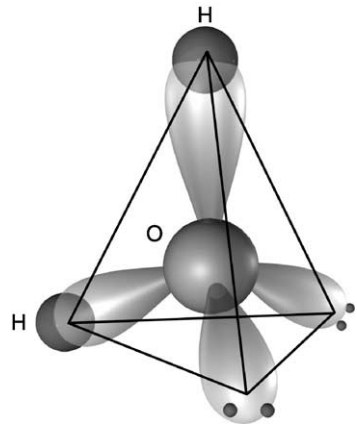

FIG. 1 Schematic orbital model of a water molecule.

the central oxygen atom provide a useful qualitative description of the electron distribution in the water molecule. Overall, the water molecule is electrically neutral, but the positive and negative charges are distributed unsymmetrically. The oxygen atom has a higher electron density than the two hydrogen atoms. This is represented as a partial negative charge on the oxygen atom and a partial positive charge on each hydrogen atom (Figure 2). The hydrogen atom is bonded covalently to the oxygen atom (called a polar covalent bond because of the unequal sharing of the electrons), with an energy of 492 $kJmol^{-1}$ (Ruscic, 2002). For an isolated water molecule (Figure 2), the calculated O–H bond length is 0.9584 Å and the H–O–H angle is 104.45° (Kern and Karplus, 1972). The experimental values vary somewhat, depending on the phase of water being investigated and the measurement method employed (Chaplin, 2004; Wallqvist and Mountain, 1999). The average van der Waals diameter for the water molecule has been reported as 2.82 Å by Franks (2000) and 3.3 Å by Fennema (1996). Molecular model values and intermediate peak radial distribution data indicate that the value is around 3.2 Å (Chaplin, 2004). Evidence discussed by Finney (2001) suggests that the van der Waals radius around a water molecule oxygen atom exhibits a small (about ±5%) but significant degree of nonsphericity, ranging between 1.6 and 1.8 Å, depending on which axis is selected (Savage, 1986).

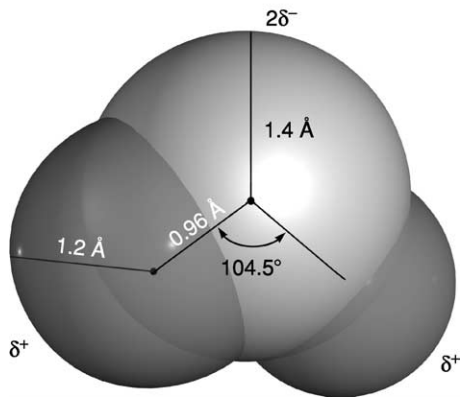

FIG. 2 Space-filling model of an isolated water molecule, in the vapor state, with associated van der Waals radii and rounded values for the O–H bond length and the H–O–H angle. Each hydrogen atom has a slight positive charge (δ^+), and each lone-pair oxygen orbital has a slight negative charge (for a total of $2\delta^-$).

B. HYDROGEN-BONDING ASSOCIATIONS

In addition to its two O–H polar covalent bonds, water molecules participate in hydrogen bonding—an intermolecular attraction between the hydrogen atom of one water molecule and an oxygen lone pair of another water molecule. The hydrogen bond is thought to be approximately 90% electrostatic and 10% covalent in nature (Chaplin, 2004). Hydrogen bonding is a dominant interaction between water molecules and pervasively affects the structure and behavior of water. The most basic hydrogen-bonding situation occurs in the water dimer (Figure 3), where one hydrogen bond exists between two water molecules in the vapor phase. The measured hydrogen-bond length [R(O···O)] in the vapor phase water dimer is about 2.98 Å, which is significantly longer than the lengths in both liquid water (2.85 Å) and regular ice (2.74 Å) (Ludwig, 2001). The shortening of the R(O···O) distance in liquid water and regular ice (i.e., stronger hydrogen bonding networks) is due to the cooperative nature of hydrogen bonding discussed later. Details of hydrogen-bond geometry in liquid water have been investigated by Modig *et al.* (2003) from 0 to 80 °C by combining measurements of the proton magnetic shielding tensor with *ab initio* density functional calculations. Their results suggest a substantial hydrogen-bond distortion, which increases in nonlinearity and distance with increasing temperature.

The hydrogen-bonded water pentamer is illustrated in Figure 4. Using natural bond orbital (NBO) terminology, the two hydrogen–oxygen-bonding orbitals of the central water molecule can act as charge acceptors, and the two oxygen lone-pair orbitals of the central water molecule can act as charge donors (Ludwig, 2001). Another terminology convention present in the

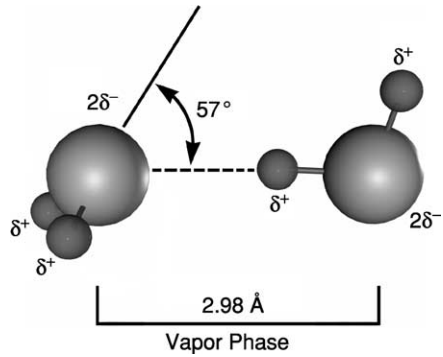

FIG. 3 The vapor phase water dimer structure. Polar covalent bonds are shown as solid lines and the hydrogen bond as a dashed line (adapted from Ludwig, 2001).

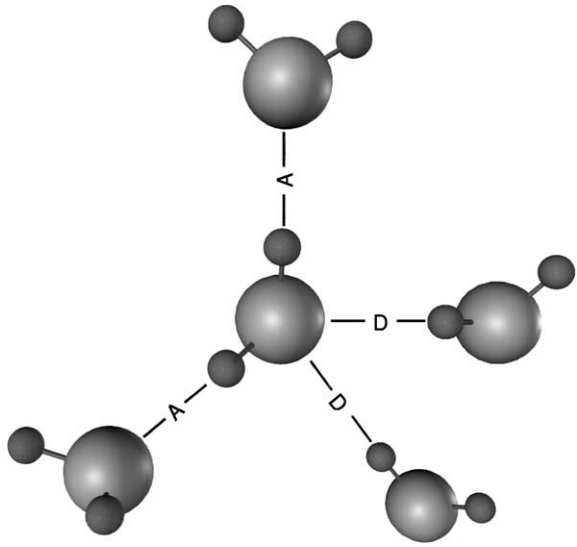

FIG. 4 The hydrogen-bonded water pentamer, using natural bond orbital (NBO) terminology, the two hydrogen-oxygen bonding orbitals of the central water molecule can act as charge acceptors (A), and the two oxygen lone-pair orbitals of the central water molecule can act as charge donors (D).

literature (e.g., Fennema, 1996; Franks, 2000) refers to the two hydrogen–oxygen-bonding orbitals as proton (or hydrogen-bond) donors and the two oxygen lone-pair orbitals as proton (or hydrogen-bond) acceptors. The difference in the two approaches is what is being accepted and donated—the charge or the proton. Regardless of the terminology used, each water molecule has the potential of forming up to four hydrogen bonds with four other water molecules, resulting in a three-dimensional hydrogen-bonding structure. The actual number, strength, and duration of the hydrogen bonds that form depend on the phase of water being investigated. In ice, each water molecule is involved in four hydrogen bonds, each about 3 $kJmol^{-1}$ stronger than the energy per hydrogen bond in liquid water (23.3 $kJmol^{-1}$ — energy required for breaking and completely separating the hydrogen bond) (Chaplin, 2004; Suresh and Naik, 2000). In liquid water, the number of hydrogen bonds per liquid water molecule has been difficult to quantify. An average value of approximately 3.4 hydrogen bonds per liquid water molecule is given in Stryer (1995). Based on computer simulations, most water molecules have two or three instantaneous hydrogen bonds per liquid water molecule, some have four, and very few have five (one more hydrogen bond than the maximum of four proposed earlier) (Ball, 2001).

The number of hydrogen bonds per molecule in liquid water depends on the balance between the favorable energetic aspect of optimal hydrogen bonding and the unfavorable entropy considerations resulting from restrictions in water molecule location (Wallqvist and Mountain, 1999).

An important feature of hydrogen bonds in water is that they act co-operatively—in other words, there is interdependence among the bonds. The formation of a first hydrogen bond between two water molecules enhances the ability of both molecules to form even stronger second hydrogen bonds because of the existence of the first hydrogen bond (Ludwig, 2001). This cooperative hydrogen bonding results in highly transient combinations of bonds among molecules, which makes elucidating the structure of liquid water immensely more complicated than for a substance that forms stable, well-defined bonds.

C. ANOMALOUS PROPERTIES

Compared to other molecules of similar molecular weight and atomic composition, water exhibits an intriguing array of anomalous physical and chemical properties, such as large values for melting and boiling points, phase transition enthalpies, surface tension, heat capacity, and thermal conductivity (Table I). Many of the unusual properties of water are related to its ability to engage in extensive, three-dimensional hydrogen bonding, which was discussed in the previous section. The cooperative and extensive hydrogen bonding in water serves to alter the properties of water compared to compounds of similar molecular structure. For example, the melting point at atmospheric pressure of water is over 100 °C higher, the boiling point at atmospheric pressure of water is over 150 °C higher, and the critical point of

TABLE I
SUMMARY OF SOME OF THE ANOMALOUS PROPERTIES OF WATER[a]

Property	Value and units
Melting point at 1 atm	0.0 °C
Boiling point at 1 atm	100.0 °C
Enthalpy of fusion at 0 °C (ΔH_{fus})	6.012 kJmol^{-1}
Enthalpy of vaporization at 100 °C (ΔH_{vap})	40.657 kJmol^{-1}
Enthalpy of sublimation at 0 °C	50.91 kJmol^{-1}
Surface tension at 20 °C	72.75×10^{-3} Nm^{-1}
Heat capacity at 20 °C	4.1818 J/g^{-1} K^{-1}
Thermal conductivity at 20 °C	0.5984 Wm^{-1} K^{-1}

[a]From Fennema (1996).

water is over 250 °C higher than expected by extrapolation of the melting, boiling, and critical points, respectively, of other group 6A hydrides—H_2S, H_2Se, H_2Te, and H_2Po (Chaplin, 2004). Explanations for the anomalous behavior of water are rooted in the ability of water to hydrogen bond and are elucidated in detail by Chaplin (2004). For example, in the case of the boiling point, the extensive hydrogen bonding in liquid water prevents water molecules from being released easily from the surface of the water. This reduces the vapor pressure of the system. Because boiling occurs when the vapor pressure equals the external pressure, a higher temperature is required to boil water compared to the nonhydrogen bonding molecules of similar structure.

Two of water's most prominent anomalies are the liquid-phase density maximum (Figure 5) and the increase in volume upon freezing (Figure 6) (Ludwig, 2001). The density of liquid water ($^1H_2\ ^{16}O$) at atmospheric pressure increases as temperature decreases to 3.984 °C, where it exhibits a maximum density value of 0.999972 gcm^{-3} (Franks, 2000). Below 3.984 °C, the density decreases with decreasing temperature to the freezing point. If the water is kept from freezing, the density continues to decrease into the supercooled liquid region (Figure 5). If the water freezes, there is a discontinuous (i.e., step change) decrease in density (Figure 5), which corresponds

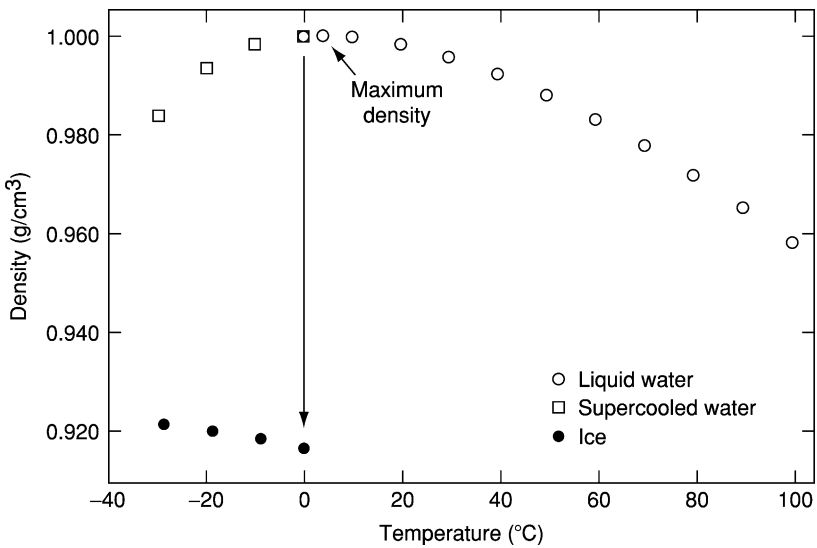

FIG. 5 The density of liquid and supercooled water as a function of temperature, illustrating the anomalous liquid phase density maximum of water (data from Lide, 2002–2003).

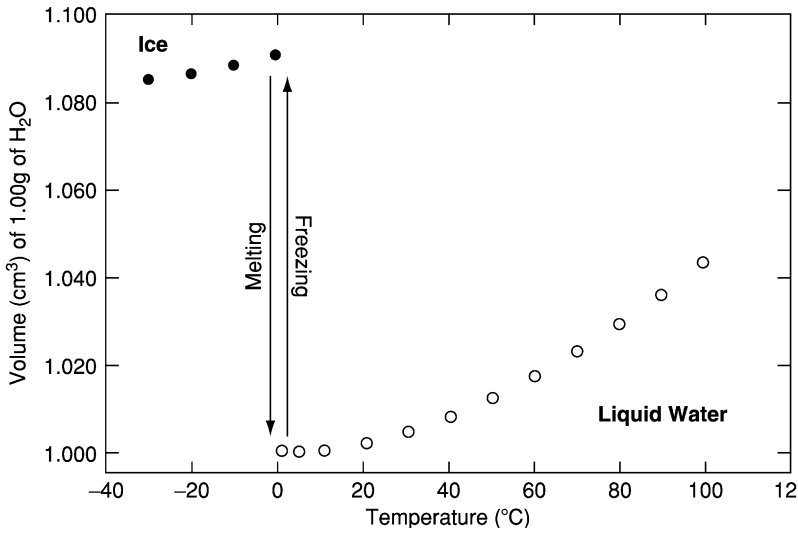

FIG. 6 The volume per 1 g of liquid and solid (ice) water as a function of temperature, illustrating the anomalous increase in the volume (or decrease in density), when liquid water freezes (data from Lide, 2002–2003).

to a discontinuous increase in volume (Figure 6). Most liquids are denser in the solid state than in the liquid state. Water, however, is unique—the solid form of water is less dense than the liquid. As can be observed in Figure 6, an increase in volume of approximately 9% accompanies the liquid-to-solid transition (freezing) of water at 0 °C and 1 atmosphere (~0.1 MPa) pressure (Kalichevsky *et al.*, 1995).

The anomalous properties of water remain an important subject of inquiry (Errington and Debenedetti, 2001; Mishima and Stanley, 1998). Chaplin (2004) gives a comprehensive overview of 40 anomalous properties of water and suggested explanations. Chaplin (2004) aptly pointed out that whether the properties of water are viewed as anomalous depends on what materials water is compared to and the interpretation of the term "anomalous." For example, Angell (2001) included a section on the nonuniqueness of water, stating that "...water is not unique, as is often supposed, but rather water is an intermediate member of a series of substances that form tetrahedral networks of different degrees of flexibility, and that, accordingly, show systematic differences of behavior." Additional references that discuss the properties of water as nonanomalous are Franks (2000), Kivelson and Tarjus (2001), and Netz *et al.* (2002).

D. ISOTOPIC COMPOSITION

Water is a mixture of varying isotopic composition (Franks, 2000). In addition to the two most common isotopes, ^{16}O and ^{1}H, there are two stable oxygen isotopes (^{17}O, ^{18}O), one stable hydrogen isotope (^{2}H, deuterium), and one radioactive hydrogen isotope (^{3}H, tritium, half-life = 12.6 years). Water also contains low concentrations of hydronium (H_3O^+) and hydroxide ions (OH^-) and their isotopic variants. In total, water consists of more than 33 chemical variants of HOH; however, these variants occur in relatively minor amounts (Fennema, 1996). Table II gives the natural abundance isotopic composition of the four major water species.

E. PHASES AND FORMS OF WATER

"*I am one thing. I am many things. I am water.*"
From *Water Dance*, by Thomas Locker (1997)

Water is a very structurally versatile molecule. Water exists in all three physical states: solid, liquid, and gas. Under extremely high temperature and pressure conditions, water can also become a supercritical fluid. Liquid water can be cooled carefully to below its freezing point without solidifying to ice, resulting in two possible forms of supercooled water. In the solid state, 13 different crystalline phases (polymorphous) and 3 amorphous forms (polyamorphous) of water are currently known. These fascinating "faces" of water are explored in detail in this section.

Water is the only form of matter occurring abundantly in all three phases (or states): solid, liquid, and gas (or vapor) (Fennema, 1996). Temperature and pressure determine the phase of water, as well as the type(s) and velocity(ies) of water molecule motion. A basic phase diagram (moderate pressure–temperature range) for pure water is shown in Figure 7. Given the

TABLE II
NATURAL ABUNDANCE ISOTOPIC COMPOSITION AND MOLECULAR WEIGHT OF THE FOUR MAJOR SPECIES IN WATER[a]

Characteristic	$^{1}H_2{}^{16}O$	$^{1}H_2{}^{18}O$	$^{1}H_2{}^{17}O$	$^{1}H^{2}H^{16}O$
Natural abundance isotopic composition (%)	99.7280%	0.2000%	0.0400%	0.0320%
Molecular weight (g/mol)	18.01056	20.01481	19.01478	19.01684

[a]Based on Franks (2000).

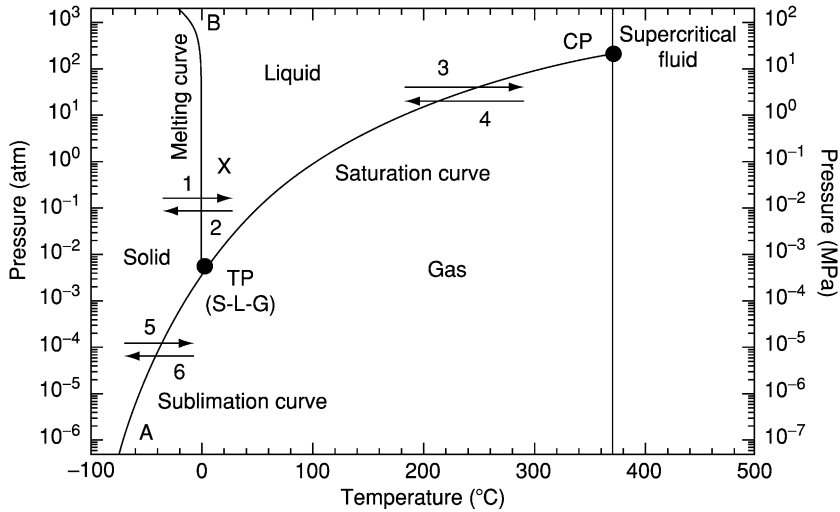

FIG. 7 Phase diagram for pure water showing the preferred physical state of water at various temperatures and pressures. The phase transitions indicated by the numbered arrows are (1) melting, (2) freezing, (3) boiling (or evaporation), (4) condensation, (5) sublimation, and (6) deposition (or ablimation). "X" marks the location on the phase diagram for water at typical room temperature (20 °C) and pressure (1 atm) conditions. TP is the triple point, where solid–liquid and gas (S-L-G) phases coexist in dynamic equilibrium. CP is the supercritical point. A and B are labels that have been added to facilitate the discussion of the sublimation and melting curves, respectively. This phase diagram was drawn using the international equations for pressure values along the phase boundary curves (melting, evaporating, and sublimation) for water (Wagner and Pruss, 1993; Wagner *et al.*, 1994).

importance of water in foods and food processing (i.e., concentration, dehydration, freezing, and freeze-drying), a thorough understanding of the phase diagram for water is of critical importance.

The phase diagram features four phase regions, three phase boundaries, and two points of particular interest: the triple point (TP) and the supercritical point (CP). Values for TP and CP from The International Association for the Properties of Water and Steam[6] (IAPWS) are 273.16 K and 611.657 Pa (IAPWS, 2002) and 647.096 K and 22.064 MPa (IAPWS, 2002), respectively. Three of the phases (solid, liquid, and gas) are bounded by equilibrium

[6]The International Association for the Properties of Water and Steam (IAPWS) provides internationally accepted values and formulations for the properties of light and heavy steam, water, and selected aqueous solutions for scientific and industrial applications. IAPWS Releases and Guidelines can be obtained online at http://www.iapws.org.

curves (sublimation curve [A to TP], melting curve [TP to B], and saturation curve [TP to CP]) that indicate the combination of pressure and temperature values at which the three reversible phase transitions occur. The liquid–gas boundary terminates at the supercritical point, and the fourth (pseudo) phase, supercritical fluid, begins. At and above the supercritical point the density of the gas becomes the same as the density of the liquid (Jones and Atkins, 2000). A liquid phase is no longer identifiable because there is no longer a dividing liquid–gas interface. Thus, by definition, what remains is a gas (a substance that fills any container it occupies) that cannot be condensed to a liquid at and above the supercritical point. A review of the properties and usefulness of supercritical water is given by Shaw *et al.* (1991).

The triple point is the location at which all three phases' boundaries intersect. At the triple point (and only at the triple point), all three phases (solid, liquid, and gas) coexist in dynamic equilibrium. Below the triple point, the solid and gas phases are next-door neighbors, and the solid-to-gas phase transition occurs directly.

One of the major differences among the phases of water at the molecular level is the motions of the water molecules. Using the phase diagram (Figure 7), we can follow the effects of temperature and pressure on the molecular mobility of water. For example, if we hold pressure constant (say at 1 atm) and increase temperature, molecular mobility increases as we move from the solid to the liquid to the gas phase regions. Conversely, if we hold temperature constant (say at 100 °C) and increase pressure, molecular mobility decreases as we move from the gas to the liquid phase region.

The temperature at which a phase transition occurs is dependent on pressure (Figure 7). At atmospheric pressure (1 atm) the solid-to-liquid phase transition occurs at 0 °C and the liquid-to-gas phase transition occurs at 100 °C. If we increase the pressure, say to 100 atm, the solid-to-liquid phase transition occurs at a temperature slightly less than 0 °C (−0.74 °C); however, the liquid-to-gas phase transition occurs at a much greater temperature (312 °C). If we decrease the pressure, say to 0.1 atm, the solid-to-liquid phase transition occurs at a temperature slightly greater than 0 °C (0.004 °C) and the liquid-to-gas phase transition occurs at a lower temperature (46 °C). If we decrease the pressure further to below the triple point, there is no solid-to-liquid phase transition; rather, the solid-to-gas phase transition occurs directly. At a pressure of 0.001 atm, the sublimation temperature is −20.16 °C.

If the phase diagram is viewed as a map (as suggested by Ball, 2000), similar to a map of the United States, with the different water phases (solid, liquid, gas) comparable to different states (i.e., Iowa, Illinois, and Wisconsin) and the phase boundaries as the state borders, we can envision

water as "traveling about" in the phase diagram. For water to do this "traveling about" in the phase diagram, changes in temperature (i.e., energy needs to be added or removed) and/or pressure are required. The amount of sensible or latent heat required to change the temperature or phase of the water (respectively) depends on the pressure. Figure 8 illustrates the steps in the phase diagram and the energy required for ice starting at −20 °C to become superheated gas (steam) at 120 °C at atmospheric pressure (1 atm). The enthalpy of fusion (ΔH_{fus}) and vaporization (ΔH_{vap}) are also given in Table I in units of $kJmol^{-1}$.

Careful cooling of pure water at atmospheric pressure can result in water that is able to remain liquid to at least 38 °C below its normal freezing point (0 °C) without crystallizing. This supercooled water is metastable and will crystallize rapidly upon being disturbed. The lower the temperature of the supercooled water, the more likely that ice will nucleate. Bulk water can be supercooled to about −38 °C (Ball, 2001; Chaplin, 2004). By increasing the pressure to about 210 MPa, liquid water may be supercooled to −92 °C (Chaplin, 2004). A second critical point (C′) has been hypothesized (Tc′ = 220 K and Pc′ = 100 MPa), below which the supercooled liquid phase separates into two distinct liquid phases: a low-density liquid (LDL) phase and a high-density liquid (HDL) phase (Mishima and Stanley, 1998; Poole *et al.*, 1992; Stanley *et al.*, 2000). Water near the hypothesized second critical point is a fluctuating mixture of LDL and HDL phases.

The effects of pressure on the phase transition of liquid water to ice (and within the ice phase itself) are complicated by the formation of several pressure-dependent ice polymorphs (Chaplin, 2004; Franks, 1984, 2000; Kalichevsky *et al.*, 1995; Ludwig, 2001). Thirteen crystalline forms of ice have been reported to date: I_h (hexagonal or normal or regular ice), I_c (cubic

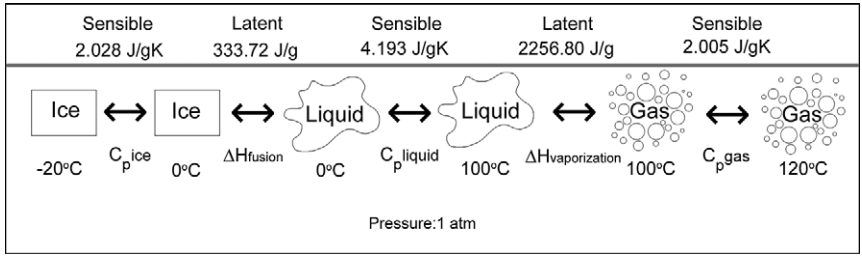

FIG. 8 Schematic illustration of the steps in the phase diagram and the energy required for ice starting at −20 °C to become superheated gas (steam) at 120 °C at atmospheric pressure (1 atm). The type and amount of heat (sensible or latent) required to change the temperature or phase are given, where C_p is the specific heat and ΔH is the change in enthalpy.

ice), and ices II–XII. Only regular ice (I_h), which is the normal form of ice and snow, is shown in Figure 7 because the other ice polymorphs occur at higher pressures and/or lower temperatures than those in Figure 7. A comprehensive phase diagram with a 0 to 800 K temperature range and a 0.1 to 10^{12} Pa pressure range, showing several of the ice polymorphs, as well as the liquid, gas, and supercritical regions, is given by Chaplin (2004). All of the ice polymorphs involve the water molecules being hydrogen bonded to four neighboring water molecules. These hydrogen bonds, however, are able to bend, stretch, and shorten under high pressure and low temperature conditions to form the various ice polymorphs. For ice I_h, application of pressure initially decreases the solid–liquid phase transition temperature, reaching a minimum of −22 °C at 207.5 MPa (2048.4 atm) (Kalichevsky *et al.*, 1995). After this minimum is reached, additional pressure results in an increase in the solid–liquid phase transition temperature and formation of different ice polymorphs. For example, the solid–liquid phase transition temperature (for ice VI to liquid water) increases to 20 °C with an increase in pressure to 882.9 MPa (Kalichevsky *et al.*, 1995). For the interested reader, Kalichevsky *et al.* (1995) and Knorr *et al.* (1998) discuss the potential application of high-pressure freezing and thawing for use in foods.

Amorphous water (also called glassy water or amorphous ice) can form when the temperature is decreased extremely rapidly below the glass transition temperature (T_g) of water (about 130 K at 0.1 MPa) (Mishima and Stanley, 1998). There are three types of amorphous ice: low-density amorphous ice (LDA), high-density amorphous ice (HDA), and very high-density amorphous ice (VHDA), with VHDA being discovered most recently (Finney *et al.*, 2002).

F. WATER MOBILITY

Water molecules exhibit three types of molecular motions: vibrational, rotational, and translational. For a nonlinear polyatomic molecule (such as water) containing N atoms, there are $3N$ coordinates needed to specify the locations of the atoms (a set of x, y, and z Cartesian coordinates for each atom). This corresponds to a total of $3N$ degrees of freedom for vibrational, rotational, and translational motions. Three degrees of freedom account for the translational energy of the molecule, three involve rotational energy, and the remaining degrees of freedom pertain to the vibrational energy $(3N - 6)$. For water with $N = 3$ atoms, there are nine total degrees of freedom (3×3): three for translational energy, three for rotational energy, and three for vibrational energy $(=[3 \times 3] - 6)$.

The water molecule can vibrate in a number of ways. In the gas phase, vibrational motion involves changes in the size and shape of the molecule

through stretching, bending, and rotation of bonds. It is intramolecular motion, i.e., motion within the molecule. As calculated earlier, water in the gas phase exhibits three vibrational modes: symmetric and asymmetric stretching of the H–O–H bonds and bending of the H–O–H bond angle (Figure 9). However, in liquid water and ice phases, vibrational motions are much more complex, mainly because they involve additional water molecules through hydrogen bonding. Chaplin (2004) gave a detailed explanation of the vibrational modes in liquid water and ice phases. Vibrational motion can be measured using infrared and Raman spectroscopy (Conway, 1981).

Rotational motion is spinning of the entire molecule around an axis in three-dimensional space. Figure 10 illustrates the rotational motion of a water molecule. Rotational motion occurs in liquid and gas phases of water and, to a limited extent, through defects in the solid phase (ice). Rotational motion of water molecules can be measured using NMR and dielectric spectroscopy (Belton, 1994).

Translational motion is the change in location of the entire molecule in three-dimensional space. Figure 11 illustrates the translational motion of a few water molecules. Translational motion is also referred to as self-diffusion or Brownian motion. Translational diffusion of a molecule can be described by a random walk, in which x is the net distance traveled by the molecule in time Δt (Figure 12). The mean-square displacement ($\overline{x^2}$) covered by a molecule in a given direction follows the Einstein-derived relationship (Eisenberg and Crothers, 1979):

$$\overline{x^2} = 2D\Delta t \tag{1}$$

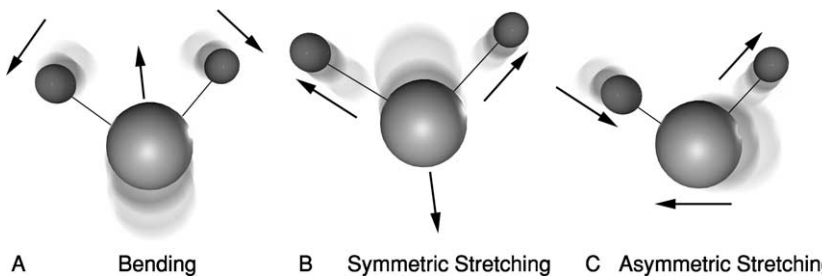

FIG. 9 Diagram illustrating the three vibrational modes ($3N-6$) of water in the gas phase. (A) The first mode is called bending, in which the water molecule moves in a scissors-like manner. (B) The second is the symmetric stretch, where the hydrogen atoms move away from (or toward) the central oxygen atom simultaneously—i.e., in-phase motion. (C) The third is the asymmetric stretch, in which one hydrogen atom approaches the central oxygen atom, while the other moves away—i.e., out-of-phase motion.

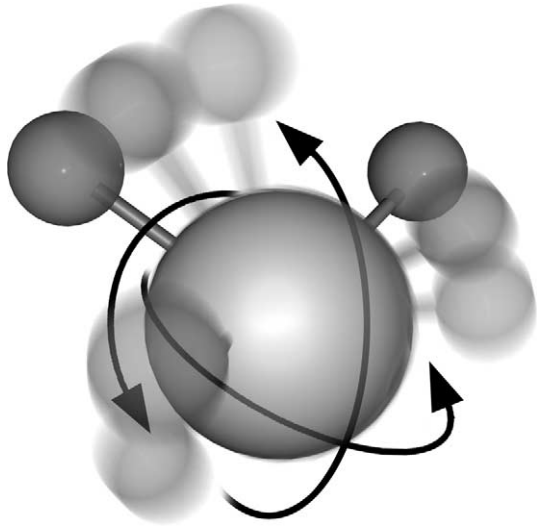

FIG. 10 Schematic illustration of the rotational motion of a water molecule. The water molecule can rotate in all three dimensions, but does not change locations.

where D is the proportionality constant referred to as the self-diffusion coefficient (m^2s^{-1}). In addition, Einstein showed that $D = k_B T/f$, and in conjunction with the Stokes expression for the friction factor f for spheres, the so-called Stokes–Einstein relationship becomes

$$D = \frac{k_B T}{6\pi\eta_s r} \tag{2}$$

where k_B is the Boltzmann constant (1.381×10^{-23} JK^{-1}), T is temperature, η_s is the dynamic viscosity of the solvent, and r is the molecular radius. For a temperature of 298 K, a viscosity of 0.8904×10^{-3} Ns/m^2, and a radius of 1.41×10^{-10} m, the D value for water in water, calculated using Eq. (2), is 1.74×10^{-9} m^2s^{-1}, which is similar in magnitude to the average experimentally determined D value, reported by Franks (1984) for water, of 2.5×10^{-9} m^2s^{-1} at 298 K.

Translational motion occurs in liquid and gas phases of water, but is virtually eliminated in the solid phase (ice). Translational motion of water molecules can be measured using NMR and magnetic resonance imaging (MRI) spectroscopy (Sun and Schmidt, 1995).

Despite the care taken to depict the three types of water motion in Figures 9 through 11, it is difficult to illustrate the dynamic three-dimensional motion of water in a static figure. A basic, but very well-done narrated

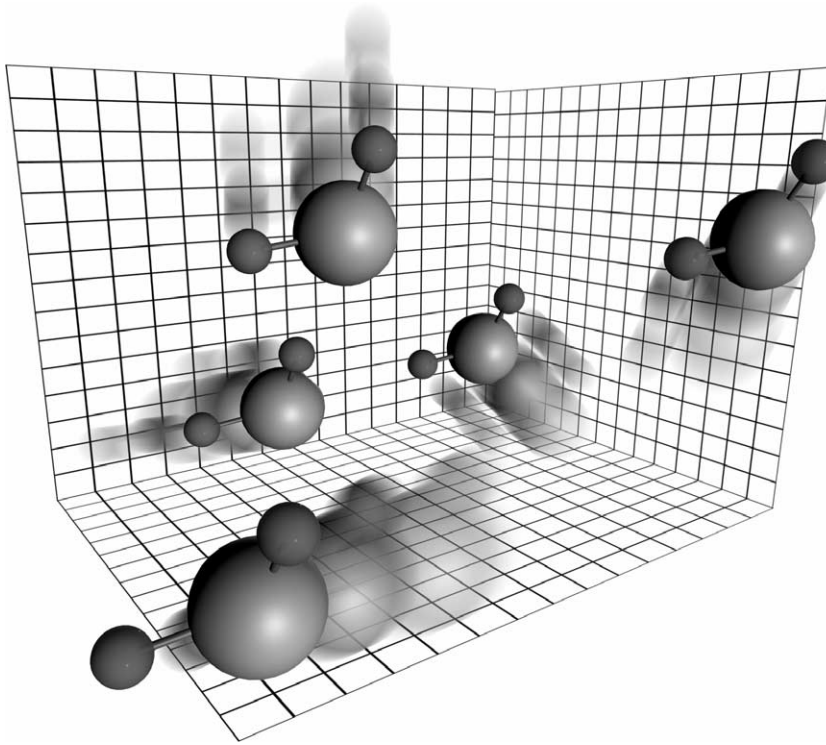

FIG. 11 Schematic illustration of the translational motion of a few water molecules. The water molecule changes locations, but does not rotate.

molecular animation of the motions of water molecules, developed originally by Tasker *et al.* (1996a,b), is available on videotape through the Films for the Humanities and Sciences; it is called "Water: A Molecular Substance" (FFH #7749).

G. WATER MODELS

Over the years, a large number of models of water structure have been developed in an attempt to reconcile all the known physical properties of water and to arrive at a molecular description of water that accounts correctly for its behavior over a large range of thermodynamic conditions. Early models of water structure have been categorized by Fennema (1996) and Ball (2001) into three general types: mixture, uniformist, and interstitial. Mixture models are based on the concept of intermolecular hydrogen bonds

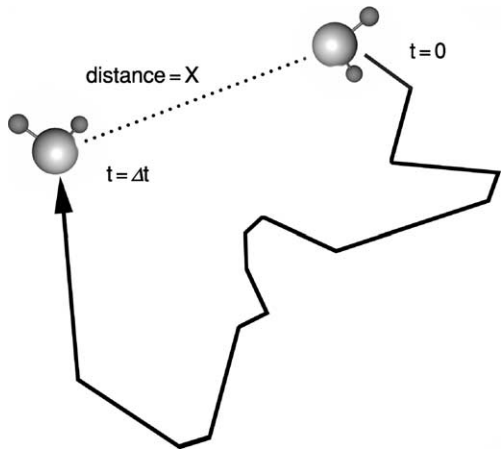

FIG. 12 Translational diffusion (also called Brownian motion) of a water molecule can be described by a random walk starting at $t = 0$ and ending at $t = \Delta t$, where x is the net distance traveled during Δt and t is time.

being momentarily ($\sim 10^{-11}$ s) concentrated in bulky clusters of water molecules that are in dynamic equilibrium with other, more dense clusters of water molecules, containing less than their full complement of hydrogen bonds (Fennema, 1996; Luck, 1981). Uniformist (also called continuum) models are based on the concept that liquid water consists of a random network of intermolecular hydrogen bonds, with frequent strains and broken bonds, that are continually undergoing topological reformation (Stillinger, 1980). Interstitial models are based on the concept that upon melting, some of the water molecules remain in place in the ice lattice and others that break loose, moving around in the empty (or interstitial) spaces (Ball, 2001; Fennema, 1996).

Reviews on water structure models include Mishima and Stanley (1998), Wallqvist and Mountain (1999), and Ludwig (2001). Mishima and Stanley (1998) concentrated their review on three relatively recent water structure hypotheses: (1) the stability limit hypothesis (Speedy, 1982), (2) the singularity-free hypothesis (Sastry *et al.*, 1996), and (3) the liquid–liquid phase transition hypothesis (Poole *et al.*, 1992).

Wallqvist and Mountain (1999) explored molecular models of water, beginning with the precomputer-era models, but mainly focused on the computer-era models. Computer simulations, which have been available since the 1960s, have contributed the missing dimension of time to the picture (or should we say movie) of the molecular structure of water. Computer simulations are powerful additions to the previous combination

of experimental and theoretical approaches to the elucidation of water structure (Wiggins, 1995). The limiting factors are the computing power and time needed for multiwater molecule simulations; thus, simulations are often limited to a few hundred water molecules in boxes with 2.5-nm edges for times equivalent to a few picoseconds (Chaplin, 2004). One of the major advances from simulated studies has been to quantify the development of the hydrogen-bond network with the thermodynamic conditions from the supercooled state to the supercritical region in passing by the ices (Guillot, 2002). Although simulations have contributed significant progress toward a self-consistent molecular model of water, much work remains to be accomplished. For a review on the progress of using computer simulation for determining water structure, see Guillot (2002).

Ludwig's (2001) review discusses water clusters and water cluster models. One of the water clusters discussed by Ludwig is the icosahedral cluster developed by Chaplin (1999). A fluctuating network of water molecules, with local icosahedral symmetry, was proposed by Chaplin (1999); it contains, when complete, 280 fully hydrogen-bonded water molecules. This structure allows explanation of a number of the anomalous properties of water, including its temperature-density and pressure-viscosity behaviors, the radial distribution pattern, the change in water properties on supercooling, and the solvation properties of ions, hydrophobic molecules, carbohydrates, and macromolecules (Chaplin, 1999, 2001, 2004).

Despite the efforts of a large number of scientists from a wide array of disciplines, to date, no single model successfully accounts for all the properties of real water. However, with each passing year, experimental and theoretical studies continue to contribute important pieces to the puzzle of the unusual properties of water, forming an increasingly coherent picture of the true nature of water.

III. WATER AND SOLIDS IN FOODS

Now we turn our attention to the water and the solids that compose the myriad of fresh and processed foods we consume. When a component is added to water (or coexists with water, as in a fresh food), the overall mobility of the water decreases, compared to that of pure water. The magnitude of the decrease depends on the number, amount, and nature of the component(s) added, as well as the effect of any processing methods used. In the past, researchers focused their attention on the relationship between water (activity, availability, mobility) and food stability. Based on the introduction of the polymer science approach to food stability by Slade and Levine (1985, 1988, 1991), the focus has shifted to the relationship

between solids (via the glass transition) and food stability. A combined approach of probing both the water and solids mobility and their individual and combined relationships to food stability is most desirable and is the approach recommended in this review. It is important to remember that the water and solids mobility values obtained are dependent on the property and measurement method selected to probe the system. This is discussed in greater detail in subsequent sections.

Before we proceed to explore the mobility of water and solids in foods, as examined by water activity, nuclear magnetic resonance, and the glass transition, we need to pause and appreciate the complex nature of the systems that we are attempting to investigate.

A. COMPLEX NATURE OF FOODS

Foods are complex, dynamically heterogeneous mixtures of macromolecules, solutes, and solvents (including water). Eads (1999) classified the complexity of food materials into three main dimensions or types: (1) compositional, (2) structural, and (3) dynamical complexity. Compositional complexity of foods ranges from a few simple compounds, such as sucrose and flavors in beverages, to hundreds of compounds in systems such as coffee (Lindsay, 1996) and aged cheeses (Eads, 1999). Structural components and structures in foods range in size from subatomic particles (10^{-15} m) to molecules to molecular assemblies to networks and composites to whole foods such as peas (0.5 cm), apples (8 cm), steaks (20 cm), and watermelon (50 cm). Structures also range in complexity from single atoms to assemblies containing thousands of molecular units, such as amino acids in the case of proteins and glucose units in the case of starch. Identifiable structures also include domains or phases in foods (Eads, 1999). Dynamical complexity in foods refers to both the changes that occur over time, because most food systems are not in equilibrium (Slade and Levine, 1991), and to the distribution of molecular motions. The characteristic duration for dynamical processes in food materials spans about 15 orders of magnitude, from femtoseconds (10^{-15} s) for absorption of light to years for recrystallization of sugars (Eads, 1999).

Ice cream serves as a wonderful (and tasty) example of a complex, dynamically heterogeneous food system. A typical ice cream mix contains milk or cream (water, lactose, casein and whey proteins, lipids, vitamins, and minerals), sucrose, stabilizers and emulsifiers, and some type of flavor (e.g., vanilla). After the ingredients are combined, the mix is pasteurized and homogenized. Homogenization creates an oil-in-water emulsion, consisting of millions of tiny droplets of milk fat dispersed in the water phase, each surrounded by a layer of proteins and emulsifiers. The sucrose is dissolved in

the water phase. The ice cream mix is whipped and frozen, which creates two more discrete structural phases—millions of tiny ice crystals and air bubbles—dispersed in the concentrated, unfrozen mix. The water undergoes a phase transition to form ice, and the dissolved sucrose becomes increasingly concentrated in the unfrozen phase, as ice continues to form. The resultant frozen ice cream contains four microscopic structures: ice crystals, air bubbles, fat droplets, and the unfrozen material (Goff, 1998). Ice cream comprises a solution, suspension, foam, and emulsion and contains extensive air/liquid, fat/liquid, and ice/liquid interfaces (Charley and Weaver, 1998). The water in ice cream may coexist in as many as four different forms: ice, glass, viscous liquid, and hydration layers on macromolecular surfaces (Eads, 1995). Over time, changes in ice cream take place. Ice crystals increase in size (ripen), yielding a coarse, undesirable texture, and lactose crystallizes, resulting in the so-called "sandiness" texture defect. For the interested reader, Hartel (1998) provides an excellent discussion of the various phase transitions important in the manufacturing and storage of ice cream.

As we proceed with discussing the various system properties and measurement methods that can be used to investigate water and solids mobility, it is important to keep in mind the influence the complexity of food systems, such as in the ice cream example just discussed, can have on our ability to measure, interpret, understand, and predict food quality, stability, and safety.

B. WATER ACTIVITY

1. Development of the water activity concept

The concept of substance "activity" was derived by Gilbert N. Lewis in 1907 from the laws of equilibrium thermodynamics and is described in detail in the text entitled "Thermodynamics and the Free Energy of Chemical Substances" by Lewis and Randell (1923). In a homogeneous mixture, each component has a chemical potential (μ), which describes how much the free energy changes per mole of substance added to the system. The chemical potential of water (μ_w) in a solution is given by

$$\mu_w = \mu_w^o + RT \ln a_w \tag{3}$$

where μ_w^o is the chemical potential of pure water in a standard state ($a_w = 1$), R is the universal gas constant (8.314 $JK^{-1}mol^{-1}$), T is temperature, and a_w is water activity. For an ideal solution, a_w equals the mole fraction of water (x_w) and varies between 0 and 1:

$$a_w = x_w = \frac{m_w}{m_w + \Sigma m_{s,i}} \tag{4}$$

where m_w is the molar concentration of water and $m_{s,i}$ is the molar concentration of each of the solutes. Equation (4) is commonly referred to as Raoult's law. Equation (4) is obeyed for ideal solutions, such as dilute sucrose solutions ($x_{sucrose} \leq 0.01$), but is poorly obeyed for concentrated solutions. Most foods exhibit marked nonideality, and calculation of a_w from composition is difficult for real food systems (Walstra, 2003). The main causes of this nonideality, as discussed by Walstra (2003), are (1) dissociation of the solute, such as in the case of NaCl, (2) solute molecule size, and (3) solvent–solute interactions. Rahman (1995) has reviewed extensively several models for predicting a_w based on composition, such as the Norrish (1966) and Ross (1975) models, which have shown moderate success for some model food systems. In general, water activity for foods is best determined experimentally.

Because the chemical potentials of water distributed in two phases (i.e., solution and vapor) must be equal, the water activity of a food can be measured by bringing the food into "equilibrium" with the air above it. At equilibrium, under conditions of constant temperature and pressure, the a_w values of the aqueous phase of a food ($a_{w,f}$) and of the air ($a_{w,v}$) are equal and can be estimated from the ratio of the partial vapor pressure of water above the food (p_v) to the vapor pressure of pure water (p_v^o) at the same temperature (Walstra, 2003):

$$a_{w,f} = a_{w,v} = \frac{p_v}{p_v^o} \tag{5}$$

Thus, the water activity of a food is equal to the relative vapor pressure p_v/p_v^o. The relative vapor pressure is also related to percentage relative humidity (%RH) divided by 100. It is critical to bear in mind the assumptions underlying the development and thus the use of Eq. (5) for determining the a_w of a food. These assumptions are examined in detail in the next section.

Before proceeding, it is worth noting that at temperatures below freezing (i.e., below the freezing point of food, in the presence of an ice phase), the definition of a_w changes to (Fennema, 1996)

$$a_w = \frac{p_{ice}}{p_{SCW}^o} \tag{6}$$

where p_{ice} is the vapor pressure of pure ice and p_{SCW}^o is the vapor pressure of pure supercooled water at a specified temperature and pressure. Because both of these vapor pressure values have been measured and/or calculated for several temperatures below freezing, a_w below freezing can be calculated using Eq. (6) (Table III). Thus, below freezing, a_w is independent of sample composition and is determined by the temperature of the system. So, below freezing pure ice and food containing ice have the same a_w at the same

TABLE III
WATER (LIQUID OR SUPERCOOLED) AND ICE VAPOR PRESSURES AND THEIR RATIO (WATER ACTIVITY BELOW FREEZING) AT 0 °C AND SEVERAL SUBFREEZING TEMPERATURES

Temperature (°C)	Vapor pressure (mmHg)		$\frac{p_{ice}}{p^o_{SCW}}$
	Liquid or supercooled water[a]	Ice[b] or food containing ice	
0	4.579	4.579	1.00
−5	3.163	3.013	0.95
−10	2.149	1.950	0.91
−15	1.436	1.241	0.86
−20	0.9406	0.776	0.83
−25	0.6053	0.476	0.79
−30	0.3816	0.2859	0.75
−35	0.2354	0.1675	0.71
−40	0.1418	0.0966	0.68

[a]Supercooled at all temperatures except 0 °C. Measured values for −15 °C and warmer (Weast, 1975). Calculated values for −20 °C and colder (Mason, 1957).
[b]Measured values from Weast (1975), except −35 °C from Mason (1957).

temperature. Consequently, below freezing a_w is not a useful concept for predicting the stability of different food systems (Fennema, 1996).

2. *Assumptions underlying the water activity concept*

The two main assumptions underlying the derivation of Eq. (5) are (1) thermodynamic equilibrium and (2) conditions of constant temperature and pressure. These assumptions, especially assumption number 1, however, are often violated in food systems. Most foods are nonequilibrium systems. The complex nature of food systems (i.e., multicomponent and multiphase) lends itself readily to conditions of nonequilibrium. Many food systems, such as baked products, are not in equilibrium because they experience various physical, chemical, and microbiological changes over time. Other food products, such as butter (a water-in-oil emulsion) and mayonnaise (an oil-in-water emulsion), are produced as nonequilibrium systems, stabilized by the use of emulsifying agents. Some food products violate the assumption of equilibrium because they exhibit hysteresis (the final a_w value is dependent on the path taken, e.g., desorption or adsorption) or delayed crystallization (i.e., lactose crystallization in ice cream and powdered milk). In the case of hysteresis, the final a_w value should be independent of the path taken and should only be dependent on temperature, pressure, and composition (i.e.,

chemical potential is a state function) (Franks, 1991). Regardless of the cause of a nonequilibrium state, a_w values in foods can change as a function of time, thus violating the assumption of thermodynamic equilibrium listed earlier.

In addition to conditions of thermodynamic equilibrium, water activity is also temperature and pressure dependent (Bell and Labuza, 2000; Kapsalis, 1987). The effect of temperature on a_w can be significant. For many food systems, at constant moisture content, water activity increases as temperature increases (Figure 13A). However, the opposite occurs for several small molecular weight solutes, such as crystalline sugars and salts. For these molecules, at constant moisture content, as temperature increases, water activity decreases (Figure 13B) (Audu *et al.*, 1978; Kapsalis, 1987; Mathlouthi and Roge, 2003). This temperature effect can also be observed for the saturated salt solutions used in constructing sorption isotherms. For example, the water activity of a saturated magnesium nitrate solution is 0.544 at 20 °C, but decreases to 0.514 at 30 °C (Greenspan, 1977). A combination of the temperature–a_w shifts illustrated in Figure 13A and B is observed for foods containing a large amount of solutes (e.g., dried fruits). At low a_w values (~0.55 to 0.75) (at constant moisture content), an increase in temperature results in an increase in a_w, after which an a_w inversion point is reached, and an increase in temperature (at constant moisture content) results in a decrease in a_w (Figure 13C). The specific location of the inversion point depends on the composition of the food and the solubility of the solutes present (Rahman, 1995).

The Clausius–Clapeyron equation can be used to predict the change in a_w with a change in temperature (Kapsalis, 1987):

$$\ln \frac{a_{w2}}{a_{w1}} = \frac{\Delta H_{st}}{R}\left[\frac{1}{T_1} - \frac{1}{T_2}\right] \tag{7}$$

where a_{w1} and a_{w2} are water activity values at temperatures T_1 and T_2 (absolute temperature, K), respectively, ΔH_{st} is the net isosteric heat of sorption at the moisture content of the sample (cal/mol), and R is the universal gas constant (1.987 cal/mol K). ΔH_{st} is defined as the difference between the total molar enthalpy change and the molar enthalpy of vaporization of pure water. The assumptions underlying Eq. (7) are that moisture content is constant and ΔH_{st} is constant over the a_w and temperature ranges considered (Kapsalis, 1987; Rahman, 1995) for each system under study.

A food system can experience rather large fluctuations in temperature during its lifetime, depending on a variety of factors, such as the location and time of year the product is manufactured and the conditions of distribution, storage, and display. For example, if a food product, such as an intermediate moisture cheese, is manufactured and packaged with an a_{w1} equal to 0.66 at

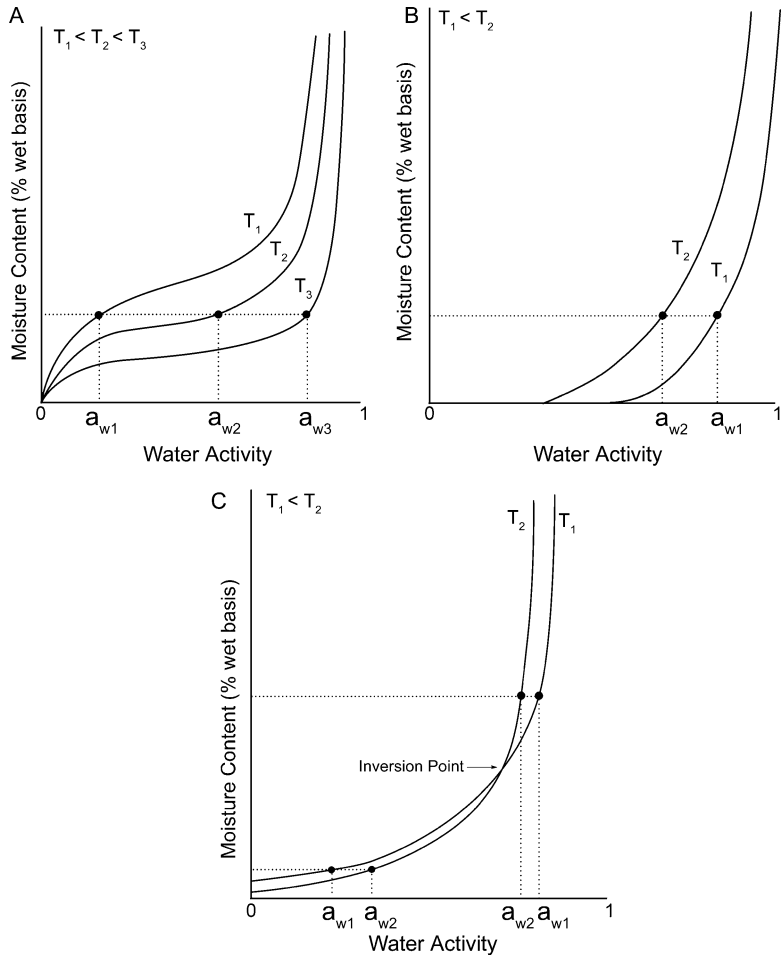

FIG. 13 Illustration of the effect of temperature (T) on a_w for (A) a complex food system, (B) a small molecular weight solute, such as fructose, and (C) foods containing large amounts of solutes, such as raisins. In all case, $T_1 < T_2 < T_3$.

25 °C (298 K) in Wisconsin and is then shipped by railroad car to Illinois in August, temperatures could increase during transport to 45 °C (318 K). Using Eq. (7) and a ΔH_{st} for cheese of 1573 cal/mol (Okos *et al.*, 1992) and assuming no moisture gain or loss, the a_{w2} of the cheese in the railcar would equal 0.78. This 0.12 increase in a_w could result in new microbiological problems and an increase in deleterious chemical reactions, such as Maillard browning. Depending on the characteristics of the product, a 10 °C change in temperature can result in a 0.03 to 0.20 change in a_w (Fennema, 1996).

Before leaving the effect of temperature on a_w topic, it is important to note that when monitoring the effect of temperature on a_w careful control and measurement of the temperature in the regions occupied by the sample and the sensor are needed. The temperature for both sample and sensor must be equal. If the temperature experienced by the sample is different than the temperature experienced by the sensor, data collected are not valid.

In contrast to the effects of temperature, the effect of pressure on a_w is relatively small and can be neglected for reasonable pressure differences. Based on thermodynamics, a change in total pressure of a system affects the vapor pressure. The change in water activity with pressure, at constant moisture content, can be calculated using Eq (8) (Bell and Labuza, 2000):

$$\ln \frac{a_{w2}}{a_{w1}} = \frac{\overline{V}_L}{RT}[P_2 - P_1] \tag{8}$$

where a_{w1} and a_{w2} are water activity values at total pressures P_1 and P_2 (in atm), respectively, $\overline{V}_L$ is the molar volume of water (18 cm^3/mol), R is the gas constant (82.06 cm^3 atm/Kmol), and T is temperature (in K). The atmospheric pressure range in the United States varies from about 1 atm in New Orleans (near sea level) to about 0.82 atm in Denver (the "mile-high" city). Using this atmospheric pressure range, a product with an a_{w1} of 0.60 at 25 °C in New Orleans would have an a_{w2} of 0.5999 at 25 °C in Denver, a negligible difference in a_w.

Strictly speaking, given the violations of the assumptions underlying Eq. (5) discussed earlier, the concept of a_w should not be applied to food systems. However, the concept of a_w has proven to be an extremely useful and practical tool in both the food industry and in food science research (Franks, 1991). Rather than discarding the use of a_w in foods, perhaps it would be more prudent at this point for one to stress the time-dependent nature (i.e., kinetics) of a_w measurements and perhaps, as suggested by Slade and Levine (1991) and Fennema (1996), to use the term relative vapor pressure (RVP, the measured term) in place of a_w (the theoretical term). To avoid confusion, the term a_w will continue to be used in this review, with the understanding that what is most often being measured is RVP.

The continued use of a_w in foods does not preclude the use of other concepts or measurement methods, such as the "food polymer science" approach proposed by Slade and Levine (1991) or rotational and translation mobility as measured by NMR. Rather, it may be most useful to combine these various approaches, recognizing the strengths, perspective (i.e., distance and time scales), and limitations of each. Then, each approach can be utilized where it is most applicable so as to build a multilevel understanding of the workings of specific food systems.

3. *Distance and timescales involved in the water activity concept*

An illustration to help conceptualize the physical meaning of the a_w parameter is given in Figure 14. Water activity is defined [Eq. (5)] as the ratio of the vapor pressure of water above a food (p_v) divided by the vapor pressure of pure water (p_v^o), measured in separate small closed containers (with a small head space) at constant temperature and atmospheric pressure. The vapor pressure in both containers is established by the macroscopic diffusion of water out of the water and out of the food. When equilibrium is reached, the vapor pressure in each container can be measured using a manometer. Thus, the a_w measurement involves water traveling over macroscopic distance scales. In addition to the manometer used in Figure 14, a_w measurements can be made using a variety of techniques, such as hygrometric instruments (i.e., resistance, capacitance, and dew point), hygroscopicity of salts, and isotherm and isopiestic methods (Rahman, 1995), each of which involves water traveling over macroscopic distance scales.

"When is equilibrium reached?" is an important follow-up, timescale question. The water activity measurement involves two interrelated timescales. The first timescale is related to the nonequilibrium nature of most

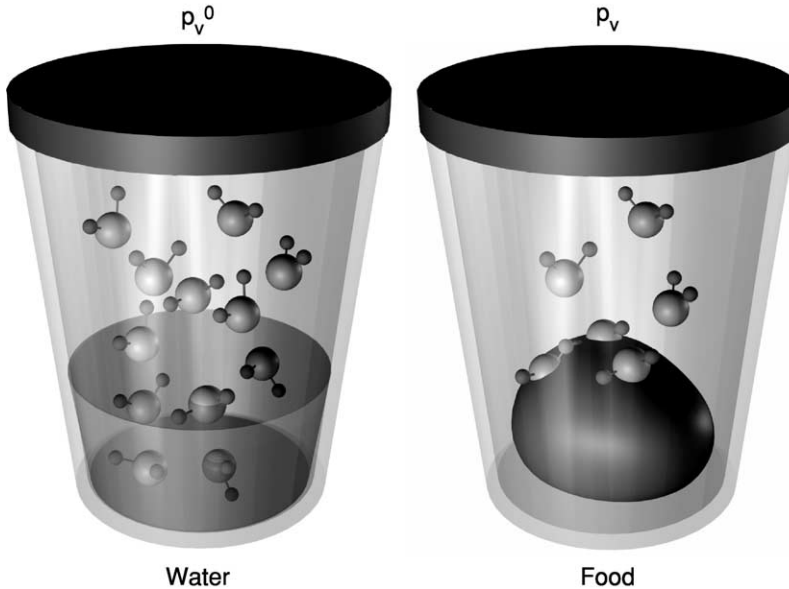

FIG. 14 Illustration of the vapor pressures measured in an a_w measurement. The vapor pressure in both the water and the food containers is established by macroscopic diffusion of water out of the sample (pure water or food).

foods, i.e., the nonequilibrium conditions within a food sample itself (discussed previously). The measured a_w value obtained would depend on the current conditions of the sample being measured (i.e., sample age, moisture content, moisture distribution among components, occurrence of any phase transitions, pH). For many foods, the change in a_w with time is relatively small and of little consequence within the shelf life of the food. Some foods change as a function of time in an attempt to reach equilibrium. For example, it is well documented that if an amorphous (noncrystalline) material, such as a sugar-based candy glass, is held at a high enough relative humidity and temperature for a sufficient length of time, the amorphous material will release the water it gained, and perhaps the water it originally contained, and crystallize (to a thermodynamically more stable state). This amorphous-to-crystalline transformation results in a dramatic change in the measured sample water activity (and the isotherm of the sample). The length of time required for water release and subsequent crystallization depends on the type of amorphous sugar (e.g., glucose versus sucrose) and the specific relative humidity (Makower and Dye, 1956). Some foods, such as butter, a water-in-oil emulsion, and mayonnaise, an oil-in-water emulsion, may never reach equilibrium. For butter, the continuous lipid phase surrounding the water has an a_w of zero, whereas the dispersed water droplets have an a_w of around 0.98 in unsalted butter and 0.91 in salted butter (25 °C). Despite the internal nonequilibrium nature of a butter sample, the a_w of butter can still be measured. However, measurement using an electronic a_w instrument takes a longer time (~30 min) compared to that for a typical food sample (~10 min) because the continuous lipid phase greatly inhibits the macroscopic diffusion of water into the head space of the measurement chamber of the instrument.

The second timescale involves equilibration of a food sample with the air or known relative humidity environment (e.g., saturated salt solutions, in the case of obtaining an isotherm). In this case, equilibration depends on the size of a sample, the measurement method used, and the nature of the sample being measured (this factor is related to the first timescale discussed previously, as illustrated with butter). For example, measuring the a_w of 2 g of corn starch at 25 °C can be done in less than 5 min using, for example, a Decagon AquaLab (Decagon, Pullman, WA) chilled-mirror a_w instrument. Measuring the isotherm for corn starch (2 g), using desiccators containing various saturated salt solutions (0.33 to 0.95 a_w at 22 °C), can take weeks to months (depending on the specific a_w), whereas measuring the isotherm for the same amount of corn starch over the same a_w values using individual proximity equilibration cells (PEC) takes from days to weeks (Lang *et al.*, 1981).

Depending on the food item, only pseudo-equilibrium (or a stationary state) may be reached in the time frame of a measurement, as a very long

time may be required for a sufficient number of water molecules to escape from the food and establish a true equilibrium. However, for many foods, this pseudo-equilibrium state may be close enough to true equilibrium, and the resultant a_w measurement is likely to fall within the uncertainties typically associated with its measurement (± 0.005 to ± 0.02 a_w; Chirife and Buera, 1996; Fennema, 1996, respectively). Chirife and Buera (1996) discussed the establishment of equilibrium in the case of sorption isotherms using a maximum tolerable weight change as the criterion and suggested that sorption determinations performed carefully using this criterion are likely to be close to equilibrium.

Automated water sorption instruments, with ultrasensitive microbalances capable of generating specific %RH values at selected temperatures, are now available, facilitating the production of isotherms in a shorter period of time, from several hours to a few days. Commercially available instruments include the dynamic vapor sorption (DVS) instrument from Surface Measurement Systems Ltd., the IGA*sorp* from Hiden Analytical, and the SGA-100 symmetric gravimetric analyzer from VTI Corporation. Literature concerning the DVS method for isotherm measurements includes Teoh *et al.* (2001), who investigated the sorption behavior of cornmeal components, and Arabosse *et al.* (2003), who compared the DVS method to the saturated salt solution method. Accuracy and repeatability of these new automated water sorption instruments, compared to standard saturated salt solution methods, are currently being investigated in the author's laboratory.

4. Usefulness of the water activity concept in foods

The modern-day study of water activity in foods began taking shape when Scott (1953, 1957; see also Christian and Scott, 1953), applied the thermodynamic concept of water activity to predict the growth of food spoilage microorganisms (van den Berg and Bruin, 1981). Since that time, the concept of water activity has been thoroughly incorporated into academic, industrial, and governmental food science and technology sectors. For example, a_w limits are currently used in the U.S. Federal Regulations on Good Manufacturing Practices and in the food industry as quality assurance specifications. However, the usefulness of a_w as an indicator of food stability and quality has been questioned over the last two decades (Franks, 1982, 1991; Slade and Levine, 1991) and remains a topic of great controversy (Chirife and Buera, 1996; Le Meste *et al.*, 2002). The approach offered here on the usefulness of a_w is based on its practical value, not its absolute theoretical correctness, which has already been investigated and discussed earlier. The compilation of ideas presented in this section on the usefulness of a_w was influenced by the following sources: Rahman (1995), Chirife and

Buera (1996), Fennema (1996), Champion *et al.* (2000), Labuza *et al.* (2001), and Le Meste *et al.* (2002).

a. Assessment of moisture content as a function of relative humidity. Water activity can be useful in determining the moisture content of a food system as a function of relative humidity at the same temperature (i.e., moisture sorption isotherms). Despite the possibility of inadequate conditions for equilibrium, an isotherm is still a useful indicator of moisture content and moisture content changes as a function of relative humidity. Moisture sorption isotherms are useful for a variety of processing and product stability applications, as discussed further later.

b. Prediction of moisture transfer. Water activity can be useful for determining the direction of possible water migration between food components or between a food and its environment. If two components with unequal water activities (e.g., crisp component 1 with an $a_w = 0.25$ and soft component 2 with an $a_w = 0.60$) are placed together in a closed chamber (e.g., a food package), they will over time equilibrate to a single a_w, with component 1 gaining water and becoming soggy and component 2 losing water and becoming hard. This concept of equalizing water activities is at the heart of the development of shelf-stable, dual-texture products, such as raisin-and-flake cereals and cake-and-filling desserts (e.g., Twinkies). This same principle of equalizing water activities applies to the interaction of a food material with its environment, as influenced by the packaging material selected. If a food is packed in moisture-impermeable packaging, such as glass or aluminum foil (>0.001 in. thick), no significant transfer of moisture with the environment will occur. However, if a food is packed in moisture-permeable (e.g., paper) or semipermeable (e.g., plastic films) packaging, the food will gain moisture if the a_w of the food is less than the relative humidity of the air or lose moisture if the a_w of the food is greater than the relative humidity of the air. Moisture sorption isotherms can be used to predict the moisture transfer rate through packaging materials or edible food coatings, and thus predict the shelf life of a food (Rahman, 1995).

c. Development of new products. Water activity and moisture sorption isotherms can be useful in the development of new or reformulated products. The water activity concept is useful in the development of foods in which reduced water contents are desired, such as in the case of intermediate-moisture foods, or in which equal water activities are required, such as in the case of dual-textured foods discussed previously. Effective selection of solutes (e.g., sugars, salts, sugar alcohols) to decrease the water activity is important when formulating a product to a desired or reduced water

activity. For example, in the reformulation of a model granola bar, the substitution of crystalline fructose for honey and brown sugar reduced a_w from 0.56 to 0.48, while maintaining the moisture content of the bar at 4.8% (wet basis) (from A.E. Staley, Krystar Application Bulletin, Number 4:88M504).

d. Determination of product stability and shelf life. Despite its thermodynamic limitations, water activity can be used for product stability and shelf life determinations. As introduced by Labuza *et al.* (1970), a water activity "map" can be used to predict what types of reactions (i.e., chemical, biochemical, physical, and microbial growth and toxin production) will occur in foods. Only a relative reaction rate is plotted versus a_w, as the actual rate is based on a kinetic phenomenon dependent on the specific food system and reaction being investigated. The combined water activity map (Figure 15) and (Table IV) provide a comprehensive and holistic way of

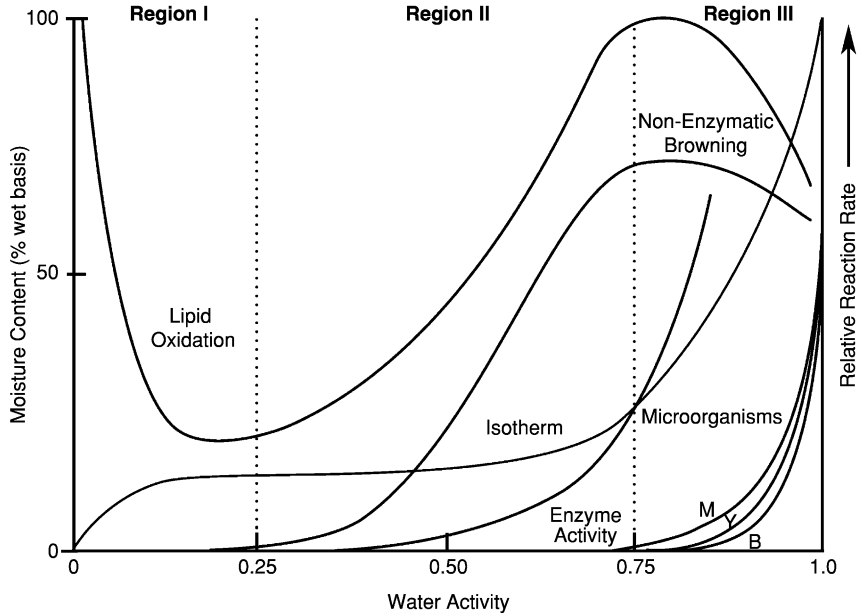

FIG. 15 A comprehensive "stability map" illustrating the general relationship between the occurrence of various reactions important in foods, as a function of water activity, superimposed on a sorption isotherm. M, mold; Y, yeast; B, bacteria. The isotherm is plotted as moisture content (left y axis) versus water activity, whereas all other curves are plotted as relative reaction rate (right *y* axis) versus water activity. Additional information corresponding to regions I, II, and III is given in Table IV.

TABLE IV
WATER ACTIVITY, MOISTURE CONTENT, RELATIVE STABILITY LEVEL, EXAMPLE PROCESSING, PRESERVATION AND PACKAGING TECHNOLOGIES, TEXTURAL ATTRIBUTES, AND EXAMPLE FOOD PRODUCTS CORRESPONDING TO EACH OF REGIONS I, II, AND III IN FIGURE 15

Characteristic	Region I	Region II	Region III
Water activity	0.0 to 0.25	0.25 to 0.75	0.75 to 1.0
Moisture content (%wb)[a]	Low (0 to 2.6%)	Intermediate (2.6 to 18%)	High (18 to 100%)
Relative stability level	High	Intermediate	Low to high, depending on technologies employed
Example processing, preservation, and packaging technologies	Dehydration, drying, extrusion	Concentration, chemical methods	Refrigeration, freezing, modified or controlled atmosphere packaging, pasteurization, canning, aseptic processing, fermentation, chemical methods
Textural attributes	Dry, hard, crisp, shrunken	Chewy, firm, flexible	Soft, juicy, moist, swollen
Example food products[b]	Snack foods, crisp cookies, some breakfast cereals	Some breakfast cereals, granola bars, soft cookies, raisins, some candy bars, IMF pet foods	Fresh fruits and vegetables, fresh meat, poultry, and fish, refrigerated dairy products, canned products

[a]Moisture content values estimated from the composite food isotherm (Figure 17) for 0.25 and 0.75 a_w values.
[b]See Figure 17 for additional product examples.

viewing the pervasive role water plays in foods, from relative stability levels to food processing techniques to textural attributes to example food products. Since its introduction in 1970, the a_w stability map has been referenced and/or reproduced in various forms thousands of times. However, the a_w stability map is not without its limitations. As pointed out by Karel *et al.* (1993), such maps do not always take into consideration the occurrence of phase transitions and time-dependent, nonequilibrium phenomena. Roos (1995) introduced a modified version of the a_w stability map, which is discussed in the glass transition section of this review.

Labuza *et al.* (1970) originally partitioned the stability map into three zones: zone I ranged from 0.0 to 0.25 a_w, zone II ranged from 0.25 to 0.80 a_w,

and zone III ranged from 0.80 to 1.0 a_w. Different reproductions of the map have subsequently used slightly different a_w partitioning values ($\pm$ 0.05) and some have included small range bars between the zones (e.g., Fennema, 1996; Rockland, 1987). Labuza (1984) also introduced an alternative isotherm partition scheme: dry foods 0.0 to 0.6 a_w, intermediate-moisture foods 0.60 to 0.92 a_w, and tissue foods greater than 0.92 a_w. Labuza pointed out that a_w does not begin to decrease much below 0.99 until the moisture content is reduced to about 1 g water/g solid or about 50% moisture content (wb).

Virtually all water containing foods can be categorized using the stability map/table scheme presented in Figure 15 and Table IV. For example, fresh meat (e.g., ground beef, chicken, pork) is located in zone III of the stability map, with an average moisture content of 73% and a_w of 0.98. Refrigeration and freezing are used to extend the shelf life of meat to days and months, respectively. Baked products, such as bread, are a bit more complicated. Bread can typically have a moisture content of approximately 36% and an a_w of 0.96 and is located in region III of the stability map. Baking, used to produce bread, decreases the moisture content of a bread dough, while chemical preservatives methods, such as the use of potassium sorbate as a mold inhibitor, are used to extend the shelf life of the bread from days to weeks.

Chirife and Buera (1996) have extensively reviewed the concerns about using water activity as a predictor of microbial viability and growth. One of those often-cited concerns is that the microbial response can differ at a particular a_w value, depending on the type of solute used (solute-specific effects). Such a solute-specific effect on the growth of *Staphylococcus aureus* is illustrated in Figure 16, where it can be seen that the minimum a_w value for growth is dependent on the solute system used to adjust water activity. However, as noted by Chirife (1994), although the minimum a_w value for growth is clearly dependent on the solute system used, *S. aureus* does not grow below the widely accepted minimum a_w value of 0.86. For different solutes, the variation in minimum a_w value for growth is related to two main effects: (1) the ability of the solute to decrease the a_w of the food medium and/or (2) the ability of the solute to exhibit specific antibacterial activities, including the ability to permeate the bacterial cell membrane (Chirife and Buera, 1996).

Chirife and Buera (1996) likened the solute-specific effect on a_w to that on pH. The solute effect on pH has not precluded the widespread usage of pH in food preservation. Rather, it is important to understand and quantify its limitations, but not discontinue its usage. For example, it is important to quantify the specific inhibitory effects of various food grade acids and to establish safe pH limits corresponding to the less inhibitory ones rather than

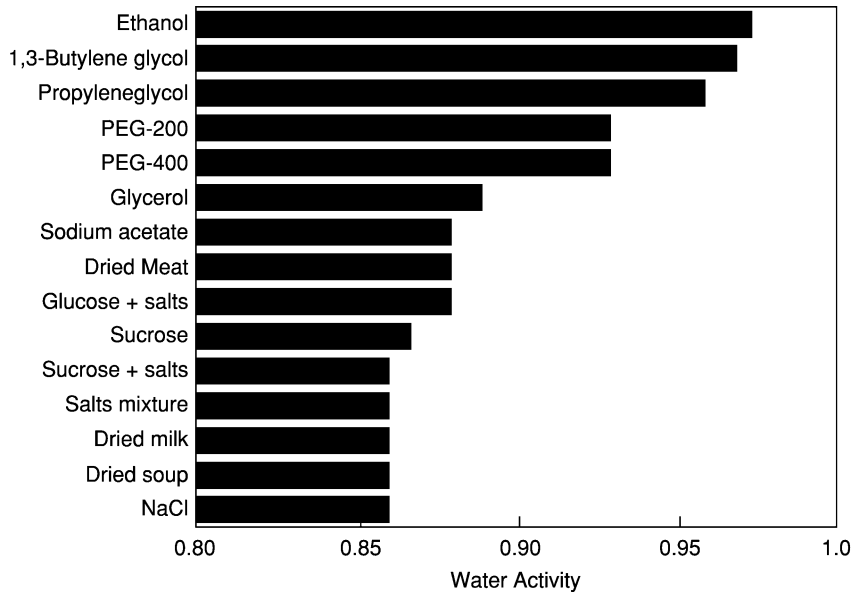

FIG. 16 Minimum a_w for growth of *Staphylococcus aureus* in specific solute systems at 30 to 37 °C (data from Chirife and Buera, 1996).

the most inhibitory ones. Chirife and Buera (1996) recommended the same approach used for pH for use with a_w values in foods. Another often-cited concern about using water activity for the prediction of microbial viability involves the nonequilibrium nature of the water activity parameter. However, Chirife and Buera (1996) argued that nonequilibrium effects are in many cases slow, i.e., slower than the shelf life of a food, and/or so small that they do not seriously detract from the use of the a_w concept as a predictor of microbial stability. Both concerns discussed earlier, regarding the validity of the a_w concept for use as a predictor of microbial viability, should not be overlooked, but rather carefully taken into account, along with other factors that affect viability (e.g., temperature, pH, oxygen level, and sample preparation and history). The cumulative effect of factors such as these on microbial viability is the basis of Hurdle technology proposed by Leistner (1987). Also, the use of other possible stability-predicting parameters, such as molecular mobility, should continue to be investigated.

e. Process design and control. Water activity and moisture sorption isotherms play important roles in the design, operation, and control of water-management unit operations, such as concentration, drying, osmotic

dehydration, freezing, freeze-concentration, freeze-drying, and reverse osmosis. For example, in drying by diffusion operations (e.g., air drying), the driving force for water removal is the difference between the vapor pressure of water at the surface of a food and the partial vapor pressure of water in the air. Thus, the drying rate depends on the a_w of a food throughout a drying process (Rahman, 1995).

5. *Measurement of water activity in foods*

A variety of measurement methods have been developed for determining the water activity of food materials and are well described in texts such as Rahman (1995), Wiederhold (1997), and Bell and Labuza (2000). In general, water activity is a relatively easy parameter to measure, which can be an advantage, especially for use in the food industry. Depending on the technique selected, the water activity of a food material can be measured in a time frame of minutes (e.g., electronic instrument). In addition, individuals can be trained, with a limited amount of instruction, to make water activity measurements. Consequently, when appropriate, water activity measurements can be made relatively quickly by personnel overseeing a manufacturing line for quality assurance purposes. Measurement protocols, such as calibration procedures and proper temperature control, should be implemented to assure the accuracy of online a_w measurements.

Two important, but often under emphasized, aspects of measuring a_w values and isotherms in foods are accuracy and repeatability. Variation in a_w and isotherm values can be due to inherent variation in biological materials, as well as differences in measurement methods, protocols, and equipment employed. Wolf *et al*. (1985) presented the results of a COST 90 Project on the standardization of saturated salt solution isotherm measurement methodology and Lewicki and Pomaranska-Lazuka (2003) discussed errors in the static desiccator method.

6. *Composite food sorption isotherm*

Typically, sorption isotherms are constructed for a single food ingredient or food system. An alternative approach is to plot the moisture content versus water activity (or relative vapor pressure) values for a variety of "as is" food ingredients and food systems. The result is a composite food isotherm (Figure 17). The composite isotherm fits the typical shape observed for a sorption isotherm for an individual food system, with a few products falling above or below the isotherm curve (chewing gum, honey, raisins, bread, and colby and cheddar cheeses). Slade and Levine (1991) were the first to construct such a plot using moisture content and a_w values from van den

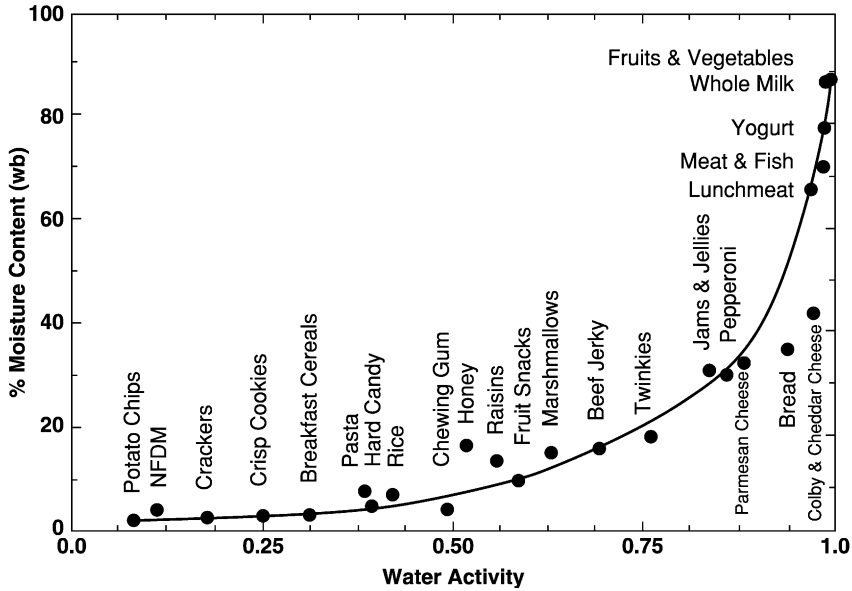

FIG. 17 Water activity (or relative vapor pressure) and moisture content (%, wb) values plotted for a variety of food materials (“as is”), resulting in a composite (or universal) food isotherm. Potato chip and nonfat dry milk (NFDM) data are from van den Berg (1986). All other data are from the author’s laboratory (at 20 or 25 ± 1 °C). Water activity and moisture content values for the breakfast cereal and fruit and vegetable categories had the largest ranges (expressed here as standard deviation): 0.311 ± 0.073 a_w and $2.94 \pm 1.55\%$ mc (wb) and 0.995 ± 0.004 a_w and $89.8 \pm 3.90\%$ mc (wb), respectively. The curve is to guide the eye—it is not a fitted line.

Berg (1986). An advanced version of the Slade and Levine (1991) plot is given later in this review (see Figure 35). Slade and Levine (1991) noted that the overall shape of the resulting curve resembled that of a typical sorption isotherm for a single food material, with a few exceptions (raisin, bread, and cheese; similar results are observed in Figure 17, with the addition of honey). Slade and Levine (1991) noted that raisins exhibit a lower a_w than expected for their moisture content. They attributed this anomalous behavior to desorption hysteresis, as raisins are produced by the dehydration of grapes. However, bread and cheese are produced by thermosetting processes, resulting in a relatively high a_w with a relatively low moisture content. Slade and Levine have subsequently published their isotherm, referring to it as a “universal sorption isotherm” (Slade and Levine, 1998, 2002). A similar plot is included in Walstra (2003), who used a log scale for the a_w axis. Walstra noted two exceptions in his plot. The first is a brine solution

(described as almost saturated with NaCl), and the second is high fat content foods such as cream and margarine. Skim milk and cream have the same aqueous phase, resulting in the same a_w, but different amounts of water. Thus, skim milk and cream have the same a_w, but cream has a lower moisture content compared to skim milk (e.g., 58% moisture content, wb, for heavy whipping cream and 91% moisture content, wb, for nonfat milk).

C. NUCLEAR MAGNETIC RESONANCE

Since the simultaneous discovery of nuclear magnetic resonance by Bloch at Stanford and Purcell at Harvard in 1946, NMR has been applied to countless problems and has benefited virtually every branch of science. Such a wide array of NMR methods exists that it is not possible to adequately describe or even mention all of them in this review. Thus, the approach taken here is to provide a brief section explaining basic NMR principles and to focus on the usefulness of NMR by providing selected examples of NMR techniques used to characterize the mobility of water and solids in food systems. In addition, some NMR techniques useful for determining the glass transition temperature are included in the glass transition section of this review. An excellent comprehensive overview of how to apply selected NMR methods to investigate specific food properties is given by Eads (1999). Eads (1999) links magnetic resonance observables to food analytical quantities, discusses the influence of sample complexity on magnetic resonance observables, and provides the reader with numerous spectroscopic strategies for defeating or embracing the effects of sample complexity. A more specific review by Schmidt (1999) focuses on the usefulness of various NMR techniques to examine the physical and sensory properties of food systems.

1. Principles of NMR

Anomalous to its low-frequency, long wavelength position in the electromagnetic spectrum (radio wave region; 10^9- to 10^3-Hz frequency range and 10^- to 3×10^7-cm wavelength range), NMR is associated with nuclear spin transitions (Belton, 1995). Atomic nuclei with an odd number of protons or neutrons possess a nonzero spin value (I), which can be thought of as being similar to the rotation of a charged nucleus. The strength and direction of the magnetic field surrounding each spinning nucleus can be described by a vector quantity known as the magnetic moment (μ_n), which can interact with a magnetic field. Thus, the first step common to all types of NMR experiments is that the sample to be analyzed is placed in a probe (containing a radio frequency coil), which is located in a strong externally applied magnetic field (B_0, in units of Tesla or T) (Figure 18). The torque exerted by B_0 on the

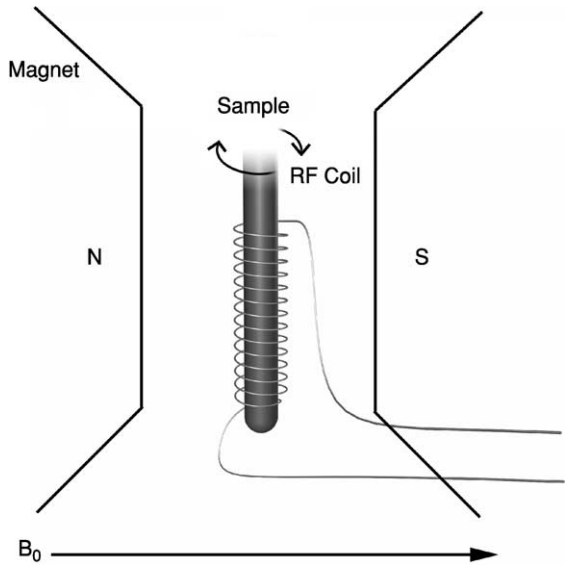

FIG. 18 Schematic representation of an NMR experiment. A sample is placed in a probe containing a radio frequency coil, which is located in a strong applied magnetic field, B_0. The coil is tuned to resonate at the frequency of the applied radio frequency field, B_1.

spinning nucleus causes precession of the magnetic moment (Figure 19), where the frequency of precession is proportional to the strength of B_0:

$$\omega_0 = \gamma B_0 \tag{9}$$

where ω_0 is the angular frequency in radians per second (also called the Larmor or resonance frequency) and γ is the magnetogyric ratio (rad $\text{Tesla}^{-1}\text{s}^{-1}$), which is a unique constant for each nucleus. The angular frequency can also be expressed in frequency units (s^{-1}, Hz), as $\nu = \omega_0/2\pi$:

$$\nu = \frac{\gamma B_0}{2\pi} \tag{10}$$

In the presence of B_0, nonzero spin nuclei adopt a specific number of orientations. The number of allowed orientations is dependent on the spin value and is equal to $(2\text{I} + 1)$. For the simplest case of $\text{I} = 1/2$, two orientations are allowed: one aligned parallel to B_0 and one antiparallel. Nuclei with $\text{I} > 1/2$ have a quadrupole moment (called quadrupolar nuclei) that allows them to interact with electric fields produced by neighboring nuclei and electrons.

Water has three stable nuclei that possess nonzero spin values: proton (^{1}H), deuterium (^{2}H), and oxygen-17 (^{17}O). The spin values and number of

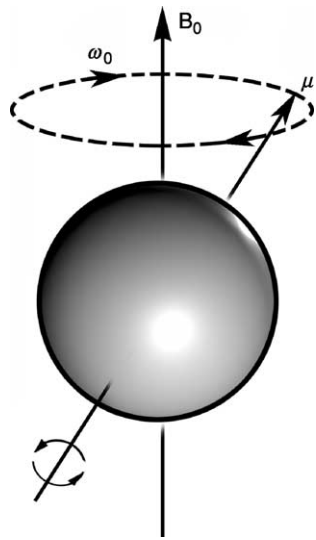

FIG. 19 An external magnetic field (B_0) applied to a nucleus causes the nucleus to precess at a frequency (ω_0) proportional to the strength of the magnetic field [Eq. (9)].

allowed orientations, as well as other NMR parameters, for the three NMR-active water nuclei are given in Table V. Each orientation has a different energy level, with the magnetic moments parallel to the applied magnetic field having slightly lower energy than those that are antiparallel, Figure 20 illustrates the energy difference, in the absence and presence of B_0, for ^{1}H nuclei, where I = 1/2. In the absence of B_0, magnetic nuclei are oriented randomly and all have the same energy level. In the presence of B_0, an excess of magnetic nuclei align parallel to B_0 and have a lower energy level than those that align antiparallel to B_0. The number of nuclei in the parallel and antiparallel positions is determined by the Boltzmann distribution [Eq. (11)]:

$$\frac{N_\alpha}{N_\beta} = e^{\Delta E/kT} \tag{11}$$

where N_α and N_β are the numbers of nuclei in the α (lower energy) and β (higher energy) positions, respectively, ΔE is the energy difference between the states and is equal to $h\nu$ (h is Planck's constant, 6.6×10^{-34} Js), k is the Boltzmann constant (1.38×10^{-23} JK^{-1}), and T is temperature (in K). There is a slight excess of parallel nuclei (N_α), which results in the creation of sample magnetization. The NMR spectrum is a measure of the energy required to cause a transition between energy levels and depends on the strength of B_0 (Belton, 1995). Typical NMR magnetic field strengths (0.2 to

TABLE V
PARAMETERS FOR THREE STABLE NMR-ACTIVE WATER NUCLEI[a]

Isotope	Spin value (I)	Natural abundance (%)	Number of allowed orientations	Gyromagnetic ratio (γ) (10^7 rad $T^{-1}s^{-1}$)	Relative sensitivity[b]	Frequency at 2.35 T (MHz)
^1H	1/2	99.98	2	26.75	1.00	300.000
^2H	1	1.5×10^{-2}	3	4.1	9.65×10^{-3}	15.351
^{17}O	5/2	3.7×10^{-2}	6	−3.6	2.91×10^{-2}	13.557

[a]From Kemp (1986).
[b]Sensitivity relative to proton. To calculate the absolute sensitivity, multiply by the natural abundance.

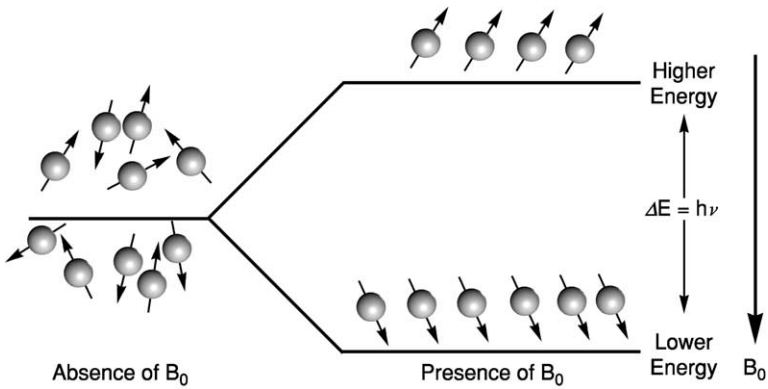

FIG. 20 Schematic illustration of magnetic nuclei, for the case of I = 1/2, in the absence and presence of B_0.

21 Tesla, which corresponds to ^1H resonance frequencies of 8.5 to 900 MHz, respectively) result in large differences in resonance frequency (see Table V for frequencies at $B_0 = 2.35$ T), making it possible to observe each NMR-active nucleus independently.

In a basic pulsed NMR experiment (for I = 1/2), when a sample is placed in the applied magnetic field (B_0), the nuclear spins distribute themselves between parallel and antiparallel positions, according to Boltzmann distribution [Eq. (11)] (Figure 21A). The number of spins in the parallel position is slightly greater than that in the antiparallel position. At equilibrium, the spins are precessing randomly (i.e., lack phase coherence). The populations

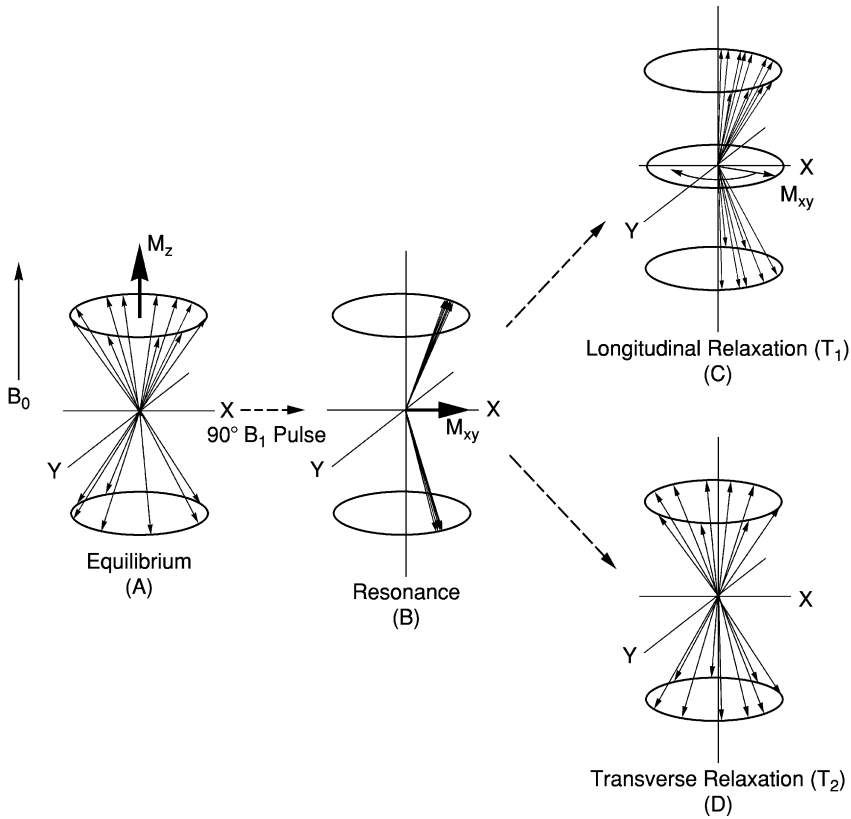

FIG. 21 Schematic illustration of the changes in spin states experienced by I = 1/2 nuclei during a basic NMR experiment. (A) In the presence of B_0, nuclear spins are distributed in parallel (lower energy) and antiparallel (higher energy) positions, according to the Boltzmann distribution [Eq. (11)]. The spins are precessing randomly (i.e., lack phase coherence). Net magnetization along the z axis (M_z) is at a maximum. (B) Immediately following application of a 90° B_1 pulse, the populations of parallel and antiparallel positions are equalized, and the spins precess in phase (i.e., exhibit phase coherence) at the Larmor frequency. The sample magnetization (M_{xy}) is at a maximum value. (C) The longitudinal relaxation process restores the equilibrium distribution of spins to the parallel and antiparallel positions. (D) The transverse relaxation process is a loss of phase coherence of the spins. Longitudinal and transverse relaxation processes occur simultaneously.

of parallel and antiparallel positions are equalized by the absorption of photons with energy equal to the difference in energy between the spin states (Figure 21B). This excitation energy is supplied to nuclei in a sample by an oscillating magnetic field (B_1) at right angles to B_0, through the coils of the

NMR probe, with a frequency equal to the Larmor frequency. In pulsed NMR, the excitation field is applied in a short pulse (or pulse sequence), usually of a few microseconds. Before the B_1 pulse is applied, the magnetic moments are out of phase with one another and the net magnetization lies along the z axis (M_z), and M_z is at a maximum value (Figure 21A); however, the net magnetization in the x–y plane (the signal detection plane) (M_{xy}) is zero. When the B_1 pulse is applied, the magnetic moments get in phase with one another (called phase coherence), and the sample magnetization precesses about B_1. The angle of precession (θ; called the flip or tip angle), which depends on the duration and strength of B_1, determines the magnitude of M_{xy}. For example, a flip angle of $\theta = 90°$ (or $2/\pi$) focuses the entire sample magnetization in the x–y plane, and M_{xy} is at a maximum value (Figure 21B).

Immediately after the 90° B_1 pulse is turned off, the sample magnetization returns to precessing about B_0. This process, referred to as relaxation, produces an electromotive force or voltage. Detection of the loss of energy (through the process of relaxation) occurs through the same coil used for excitation. As the magnetization relaxes, it contains both a longitudinal component (along the z axis; Figure 21C) and a transverse component (in the x–y plane; Figure 21D). The magnitude of the transverse relaxing signal, as a function of time [$M_y(t)$], is called the free induction decay (FID). The FID can be analyzed directly (as discussed later) or can be Fourier transformed from the time domain into the frequency domain, yielding an NMR spectrum. A great deal of chemical information (e.g., molecular structure and chemical analysis) can be extracted from an NMR spectrum, as each resonance peak provides fingerprint-like information, including position (called chemical shift, δ), area (or intensity), width, and multiplicity (called spin–spin or J coupling).

The decay of the longitudinal component is called longitudinal relaxation or spin–lattice relaxation and is characterized by a time constant T_1 (s) or a rate constant R_1 (s^{-1}), which equals $1/T_1$. The longitudinal relaxation process restores the equilibrium distribution of spins to the parallel (lower energy) and antiparallel (higher energy) positions (Figure 21C). Longitudinal relaxation occurs because of the existence of magnetic fields fluctuating at the correct frequency, which are able to induce transitions between the antiparallel and the parallel positions of the spins in the applied magnetic field. If these fluctuations are associated with a lattice, then exchange of energy can occur between the spin system (the nuclei being probed) and the lattice (the molecular assembly in which the spins are embedded). There are many physical processes that result in locally fluctuating magnetic fields. The most important such interaction in liquids is the dipole–dipole interaction. Additional relaxation mechanisms are mentioned in the next section.

Because the excitation/detection coil is in the x–y plane and the longitudinal component relaxes along the z axis, T_1 cannot be measured directly from an NMR spectrum, but must be obtained using a pulse sequence. The most commonly used pulse sequence to measure T_1 is an inversion recovery pulse sequence (Kemp, 1986). Other commonly used pulse sequences for measuring T_1 are given in Ernst *et al.* (1987).

The decay of the transverse component is called transverse relaxation (or spin–spin relaxation) and is characterized by a time constant T_2 (s) or a rate constant R_2 (s^{-1}), which equals $1/T_2$. The transverse relaxation process is a loss of phase coherence (dephasing) of the spins after an excitation pulse (B_1) due to differences in the magnetic field experienced by individual magnetic moments and to exchange of energy between identical nuclei (Figure 21D). These processes result in a loss of magnetization in the x–y plane. Magnetic field differences arise from two distinct sources: static magnetic field inhomogeneity (imperfections in B_0, minimized by shimming) and local magnetic fields arising from intramolecular and intermolecular interactions in a sample (true or genuine transverse relaxation). The total relaxation time constant, designated as T_2^*, is a combination of both sources:

$$\frac{1}{T_2^*} = \frac{1}{T_2} + \frac{1}{T_{2(\Delta B_0)}} \tag{12}$$

where T_2 refers to the contribution from the true relaxation process and $T_{2(\Delta B_0)}$ to that from field inhomogeneity (ΔB_0). $T_{2(\Delta B_0)}$ equals $1/\pi\gamma\Delta B_0$, where $\gamma\Delta B_0$ is the spread in frequencies caused by field inhomogeneity (Eads, 1998). For single exponential relaxation (i.e., Lorentzian line shape), T_2^* can be obtained from the line width of an NMR spectrum resonance at half-height ($\Delta\nu_{1/2}$):

$$T_2^* = \frac{1}{\pi\Delta\nu_{1/2}} \tag{13}$$

Measurement of a true T_2 can be obtained using a spin-echo pulse sequence, such as the Carr–Purcell–Meiboom–Gill (CPMG) sequence, which minimizes the loss of phase coherence caused by inhomogeneities (Kemp, 1986).

A parameter related to T_2 is $T_{1\rho}$, the rotating-frame relaxation time. To obtain $T_{1\rho}$, the equilibrium spin magnetization is first subjected to a 90° pulse, which rotates the equilibrium spin magnetization along the y axis. A spin-locking frequency field (amplitude $\omega_1 = \gamma B_1$) is immediately applied for a time, τ, along the y axis. The spin-locking field is then turned off and the resultant FID is recorded. A plot of the signal amplitude as a function of

the spin-locking time, τ, exhibits an exponential decay with time constant, $T_{1\rho}$. A discussion of the potential usefulness of $T_{1\rho}$ to probe the molecular dynamics of water is given by Hills (1998).

In addition to T_1 and T_2, which reflect the rotational motion of water, NMR can also be used to measure the translational motion of water. If an additional, relatively small (compared to B_0), steady magnetic field gradient is incorporated into a pulsed NMR experimental setup, a translational diffusion coefficient (D, m^2/s) can be measured (called pulsed field gradient NMR).

Up to this point, water mobility values obtained are average values for an entire sample. However, if magnetic field gradients in the *x, y*, and *z* directions are incorporated into a pulsed NMR experimental setup, the spatial distribution aspects of water mobility (T_1, T_2, and D) can also be measured via the use of magnetic resonance imaging (MRI) techniques.

A vast number of NMR experiments can be devised using the basic NMR principles presented earlier. Eads (1999) organized all the possible NMR experiments into five classes (Table VI). The forms of data for each class, as well as references for additional study, are included in Table VI.

TABLE VI
CLASSES OF MAGNETIC RESONANCE MEASUREMENTS ADAPTED FROM EADS (1999)

Class	Forms of data	References
NMR relaxometry	Free induction decay (T_2*) or solid echo Spin echo decay (T_2) Magnetization recovery curve (T_1)	Eads (1998)
NMR diffusometry	Decay of spin echoes in the presence of a magnetic field gradient (echo attenuation curve)	Price (1996, 1997, 1998a)
High-resolution liquid and solid NMR spectroscopy	One- or two-dimensional NMR spectra	Claridge (1999); Harris (2001)
NMR imaging	Images (one-, two-, or three-dimensional array of voxel intensities) pixel-specific relaxation curves; maps, and movies (i.e., density, T_1, T_2, or D weighted)	Hills (1998); McCarthy (1994); Price (1998b)
Volume-localized NMR spectroscopy	NMR spectrum from voxel of interest	Eads (1999)

2. Connecting relaxation and mobility

NMR spin relaxation is not a spontaneous process, it requires stimulation by a suitable fluctuating field to induce an appropriate spin transition to reestablish equilibrium magnetization. There are four main mechanisms for obtaining relaxation: dipole–dipole (most significant relaxation mechanism for $I = 1/2$ nuclei), chemical shift anisotropy, spin rotation, and quadrupolar (most significant relaxation mechanism for $I > 1/2$ nuclei) (Claridge, 1999).

Both T_2 and T_1 relaxation times are coupled to molecular mobility, but the specifics of their relationship are different and vary depending on the nucleus being probed (Belton, 1995; Campbell and Dwek, 1984; Eads, 1998). In the simplest case of relaxation in a single proton pool (e.g., pure water), each water proton experiences a randomly fluctuating local magnetic field due to transient dipolar interactions with other water protons as water molecules rotate and translate (via Brownian motion). Fluctuating fields at an appropriate frequency (the Larmor frequency, ω_0) are able to induce transitions between antiparallel and parallel spin states, resulting in longitudinal relaxation. Hills (1998) and Claridge (1999) give details of the relationship between the rate of relaxation and the amplitude and frequency of fluctuating fields.

A schematic illustration of the dependence of T_1 on molecular rotational correlation time, τ_c (the average time taken for molecule to rotate through one radian), is shown in Figure 22. The dependence of T_1 on mobility shows a minimum, when $\tau_c = 1/\omega_0$ (or the product $\omega_0\tau_c = 1$). When $\tau_c \ll 1/\omega_0$, the system is in an extreme narrowing limit (also called a motionally narrowed regime), and when $\tau_c \gg 1/\omega_0$, the system is in a slow motion regime and T_1 is again large. Thus, it is possible to obtain T_1 values of equal magnitude for both liquid and solid domains, as well as for high and low temperatures.

Figure 23 illustrates the T_2 relaxation behavior of the three major mobility domains in foods—liquid, viscous liquid, and solid (crystalline and glassy). ^{1}H T_2 relaxation time values typically observed in these domains, as well as ^{1}H T_2 values specific for water in liquid and crystalline solid domains, are also given in Figure 22. The difference in T_2 relaxation behavior between liquids and solids is very dramatic and is the basis for using NMR for determining water content (Schmidt, 1991) and solid fat content (Gribnau, 1992). The dependence of T_2 relaxation on molecular correlation time is also illustrated in Figure 22. In the extreme narrowing limit, $T_2 = T_1$, whereas in the slow motion regime, T_1 becomes much longer than T_2. In general, based on Figure 22, shorter T_2 values mean less mobility.

NMR relaxation time measurements (T_1 and T_2) can provide valuable information for investigating the molecular dynamics of water in food systems. However, a number of factors can seriously complicate the analysis

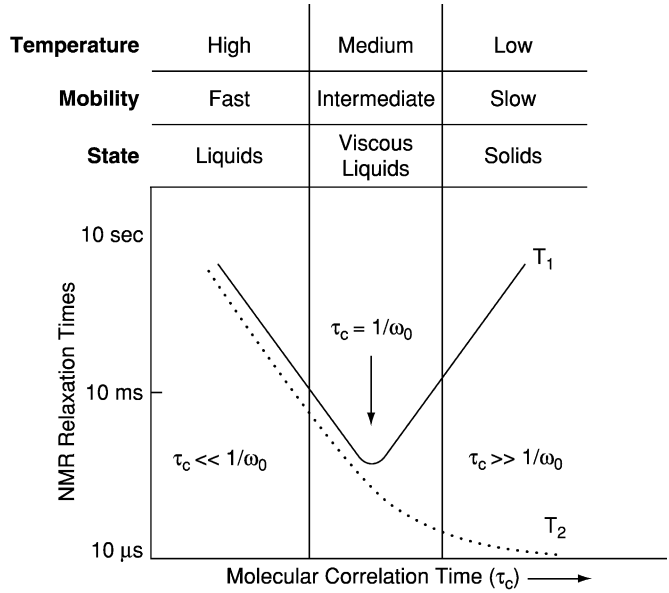

FIG. 22 A schematic illustration of the dependence of NMR relaxation times T_1 and T_2 on the molecular correlation time, τ_c, characterizing molecular mobility in a single-component system. Both slow and fast motions are effective for T_2 relaxation, but only fast motions near ω_0 are effective in T_1 relaxation.

and quantitative interpretation of the relaxation behavior of water, such as the presence of additional relaxation pathways, the water nucleus chosen, and the complex nature of most food systems. Additional pathways contributing to relaxation are discussed in detail by Belton (1990) and Eads (1999) and include (1) chemical exchange–physical exchange of protons between water and exchangeable solute protons, such as hydroxyl, amine, and carboxyl groups within homogeneous regions (also called proton exchange) (affects both T_1 and T_2); (2) diffusion exchange–physical movement between spatially separate regions (affects both T_1 and T_2); (3) cross-relaxation–transfer of z magnetization between spin states having different T_1 values (also called magnetization exchange or magnetization transfer) (affects T_1); and (4) paramagnetic relaxation–interaction of nuclear spins with unpaired electrons; occurs in the presence of paramagnetic species, such as iron, manganese, and dissolved oxygen (affects T_1 and T_2).

The water nucleus chosen also has an impact on relaxation data. Proton relaxation is affected by chemical exchange and cross-relaxation, ^{2}H by chemical exchange, and ^{17}O by proton-exchange broadening (scalar spin–spin coupling between ^{1}H and ^{17}O nuclei; affects T_2, but not T_1) (Glasel,

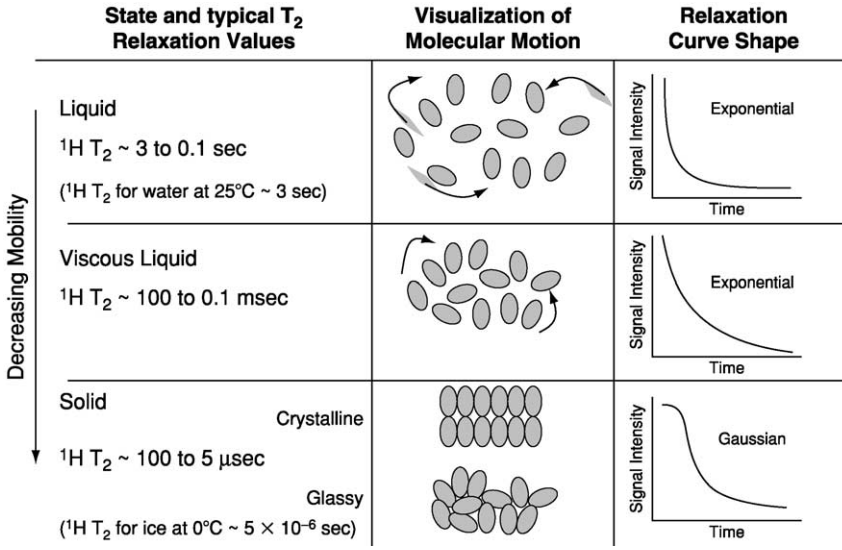

FIG. 23 A schematic illustration of the molecular motions and associated T_2 relaxation curve behavior for the three major domains in foods—liquid, viscous liquid, and solid (crystalline and glassy). Typical ^{1}H T_2 NMR relaxation time values observed in these domains, and values specific for water in liquid and crystalline domains, are listed.

1972; Halle and Karlstrom, 1983a,b). The effects of ^{17}O proton-exchange broadening can be eliminated by proton decoupling (Richardson, 1989). Deuterium and ^{17}O are quadrupolar nuclei ($I > 1/2$) and are not affected by magnetization transfer because quadrupolar relaxation is already very efficient, and these nuclei intrinsically possess weak dipolar interactions (Belton, 1990). The effects of spatial (or structural), compositional, and dynamical complexity of foods on relaxation time measurements are discussed in detail by Eads (1999). Because of the aforementioned complications, quantitative interpretation of T_2 and T_1 relaxation time measurements for water in foods often requires nucleus- and system-specific, sophisticated and detailed analysis and modeling (Belton, 1995). For the interested reader, Hills (1998) presents a comprehensive overview of water proton relaxation, ranging from that in dilute (solutions and gels) to more concentrated (rubbers and glasses) model food systems.

3. Distance and timescales involved in NMR

As discussed previously, foods display an enormous range of compositional, structural, and dynamical complexity. The structural complexity of foods can extend over distance scales ranging from subatomic to macroscopic.

Figure 24, presented originally by Belton (1995), illustrates the enormous range in distance scales that can be probed using various magnetic resonance spectroscopy and imaging techniques. Approximate distance ranges for molecular, microscopic, and macroscopic regions are provided for perspective on the left side of Figure 24. The criterion used for the demarcation between macroscopic and microscopic regions was based on the size of objects that are no longer visible with the naked or unaided eye, i.e., less than 40 μm (Hills, 1998).

Shortest-range interactions (over molecular distances of up to a few bonds away) examined by magnetic resonance are those that cause effects such as chemical shift, spin–spin coupling (also called scalar or "J"

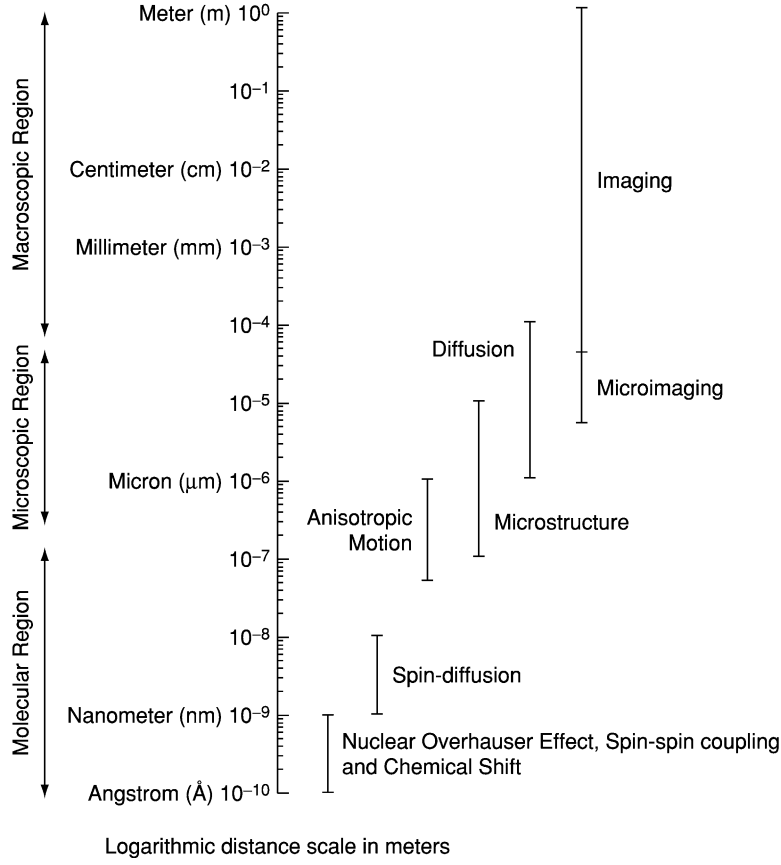

FIG. 24 The range of distance scales, from molecular to macroscopic, probed in NMR. See text for details.

coupling), and nuclear Overhauser. Chemical shift and spin–spin coupling effects occur through the electrons of chemical bonds, whereas the nuclear Overhauser effect (NOE) occurs through space. These effects form the foundation for why NMR is considered the premier structure identification tool. Somewhat larger distance scale information can be gleaned by considering the rate at which NOEs grow between spins (referred to as spin diffusion). Distance scales over which anisotropic order persists in oriented systems, such as muscle, can be calculated by combining information about the size of a residual anisotropic interaction with knowledge of translational motion values (Belton, 1995). Microstructural features of food materials, such as water and oil droplet sizes in food emulsions (Metais and Mariette, 2003; van Duynhoven *et al*., 2002), can be probed using relaxometery and diffusion techniques (Hills, 1998). Distance traveled by a molecule (e.g., water) diffusing through a food matrix (e.g., sugar glass) over time can be measured, and in turn can be used to explore the morphology of a system (e.g., restricted versus unrestricted diffusion). At the largest end of the distance scale are magnetic resonance microscopy and imaging techniques. NMR microscopy is defined by Hills (1998) as pertaining to a system in which one or more of the spatial voxel dimensions is less than 40 μm.

Because distance and time can be coupled by motion, we could also view the timescales available to be probed with NMR and would find the same staggering range (Belton, 1995). Time constants for molecular processes can be quantified by magnetic resonance techniques ranging from extremely fast (picoseconds, such as for the tumbling of water molecules) to extremely slow (tens of seconds, such as for selected chemical reactions or exchange).

4. Usefulness of NMR methods for foods

NMR is an incredibly versatile tool that can be used for a wide array of applications, including determination of molecular structure, monitoring of molecular dynamics, chemical analysis, and imaging. NMR has found broad application in the food science and food processing areas (Belton *et al*., 1993, 1995, 1999; Colquhoun and Goodfellow, 1994; Eads, 1999; Gil *et al*., 1996; Hills, 1998; O'Brien, 1992; Schmidt *et al*., 1996; Webb *et al*., 1995, 2001). The ability of NMR to quantify food properties and their spatiotemporal variation in a nondestructive, noninvasive manner is especially useful. In turn, these properties can then be related to the safety, stability, and quality of a food (Eads, 1999). Because food materials are transparent to the radio frequency electromagnetic radiation required in an NMR experiment, NMR can be used to probe virtually any type of food sample, from liquids, such as beverages, oils, and broth, to semisolids, such as cheese, mayonnaise, and bread, to solids, such as flour, powdered drink mixes, and potato chips.

Intact, "as is" food materials can be placed directly into NMR tubes for analysis. Thus, little to no sample preparation is needed beyond shaping the sample (when necessary) to fit into the bore of the magnet. In addition, it is possible to simulate various food processes (e.g., drying, freezing, microwaving, and frying) inside an NMR magnet and obtain real-time or near real-time measurements. NMR imaging has been especially useful in this regard (Duce and Hall, 1995; Hills, 1995, 1998, 1999; McCarthy, 1994; Schmidt *et al*., 1996; Sun and Schmidt, 1995). Sample size is limited only by the size of an NMR probe, which currently ranges from 0.1 to 2.5×10^5 cm^3, depending on the type of instrument employed (i.e., high-resolution spectrometer to an imaging spectrometer). Advances in NMR and MRI instrumentation, techniques, and applications are developing at an incredibly rapid rate, as discussed in Grant and Harris (2002). Many of these advances are just waiting to be applied by the insightful and ingenious food-focused researcher to further advance the study of water and solids in foods.

Because of the vast amount of information that has been published on the use of NMR to investigate food systems, it is not feasible to present a comprehensive survey of the usefulness of NMR for foods in this review. Rather, the approach taken here is to illustrate the usefulness of NMR specifically for probing water and solids mobility in foods by presenting selected papers from recent literature. Review papers and recent developments in each of the following areas are also included.

a. Molecular dynamics in concentrated sugar solutions and glasses. Hills *et al*. (2001) studied the molecular dynamics of water and sugars (sucrose and xylose) in concentrated sugar solutions and glasses above and below their glass transition temperatures. Extending previous studies on maltose (Hills and Pardoe, 1995) and saturated sucrose solutions (Hills *et al*., 1998), the approach taken was to use fast-field cycling measurements of the frequency dispersion in proton longitudinal relaxation. Reviews of applications of field-cycling NMR are given by Noack *et al*. (1997) and Belton and Wang (2001). In concentrated sucrose–water solutions well above T_g, proton frequency dispersion curves (R_1 plotted as a function of frequency) could be fitted to a single dispersion, conforming quite well to theoretical predictions. The main dispersion arises from sucrose (either the overall sucrose reorientation or from rotation of CH_2OH side chains or both), not from water. The sucrose correlation time for a 51% (w/w) sucrose solution at 298 K was calculated to be 20 ns (Hills *et al*., 2001). In concentrated sucrose–water systems well below T_g [90.1% (w/w) sucrose at 230.9 K; $T_g = 261.5$ K], a double dispersion was observed, again conforming quite well to theoretical predictions. This double dispersion strongly suggests that there are separate dispersive contributions from water and sucrose molecules. The water and

sucrose correlation times for the 90.1% (w/w) sucrose sample as a function of temperature are listed in Table VII. As can be observed, the water correlation time remains short, even in the glassy state (138 ns at 230.9 K). Hills *et al.* (2001) suggested that the systematic decrease in the correlation time for water as temperature decreases is perhaps due to an increasing decoupling of water and sucrose dynamics, as the system heads toward the glassy state. The water correlation times show no obvious break, as the temperature is lowered through the glass transition.

Sugar lattice dynamics were investigated using 100% xylose glasses in their protonated and deuterated forms. Dispersions for a 100% xylose deuterated glass (containing no water protons and no side chains) in the glassy state ($T_g = 282$ K) were able to be fitted with a single dispersion and a quadrupolar peak. This indicates that the observed dispersion arises from low-frequency vibrational modes in the three-dimensional xylose lattice. Fitting dispersion data with a stretched spectral density function yielded a single correlation time of 1.5 μs, thus showing no evidence for a distribution of correlation times corresponding to a range of amorphous environments that might have been expected to exist in the glassy matrix. The combination of NMR field-cycling and deuterium exchange was shown to be a powerful technique for investigating molecular dynamics both above and below T_g.

The composite picture that is developing [based mainly on NMR mobility and differential scanning calorimetery (DSC) T_g data] of these sugar–water glasses at temperatures below T_g is that the sugar is irrotationally frozen in a rigid three-dimensional amorphous matrix. The sugar molecules exhibit vibrational motion and experience a gradual relaxation (physical aging) toward equilibrium. The water and sugar dynamics are decoupled from one another in the glassy state. The water in the glassy system exhibits vibrational, rotational, and translational motions, albeit at rates much slower than in bulk water.

TABLE VII

TEMPERATURE DEPENDENCE OF WATER AND SUCROSE CORRELATION TIMES IN A 90.1% (W/W) SUCROSE–WATER SYSTEM ($T_g = 261.5$ K)

Temperature (K)	Water correlation time (ns)	Sucrose correlation time (ns)
298.0	265	732
268.7	202	1331
261.1	148	1299
230.9	138	1493

Other studies that have focused on mobility in sugar–water systems at or near the glass transition include Wachner and Jeffrey (1999), van den Dries *et al.* (1998, 2000a,b), and Sherwin *et al.* (2002). Wachner and Jeffrey (1999) used two-dimensional deuterium NMR to investigate reorientational dynamics in an 85% glucose–15% water system. They reported that reorientation is dominated by small-angle jumps (~3°) and a small fraction of large-angle jumps (~34°). van den Dries *et al.* (1998, 2000a,b) studied various carbohydrate glasses (maltose, glucose, and malto-oligomers) using ^{1}H NMR, DSC, electron spin resonance (ESR) spectroscopy, and Fourier transform infrared (FTIR) spectroscopy. van den Dries *et al.* (2000b) reported that increasing water content from 10 to 30% (wt%) results in a decrease in spin probe (TEMPOL) mobility at T_g, whereas water mobility as measured by ^{1}H NMR increases at T_g. They explain this apparent paradox in terms of molecular packing. Sherwin *et al.* (2002) used solid-state techniques of cross-polarization/magic-angle spinning (CP/MAS) NMR to determine the mobility of glucose within a caseinate model system as a function of water activity (0.11, 0.33, 0.43, and 0.65), temperature (25, 35, 45 °C), and added humectants (glycerol and sorbitol). They reported that glycerol yielded the lowest T_g over the entire range of a_w values and imparted the greatest mobility to solid-state glucose, followed by sorbitol and finally the control formula containing no humecant.

b. Water distribution and dynamics in native starch granules. Tang *et al.* (2000) studied the microscopic distribution and dynamics state of water within native maize (A type), potato (B type), and pea (C type—a combination of A and B types) starch granules using NMR relaxometry and diffusometry. The distribution of water proton transverse relaxation times for a water-saturated, packed bed of native potato starch granules at two temperatures is shown in Figure 25. For both temperatures, the small intensity peak centered at approximately 3 s was assigned to residual supernatant bulk water (the majority of which was removed before measurements were made). The difficult assignments in the relaxation time distribution were the two peaks centered at approximately 8 and 50 ms at 290 K. The 50-ms relaxation time peak was assigned to bulk water in external interstitial spaces between the granules. This assignment implies that extragranular water exists as a thin layer between closely packed granules and that its relatively short relaxation time of 50 ms (compared to 3 s for free bulk water) was caused by fast proton exchange with starch hydroxyl protons. At 290 K, the 8-ms relaxation peak with a shoulder resolved into two separate peaks at 1 and 8 ms at 277 K. The 1 and 8-ms peaks were assigned to water inside granules.

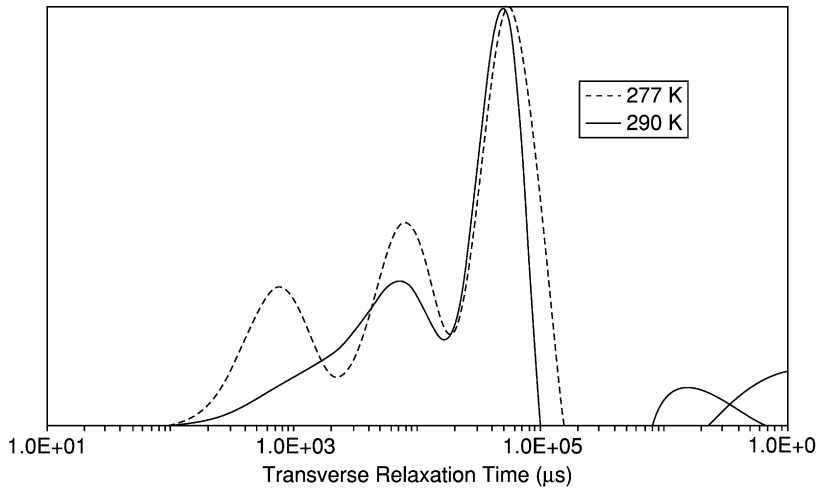

FIG. 25 The distribution of water proton transverse relaxation times for a water-saturated, packed bed of potato starch granules at two temperatures [reproduced with permission from Tang *et al*. (2000)].

Based on additional freezing and drying experiments, in addition to extragranular water (with a water proton transverse relaxation time of about 50 ms), Tang *et al*. (2000) identified three water populations inside native potato starch granules: (1) water in amorphous growth rings, (2) water in semicrystalline lamellae, and (3) water located in hexagonal channels within B type amylopectin crystals (called channel water). Water populations 1 and 2 above were found to be orientationally disordered and exchanging with each other on a millisecond time scale at 290 K. NMR diffusometry showed that water in packed granule beds undergoes translational diffusion in a two-dimensional space, either in thin layers between granules and/or in amorphous growth rings within granules. So-called channel water was characterized by a 1-kHz deuterium doublet splitting and was found to be in slow exchange with water in the other compartments on an NMR timescale. For the smaller maize granules, there was no evidence for the existence of channel water and all intragranule water populations were in fast exchange. For pea starch, NMR water proton and deuterium data showed composite A and B type starch behavior. For the interested reader, Tang and Hills (2001) also discuss the microscopic distribution of water among various subgranular compartments of native starches.

Other research using NMR techniques to study mobility in starch systems includes Li *et al*. (1998), who investigated the mobility of "unfreezable" and "freezable" water in waxy cornstarch using ^{1}H and ^{2}H NMR; Choi and Kerr

(2003a,b), who probed molecular mobility in regular and chemically modified wheat starch using ^{1}H NMR; Gonera and Cornillion (2002), who examined the effect of additives (guar gum, xanthan, glucose, and sucrose) on starch (corn, waxy maize, and potato) gelatinization using ^{1}H NMR relaxometry; and McCarthy *et al.* (2002), who monitored postcooking changes in moisture distribution over time in lasagna pasta.

c. Determination of self-diffusion coefficients in casein dispersions and gels. Mariette *et al.* (2002) used ^{1}H diffusometry to measure the self-diffusion coefficients of water and casein in casein solutions and gels. In the case of water self-diffusion measurements, they found that the water self-diffusion coefficient was insensitive to the structure of the casein whether in solution (Na-caseinate and micellar casein) or in a gelled state (acid gels and rennet gels). Figure 26 illustrates this observation, showing no difference between the water self-diffusion coefficients in a micellar casein dispersion (similar to Na-caseinate data, not shown) and in acid and rennet gels, throughout the protein concentration range investigated. The effect of casein concentration on the water self-diffusion coefficient was explained by obstruction from the casein molecule. In the case of protein self-diffusion measurements, researchers calculated an average casein self-diffusion coefficient of 3.4×10^{-12} m^2s^{-1} for a concentration of 0.08 g protein/g water. They noted that a large deviation from linearity was observed in an echo attenuation plot for a casein dispersion. However, they attributed this nonlinearity mainly to an effect of micelle size distribution and secondarily to the presence of a small amount of noncasein protein rather than to restricted diffusion behavior. For an overview of diffusion measurements by NMR and

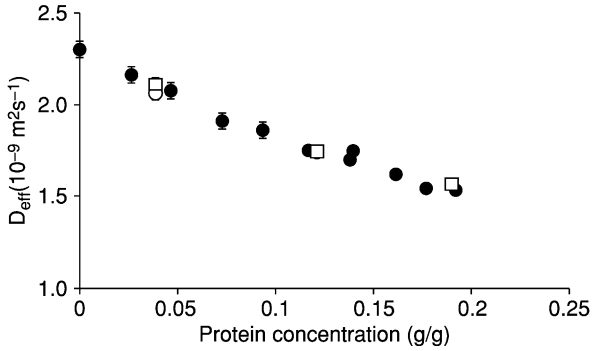

FIG. 26 Observed water self-diffusion coefficients as a function of the protein concentration (g protein/g water) for micellar casein dispersions (●), for acid gels (○), and for rennet gels (□) [reproduced with permission from Mariette *et al.* (2002)].

their applications, the interested reader is referred to excellent reviews by Price (1996, 1997, 1998a) and a special issue on NMR and diffusion in *Magnetic Resonance in Chemistry* (Morris, 2002a). The latter includes a very good discussion by Sorland and Aksnes (2002) on artifacts and pitfalls in NMR diffusion measurements.

Diffusion-ordered NMR spectroscopy (DOSY), a relatively recent adaptation of pulsed-field gradient spin–echo NMR, can be used to separate the NMR signals of different components of a mixture on the basis of their diffusion characteristics (Morris, 2002b). The first step in such an experiment is to obtain spectra attenuated by diffusion. Next, a diffusion coefficient and an estimated standard error are calculated for each resolved signal in the spectrum. A two-dimensional DOSY spectrum is then synthesized, in which the one-dimensional spectrum is extended into a second, diffusion domain (Pelta *et al.*, 2002). DOSY experiments employ a variety of pulse sequences, mainly variants of a pulsed-field gradient-stimulated echo (PFGSTE) sequence. A new one-shot sequence for high-resolution DOSY was introduced by Pelta *et al.* (2002), which allows data acquisition times of less than 1 min.

For examples of applications of DOSY, the reader is referred to Morris and Johnson (1993), Chen *et al.* (1995), Olson (1999), and Sobolev *et al.* (2003). Most relevant to the focus of this review is Olson (1999), who applied DOSY to investigate changes in water diffusion coefficients in gelatinized dent corn starch–water systems during retrogradation. Preliminary two-dimensional DOSY spectra revealed a distribution of water diffusion coefficients in retrograding starch gels, which increased as a function of both increasing starch concentration and time.

d. Measurement of solids mobility in low and high concentration solids systems. Low starch concentrations are used in a wide variety of food products, such as salad dressings, gravy mixes, and condiments. However, it is difficult with traditional solids techniques to probe changes in mobility (i.e., as affected by processing or as a function of storage time) of solid components. Cross-relaxation spectroscopy (CRS) allows for the observation of solids mobility at low solids concentrations, and the ability to monitor liquid properties independent of interference from solids. Lewen *et al.* (2003) employed cross-relaxation NMR to measure the mobility of water and solids in low starch concentration gels (5 to 25%). Parameters obtained from their CRS experiment were rate of magnetization transfer (R), solid transverse relaxation time constant (T_{2B}), liquid longitudinal relaxation time constant (T_{1A}), liquid transverse relaxation time constant (T_{2A}), and the number of solid protons that participate in cross-relaxation (M_0^B). As starch gels aged over a 29-day period (at 23 °C), it was found that T_{2B} did not change significantly, whereas M_0^B increased for each starch gel

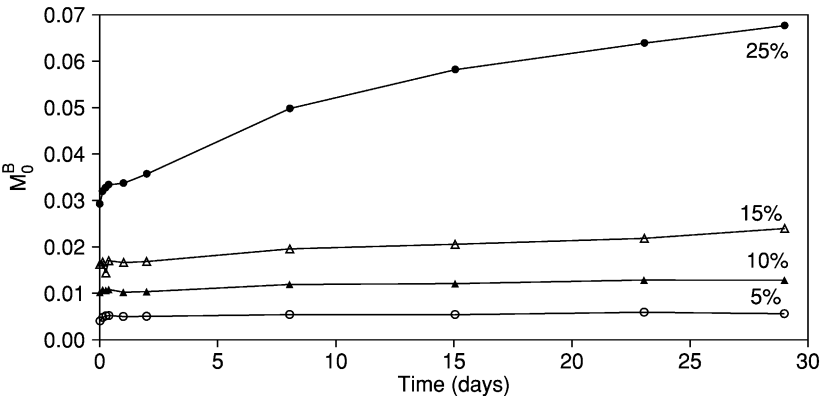

FIG. 27 Plot of $M_0{}^B$ for the 5 to 25% starch gel samples over a 29-day period after gelatinization [reproduced with permission from Lewen *et al.* (2003)].

concentration. Results for M_0^B are reproduced in Figure 27. These CRS results suggest that during retrogradation in low concentration starch systems, the highly mobile starch fraction converted to the less mobile solid state (increase in M_0^B), due to reassociation of starch molecules, but that the mobility of the solid component (constant T_{2B}) did not change over time.

Roudaut *et al.* (1999a) used low-frequency pulsed-proton NMR and dielectric dynamic mechanical spectroscopies to study molecular mobility in glassy bread (<9%) as a function of temperature. Based on NMR results, they reported that some (if not all) of the water molecules were much more mobile than the polymer matrix whose relaxation time could not be measured within the 20-μs dead time of the RF probe.

Magnetic resonance imaging techniques, such as stray field (STRAFI), single-point imaging (SPI), and single-point ramped imaging with T_1 enhancement (SPRITE), have been developed to obtain "solid-state" images for high concentration solids systems (Balcom *et al.*, 1996; Chudek and Hunter, 2002; Cornillon and Salim, 2000; Eads and Axelson, 1995). These techniques offer great potential for imaging the processing of low-moisture food systems, such as crackers, cookies, and snack foods. In addition, Eads and Axelson (1995) gave an example of using SPI to produce a mobility map for solid domains in a dilute particle gel of starch crystallites. Lee *et al.* (2002) used SPRITE (a refinement of SPI) to investigate the spatial distribution of nonfrozen water in beef, orange juice, and dough during freezing and frozen storage. Ziegler *et al.* (2003) used SPRITE to study moisture migration during the drying of starch-molded confectionery. Moisture profiles

within a porous bed of molding starch, where total proton density is low and T_2^* is quite short, were visualized using SPRITE. Similar images were not possible to obtain using more traditional spin–echo techniques.

e. Relationship between water and solids mobility and chemical and microbial stability. Kou *et al.* (1999) investigated the relationship between water and solids mobility and conidia mold germination. Water activity, a suite of NMR techniques, including ^{2}H NMR rotational mobility (R_1, R_2, and R_2^*), ^{1}H NMR translational mobility (water self-diffusion coefficient, D), and ^{13}C CP/MAS NMR ($T_{1\rho}$) solids mobility, and DSC were used to fully characterize water and solids mobility and T_g of the systems. Water content, a_w, and ^{2}H NMR R_1 and R_2 relaxation rates were found not to predict mold germination time. These workers concluded that the self-diffusion coefficient (translational mobility of water), DSC T_g (overall system mobility), and, to a more limited extent, ^{2}H NMR R_2^* relaxation rate and ^{13}C $T_{1\rho}$ (solids mobility) could provide alternative measures to augment a_w for predicting food stability and safety. Figure 28 shows water self-diffusion coefficient (D) as a function of weight fraction of solids for samples of sucrose, instant dent #1 starch, and a 1:1 sucrose/starch mixture. For starch and the sucrose/starch mixture, D decreased almost 10-fold near the corresponding weight fraction

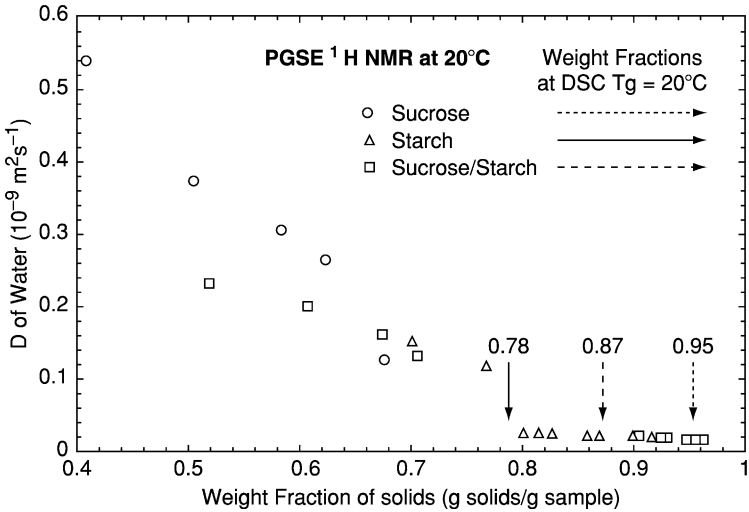

FIG. 28 Water self-diffusion coefficient plotted as a function of weight fraction of solids for samples of sucrose, instant #1 dent starch, and a 1:1 sucrose/starch mixture at 20 °C. The corresponding weight fractions at the DSC T_g equal to 20 °C are given for reference [reproduced with permission from Kou *et al.* (1999)].

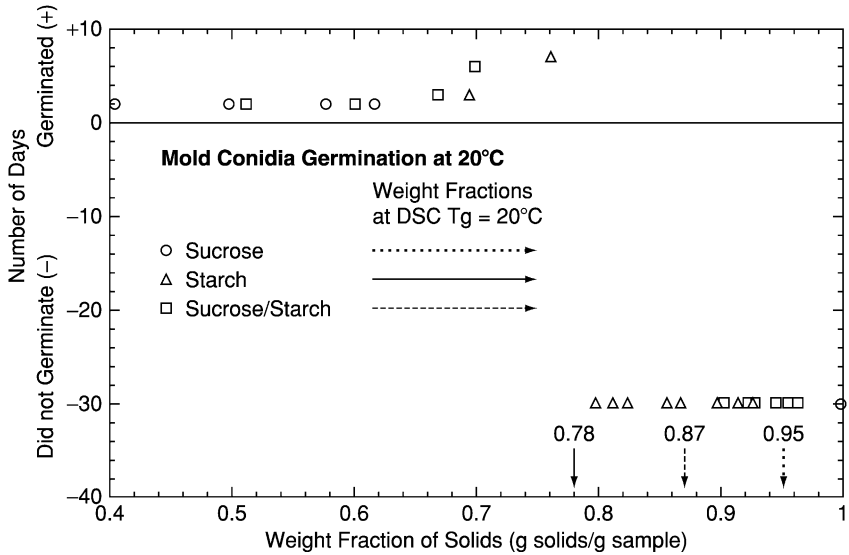

FIG. 29 *Aspergillus niger* conidia germination time as a function of weight fraction of solids at 20 °C for samples of sucrose, instant #1 dent starch, and a 1:1 sucrose/starch mixture. The corresponding weight fractions at the DSC T_g equal to 20 °C are given for reference. Conidia that did not germinate after 30 days were plotted on the graph as "did not germinate (−30 days)" [reproduced with permission from Kou *et al.* (1999)].

at which the DSC T_g was equal to 20 °C (the experimental temperature). Samples with D lower than this substantially reduced D no longer supported conidia mold germination, as shown in Figure 29. For sucrose, only samples with $a_w > 0.866$ were measured, as sucrose below this saturation a_w value (at 20 °C) remained in crystalline form.

Bell *et al.* (2002) investigated the relationship between water mobility as measured by oxygen-17 NMR (transverse relaxation rate obtained from linewidth at half-height) and chemical stability in glassy and rubbery polyvinylpyrrolidone (PVP) systems. Reported results suggest that water mobility in PVP model systems was not related to T_g. The study did not find a link between water mobility and reaction kinetics data (half-lives) for degradation of aspartame, loss of thiamin and glycine, and stability of invertase.

5. *Measurements utilizing NMR techniques for foods*

As described previously, there are a number of significant advantages to using NMR to examine food systems, such as the noninvasive and nondestructive nature of the technique, the limitless types of food samples that can

be probed, the ease of sample preparation, and the numerous pulse sequences and methods that can be employed to either embrace or overcome sample complexity. However, along with the bountiful advantages of NMR come three general disadvantages: (1) poor sensitivity, (2) high equipment costs, and (3) often times, the need for highly trained/experienced personnel for data collection and interpretation.

The relatively low sensitivity of NMR, compared to other spectroscopic techniques, such as infrared (IR) or ultraviolet (UV) spectroscopy, arises from the small differences between spin energy levels and thus small population differences exploited in an NMR technique. However, with the advent of higher external magnetic field strengths, the sensitivity of NMR has improved to nanomolar levels (Eads, 1999). In addition, NMR can be coupled with other techniques (referred to as hyphenated NMR), such as liquid chromatography-NMR (LC-NMR), so as to take advantage of the benefits of each technique, while overcoming their individual disadvantages (Duarte *et al*., 2003; Spraul *et al*., 2001).

The initial investment in NMR equipment can be rather expensive, with the magnitude of the cost depending on the equipment required and the type(s) of experiments to be performed. For example, a 400-MHz high-resolution spectrometer, for running a variety of advanced level experiments, costs approximately $400,000 for a well-equipped liquids system to $500,000 for an instrument with solids capabilities. However, a 20-MHz low-resolution tabletop NMR, for running relatively routine relaxometry analyses, costs $50,000, plus an additional $10,000 for a gradient accessory for enabling diffusion measurements. An additional important cost consideration, not reflected in the aforementioned prices, is the operational costs associated with using and maintaining the instruments, such as for personnel, liquid nitrogen and helium refills for high-resolution instruments, and use of consumables.

Measurements obtained utilizing NMR techniques can be made on virtually any food. However, depending on the nature of these measurements, the training needed by a person obtaining such measurements varies widely. For example, in the case of a routine online analysis, such as using NMR to measure sample moisture content, quality assurance personnel can be trained to obtain such measurements; however, calibration and upkeep of an instrument by more highly trained personnel may still be required. In contrast, in the case of experimental research, such as using NMR to probe water dynamics during processing, design of experiments and collection and interpretation of resultant relaxation or diffusion data require highly trained personnel with experience in carrying out sophisticated and detailed data analysis. In fact, if Hills (1999) is correct in saying that the most challenging task for the future is to develop realistic theoretical models capable of

incorporating all NMR and MRI data from all distance scales in an integrated fashion (and I believe he is!), then very highly trained and experienced NMR personnel are needed now more than ever before.

In addition to the three general advantages/disadvantages of NMR discussed earlier, there are also specific advantages/disadvantages associated with particular magnetic resonance techniques and experiments. For a thorough discussion of pros and cons associated with various NMR techniques for investigating intact food materials, see Eads (1999).

6. *Relationship between NMR relaxation rates and* a_w

A relationship between NMR T_1 and T_2 relaxation rates and a_w seems likely, as both parameters are a measure of the mobility of water in a system, although one reflects molecular mobility and the other macroscopic mobility, respectively. Richardson *et al.* (1987), who plotted ^2H and ^{17}O NMR R_2 data as a function of a_w for corn starch, showed linear behavior for both nuclei. For ^{17}O data, linear behavior extended from 0.97 to 0.80 a_w, below which ^{17}O NMR measurements could not be obtained, because linewidths for higher concentrations (>83% starch) were larger than the bandwidth of the spectrometer used. For ^2H data, there were two linear regions: region A, from 0.99 to 0.23 a_w, and region B, from 0.23 to 0.11 a_w. The break between the two regions of ^2H data corresponded closely to the value of $a_w = 0.20$ given by van den Berg (1981) for the approximate BET monolayer value for starch.

Hills (1998, 1999) proposed an empirically derived relationship between NMR relaxation rates and a_w. The model begins by describing observed "average" values for NMR (T_{av}^{-1}) and $a_w(a_{av})$ parameters as a weighted average of values over all water states:

$$T_{av}^{-1} = \sum_i p_i T_i^{-1} \tag{14}$$

$$a_{av} = \sum_i p_i a_i \tag{15}$$

where T_i^{-1} and a_i are the intrinsic relaxation rate and water activity of the ith state of water in a system and p_i is the fractional population of that state.

Eq. (14), which was originally postulated by Zimmerman and Brittin (1957), assumes fast exchange between all hydration states (i) and neglects the complexities of cross-relaxation and proton exchange. Equation (15) is consistent with the Ergodic theorem of statistical thermodynamics, which states that at equilibrium, a time-averaged property of an individual water molecule, as it diffuses between different states in a system, is equal to a

time-independent ensemble-averaged property [Eq. (15) being an ensemble-averaged expression], but ignores configurational entropy effects (Hills, 1998, 1999; Hills *et al.*, 1999). Next, Hills simplified both Eqs. (14) and (15) to a case of two states of water in fast exchange (e.g., bulk water exchanging with hydration water), yielding the following two equations, respectively:

$$T_{av}^{-1} = T_b^{-1} - \frac{m_o\left(T_b^{-1} - T_h^{-1}\right)}{W} \tag{16}$$

$$a_{av} = a_b - \frac{m_o(a_b - a_h)}{W} \tag{17}$$

where m_o is the weight of hydration water per unit weight of dry biopolymer, W is water content, defined as the weight of water per unit weight of dry solid, and water activity of bulk water (a_b) is set equal to 1. It should be noted that Eq. (16) is only valid when water relaxation is single exponential (requires rapid diffusive exchange between all water populations) and Eq. (17) is only valid for $W > m_o$, as W values less than m_o correspond to the removal of hydration water, a region of an isotherm where the BET isotherm equation is applicable (Hills *et al.*, 1996a).

Based on the correspondence between Eq. (16) and (17), Hills combined the two equations by rearranging Eq. (17) to solve for m_o/W and then substituting the results of this term into Eq. (16), yielding Eq. (18), which linearly correlates NMR relaxation rates to water activity:

$$T_{av}^{-1} = T_b^{-1} + C(1 - a_{av}) \tag{18}$$

where the constant C is $(T_h^{-1} - T_b^{-1})/(1 - a_h)$. This combined equation is valid within the limitations given for the individual equations (two states of water in exchange, water relaxation is single exponential, and $W > m_o$). Breaks in linearity (i.e., changes in slope) between otherwise linear regions indicate that one of the states of water has been removed or a new one has been introduced.

The linear relationship between ^{1}H NMR transverse relaxation rate and $(1 - a_{av})$ is shown in Figure 30 for pregelled potato starch (Hills *et al.*, 1999). The change in slope at about 0.90 a_w corresponds to the bulk water break (i.e., the removal of bulk water) in a corresponding adsorption isotherm. Equation (18) has been applied successfully to beds of Sephadex microspheres and silica particles using both ^{1}H NMR (Hills *et al.*, 1996b) and ^{17}O NMR, the latter of which is free from the complication of proton exchange when measured using proton decoupling (Hills and Manning, 1998).

Hills *et al.* (1999) clearly expressed the point that there is no implied fundamental physical relationship between a_w, an equilibrium thermodynamic quantity, and NMR relaxation, a nonequilibrium kinetic event, in

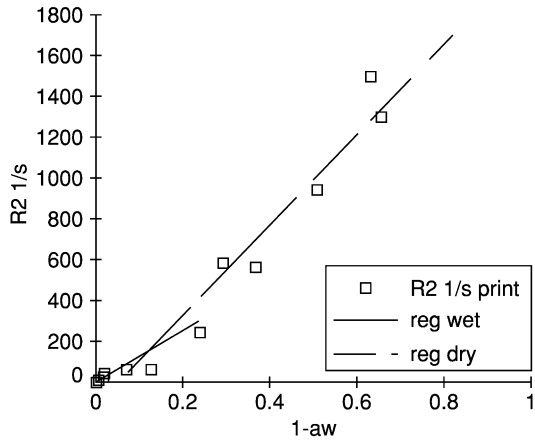

FIG. 30 Linear relationship between ^{1}H NMR transverse relaxation rate (recall $R_2 = 1/T_2$) and $(1 - a_w)$ for pregelled potato starch [reproduced with permission from Hills *et al.* (1999)].

this theory. Rather, all that is suggested is that the changing states of water in a biopolymer system affect both water activity and NMR relaxation similarly.

D. GLASS TRANSITION

Widespread application of the glass transition concept in foods is attributed to Slade and Levine and their introduction in the 1980s of the "food polymer science" approach for the assessment of food quality and safety—beyond that of the "water activity" concept of moisture management (e.g., Slade and Levine, 1985, 1988, 1991, 1995, 1998, 2002, 2003). One of the key elements of the food polymer science approach is the importance of "the glass transition temperature ... as a physicochemical parameter that can determine processibility, product properties, quality, stability, and safety of food systems" (Slade and Levine, 1991). Levine (2002) provided his own personal chronology of key milestones in the application of polymer science concepts to foods. Levine attributes his finding and reading of a paper, in 1979, by Felix Franks and co-workers (1977) on biological cryoprotection as the beginning of the story. Levine (2002) also cites a number of historical papers he read on glasses, glassy states, and glass transitions, including a seminal review by White and Cakebread (1966) and van den Berg's 1981 doctoral thesis, which helped shape the "food polymer science" approach.

Since its introduction, the food polymer science approach has been used to understand structure–function relationships in foods, the effect of

plasticization by water on a number of thermal and mechanical properties of foods, and the relative stability of foods in a nonequilibrium glassy state versus the instability in a rubbery or viscous liquid state (Slade and Levine, 2003). The glass transition concept has been especially useful in understanding and enhancing the processing, quality, and stability of concentrated foods, i.e., low-moisture and frozen foods.

Based on the pioneering efforts of Slade and Levine, there has been a constantly increasing number of studies, review papers, book chapters, books, symposia, conferences, and short courses devoted to investigating, teaching, and critically evaluating applications of the glass transition concept to foods. Because of the large number of excellent recent books and book chapters (Blanshard and Lillford, 1993; Levine, 2002; Rahman, 1995; Roos, 1995) and review articles (Bhandari and Howes, 2000; Champion *et al*., 2000; Hancock and Zografi, 1997; Le Meste *et al*., 2002; Roos, 2003; Roos and Karel, 1991; Roos *et al*., 1996; Slade and Levine, 1991, 2003) on the subject, the approach taken here is to briefly summarize the current status of the glass transition concept and its measurement methods and to highlight its usefulness and limitations in foods.

1. Physical states and state transitions

Matter can exist in three basic physical states: solid, liquid, and gas. Interconversions between these physical states are termed phase transitions and are caused by a change in temperature and/or pressure. Phase transitions can be classified into two main groups: first order and second order. This classification is based on observed discontinuities that occur in state functions at transition temperatures (Roos, 1995). First-order phase transitions are those for which the first derivatives of the chemical potential and of Gibbs free energy exhibit discontinuous changes at the transition temperature. During first-order transitions, the physical state of matter (at constant pressure) transitions isothermally from one state to another by an absorption (i.e., solid to liquid) or release (i.e., liquid to solid) of latent heat. Phase transitions that occur among the three basic physical states are first-order transitions and take place at very well-defined temperatures. Recall the six phase transitions (three pairs of two—melting and crystallization; evaporation and condensation; sublimation and ablimation) that occur in water, as shown in the phase diagram for pure water (in Figure 7).

Second-order phase transitions are those for which the second derivatives of the chemical potential and of Gibbs free energy exhibit discontinuous changes at the transition temperature. During second-order transitions (at constant pressure), there is no latent heat of the phase change, but there is a discontinuity in heat capacity (i.e., heat capacity is different in the two

phases). The glass transition is often labeled as a second-order phase transition, as it has some apparent features of a second-order phase transition at very slow rates of heating or cooling (i.e., exhibits step changes in heat capacity and thermal expansion coefficient with temperature) (Roos, 1995). However, it exhibits other features (e.g., it occurs over a temperature range and is time and measurement method dependent) that suggest that it should not be classified as a second-order transition, but rather as a kinetic and relaxational transition (Labuza *et al*., 2001). In addition, because the glass transition is a property of a nonequilibrium system, it cannot be classified as a pure phase transition, but is rather considered as a state transition (Roos, 2003; Slade and Levine, 1991).

Food materials (ingredients or whole systems) can be composed of matter in one, two, or all three physical states: solid (crystalline or amorphous or a combination of both), liquid, and gas. The crystalline state is an equilibrium solid state, whereas the amorphous glassy state is nonequilibrium solid state. The main transitions that occur between the physical states of materials of importance to foods are summarized by Roos and Karel (1991) and Roos (2002). The most important parameters affecting the physical state of foods, as well as their physicochemical properties and transition temperatures, are temperature, time, and water content (Slade and Levine, 1988; Roos, 1995). Pressure is not included in this list, as food materials usually exist under constant pressure conditions.

The physical state of relevance to the glass transition is the amorphous solid state. The amorphous solid state is an energetically metastable, nonequilibrium state that retains the disorder of a liquid state (Rahman, 1995; Roos, 1995). An amorphous material can be in either a supercooled liquid state (also called the rubbery state or rubber) or a solid state (also called the glassy state, glass, or solid solution). A common feature of amorphous solid materials is that they contain excess free energy and entropy, as compared to their crystalline counterparts at the same temperature and pressure conditions (Roos, 1995). The transformation between supercooled liquid and solid amorphous states is known as the glass transition and is illustrated schematically in Figure 31. The viscosity of amorphous materials in the glassy state is typically $\geq 10^{12}$ Pa second. Over the glass transition temperature range, Young's modulus (E) drops dramatically from about 10^9 to 10^6 Pa (Sperling, 1986). A number of methods can be used to produce materials in the amorphous solid state. These methods usually involve two events (Figure 31): (1) rapid evaporation of solvent molecules (decrease in water content) and/or (2) sufficiently rapid cooling of a material to avoid formation of an equilibrium crystalline state (decrease in temperature). Also, depending on the rate of solvent removal and/or cooling into an amorphous solid state, glasses with different properties can be formed (Roos, 2003). For

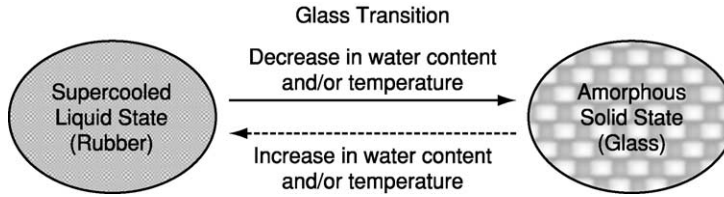

FIG. 31 Schematic diagram illustrating the transition between a supercooled liquid state (rubber) and an amorphous solid state (glass). The glass transition event is typically caused by a decrease in water content and/or temperature. The reversibility of the transition, as indicated by the dotted arrow, is material dependent (see text for further discussion of the reversibility of the transition).

example, a glass formed using a fast cooling rate possesses greater free volume and enthalpy and has a higher T_g value compared to a glass formed using a slow cooling rate (Hsu *et al.*, 2003; Roos, 2003; Schmidt and Lammert, 1996). As illustrated by the dotted arrow in Figure 31, a glass transition event may be reversible, depending on the material under study. The reversibility of the glass transition in food systems is discussed in more detail in the next section. Various food ingredients and food systems are produced in the amorphous state using a variety of processing methods that include one or both of the aforementioned events, such as spray-drying, freeze-drying, melting and subsequent quick-cooling, extrusion, baking, and encapsulation. Examples of products that contain amorphous or partially amorphous structures below their T_g are extruded snacks and breakfast cereals, low-moisture cookies and crackers, pasta, hard sugar-based candies, powdered drink mixes, and cotton candy.

Once in the amorphous solid state, undesirable changes in the properties of amorphous ingredients and foods (e.g., stickiness, caking, collapse, loss of crispness) can occur via a reversal in the two events discussed earlier: (1) an increase in moisture content (water plasticization) so that the T_g of a material is decreased to below room temperature and (2) an increase in temperature [thermal plasticization (Roos, 2003)] so that the temperature of the material rises above its T_g. In both cases and their combination, the once glassy material is now in a rubbery or liquid state and is undesirable and/or unfit for consumption.

State diagrams are very useful tools in the characterization of amorphous ingredients and food systems (Roos, 1995; Slade and Levine, 1991). Slade and Levine (1988, 1991), acknowledging the earlier work of Franks *et al.* (1977) and MacKenzie (1977), formulated a state diagram (called a ''dynamics map'' or ''mobility transformation map'') for food systems that includes four dimensions: temperature, concentration, pressure, and time. This state

diagram includes both equilibrium and nonequilibrium thermodynamics in a single figure. The equilibrium regions of the diagram are completely described in two dimensions: temperature and concentration (at constant pressure). However, the nonequilibrium regions require inclusion of the third dimension of time, expressed by Slade and Levine (1991) as t/τ, where τ is a relaxation time. Expressing the time in this dimensionless manner allows the time dependence of a dynamic process to be defined in terms of the relationship between an experimental timescale and the time frame of a relaxation process (Slade and Levine, 1991). The concept of mobility, as one of the underlying principles of the food polymer science approach, was stressed by Slade and Levine (1988), as they introduced their ''dynamics map'':

> 'Mobility' will be used as a transcendent principle to connote all of these interdependent concepts embodied in the dynamics map in Figure 1. Thus, mobility will be the key to all transformations, as well as the basis for defining appropriate reference states (page 1842).

A simplified state diagram (assuming constant pressure and omitting the time-dependence aspect) can be used to show the physical state of a material as a function of temperature and concentration (often expressed as percent weight fraction of solids). A general state diagram typical for a water-soluble food component (e.g., sucrose) is shown in Figure 32. This state diagram is composed of three main curves [the freezing curve (AB), the solubility curve (BC), and the glass transition curve (DEF)] and several anchor points, each of which is defined in the legend for Figure 32. For the interested reader, Slade and Levine (1991) and Roos (1995) not only furnish comprehensive explanations of the state diagram, but also give a variety of material-specific state diagrams (e.g., sucrose, glucose, lactose, fructose, starch, cereal proteins, and PVP-40).

Two locations on the state diagram are of particular interest to the glass transition concept. The first location is the high weight fraction of solids (i.e., low moisture content region) portion (DE) of the glass transition temperature curve (DEF), which is important for the processing and stability of low-moisture ingredients and foods. This low water content region is the main focus of this review. As illustrated in Figure 32, the glass transition temperature of an amorphous food decreases rapidly as moisture content increases (i.e., decreasing weight fraction of solids).

The second location of interest is the T_g associated with a maximally freeze-concentrated solute matrix, T_g' (point E), which is important to the processing and stability of frozen foods. The freezing of most foods results in the formation of an amorphous freeze-concentrated phase that is plasticized

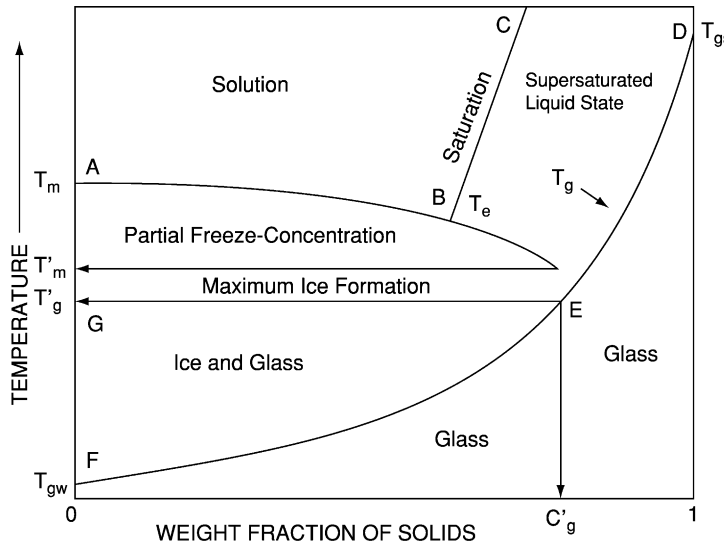

FIG. 32 General state diagram, typical of a water-soluble food component (e.g., sucrose), composed of three curves, the freezing curve (AB), the solubility curve (BC), and the glass transition curve (DEF), and several anchor points. T_m is the equilibrium melting temperature of pure ice, T'_m is the onset melting temperature of ice in contact with a maximally freeze-concentrated solution, T'_g is the glass transition temperature of a maximally freeze-concentrated solute matrix, C'_g is the solute concentration in a maximally freeze-concentrated solute matrix, T_e is a eutectic point, T_{gw} is the glass transition temperature of pure water [often given as $-135\,^{\circ}C$ (Angell, 1983)], and T_{gs} is the glass transition temperature of an anhydrous amorphous material [adapted from Roos (1995) and Rahman (1995)].

by unfrozen water within the aqueous phase. At sufficiently low temperatures ($< T'_g$), the freeze-concentrated phase solidifies into a glassy state (called vitrification), and ice formation ceases due to kinetic restrictions (Roos *et al.*, 1996; Slade and Levine, 1988). The importance of T'_g in frozen food systems is discussed in detail by Slade and Levine (1991), Roos (1995), Goff and Sahagian (1996), Roos *et al.* (1996), and Matveev and Ablett (2002).

State diagrams are an integral part of the food polymer science approach and are further explored and expanded upon in Section III.D.5. For the interested reader, Javenkoski (2001) developed instructional visualization media (three QuickTime animations) for aqueous phase transitions in food systems and investigated their use for improving the comprehension of phase transitions by students enrolled in an introductory food science and human nutrition course.

2. *Definition and assignment of glass transition*

From a conceptual point of view, the glass transition is a phenomenological passage from a glassy solid state, in which short-range vibrational processes are occurring, to a rubbery–liquid state, in which long-range translational and rotational (cooperative) processes are occurring, within a finite temperature range (Seyler, 1994c). The glass transition temperature (T_g) is a single temperature value that represents this finite temperature range. In addition to this widely accepted conceptual view of the glass transition, the ASTM has provided a standard definition and discussion of the glass transition and glass transition temperature. These are given here, as excerpted from Designation: E 1142, Terminology Relating to Thermophysical Properties (ASTM E 1142-97):

> **glass transition**—reversible change in an amorphous material or in amorphous regions of a partially crystalline material, from (or to) a viscous or rubbery condition to (or from) a hard and relatively brittle one.
>
> **discussion**—The glass transition generally occurs over a relatively narrow temperature range and is similar to the solidification of a liquid to a glassy state. Not only do hardness and brittleness undergo rapid changes in this temperature region, but other properties, such as coefficient of thermal expansion and specific heat capacity, also change rapidly. This phenomenon sometimes is referred to as a second order transition, rubber transition, or rubbery transition. When more than one amorphous transition occurs in a material, the one associated with segmental motions of the backbone molecular chain, or accompanied by the largest change in properties is usually considered to be the glass transition.
>
> **glass transition temperature**—a temperature chosen to represent the temperature range over which the glass transition takes place.
>
> **discussion**—The glass transition temperature can be determined readily by observing the temperature region at which a significant change takes place in some specific electrical, mechanical, thermal, or other physical property. Moreover, the observed temperature can vary significantly depending on the property chosen for observation and on details of the experimental technique (for example, heating rate, frequency of test). Therefore, the observed T_g should be considered valid only for that particular technique and set of test conditions.

Three aspects of the ASTM definitions and discussions just given require further attention, especially when applied to food systems. The first is the reversible nature of the glass transition. In the proceedings of the 1993 ASTM Assignment of the Glass Transition symposium (Seyler, 1994a), Seyler (1994c) stated that the glass transition is not reversible, but rather more accurately described as ''bidirectional with hysteresis.'' In the case of some food ingredients and food systems, we may have to take this suggested

redefinition one step further. Because of the complex nature of foods and the possible irreversible effects of processing (e.g., heating and/or moisture uptake) on a material, the glass transition may occur at a very different temperature after processing (or measuring with an analytical method) compared to before processing. For example, gelatinization (via heat and moisture uptake) of starch and denaturation (e.g., by heat, acidic pH, or mechanical shear) of protein are two frequently encountered processes occurring in foods, which result in irreversible changes in these food polymers. If these irreversible changes occur while the glass transition is being measured, the glass transition will not be located in the same temperature range upon replicate measurement of the same sample; there will be a new glass transition, reflective of the new nature of the material. Thus, for foods, the definition needs to include the possibility that the glass transition can be only unidirectional in some cases (e.g., starch and protein) and bidirectional in others (e.g., sugar glasses).

The second issue with the ASTM definition is the statement in the glass transition discussion that "the glass transition generally occurs over a relatively narrow temperature range." Exactly what is meant by "relatively narrow" is not defined specifically. However, literature sources suggest that the temperature range may not be as narrow as that implied by the ASTM discussion. Wunderlich (1990) gave a general temperature range for the glass transition of 5 to 20 K (based on DSC), and Sperling (1986) gave a general range of 20 to 30 °C (based on a change in modulus). In an actual sample, Bair (1994) reported a DSC T_g range for polycarbonate of 17 °C (calculated as T_g end point minus T_g onset). These sources suggest that even for well-behaved synthetic polymers, the T_g range can be rather broad. Because of the complex, heterogeneous nature of many food systems, the temperature range over which the glass transition occurs in foods can also be quite large. Kou *et al.* (1999) reported an average T_g range (calculated as T_g end point minus T_g onset) of 10.25 °C for sucrose, 14.23 °C for starch, and 12.87 °C for a 1:1 sucrose/starch mixture. In general, the more complex a system, the broader and more difficult it will be to observe the glass transition. For the interested reader, Bair (1994) uses changes in an uncured, low molecular weight, light-sensitive acrylate adhesive to illustrate how broad and complex T_g can become with processing.

One additional point before we leave this second issue concerns the reporting of T_g. Regardless of how broad or narrow the glass transition is for a particular food system, it is important to recognize (and conceptualize) that the glass transition occurs over a temperature *range* and not at a single temperature value. As pointed out by Peleg (1997), the difference in terminology (glass transition temperature and temperature range) is more than just semantic and has several theoretical and practical implications. Because of

the confusion associated with using a single temperature value to represent an entire T_g range, this author strongly recommends that, when possible, researchers report not only the observed T_g value (and how it was assigned), but also the T_g range. For example, in the case of DSC, report the T_g midpoint value as T_g and, for the range, report both onset and end point T_g values. In addition to these three temperature values (T_g onset, T_g midpoint, and T_g end point) and the change in heat capacity (ΔCp), Wunderlich (1994) suggested reporting two other useful temperatures to characterize the DSC glass transition: T_1 and T_2, which are identified as the intersections of the tangent at T_g with the extrapolated glass and liquid heat capacities, respectively. Wunderlich (1994) also suggested that when using DSC, the glass transition should be measured on cooling at a specified cooling rate. Many researchers, however, measure the transition during heating rather than cooling.

The third issue with the ASTM definitions and discussions given earlier was raised in the earlier T_g discussion, where it was stated that "the observed glass transition temperature can vary significantly depending on the property chosen for observation and on details of the experimental technique." This issue was also discussed throughout the proceedings of the aforementioned 1993 ASTM symposium (Seyler, 1994a). Regarding assignment of the glass transition, Seyler (1994b) stated that "we do not measure THE glass transition temperature [of a sample] but rather make measurements to observe the glass transition and then assign a temperature, T_g, to mark its occurrence." As discussed in detail in the next section, the glass transition can be observed (and marked) by a number of analytical methods. The T_g obtained, however, is not a single value, but rather occurs over a temperature range (as discussed previously) and, moreover, is dependent on a myriad of intrinsic and extrinsic factors associated with a given sample and method. Therefore, in order to assign the glass transition reliably and reproducibly, a complete description of a system must also be given (Seyler, 1994c). This description must not only include the method and property whose changes are being used to identify the glass transition, but also a detailed accounting of the conditions of the sample, test, and atmosphere. This concept is illustrated in Figure 33, in which the large box encompasses the system that yields T_g. To accurately communicate the assigned T_g, we must not simply report a T_g value, but rather a T_g value plus SYSTEM details (Seyler, 1994c).

One final but very important point needs to be made regarding the glass transition. As highlighted by Ludescher *et al.* (2001), it must be kept in mind that the glass transition is a macroscopic manifestation of cooperative changes in molecular mobility (specifically, translational mobility) of individual molecules in a continuous amorphous phase—where the change in

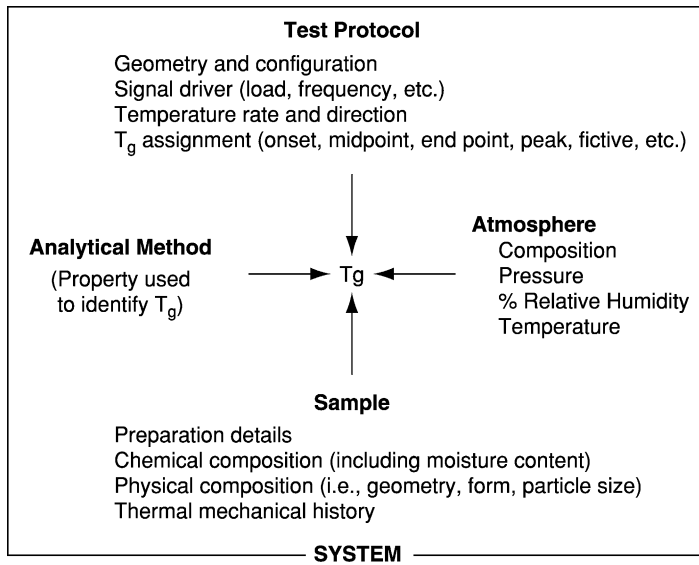

FIG. 33 An analytical method used to assign a T_g value to a sample. The large outer box encompasses the system that yielded the T_g value. Thus, in order to communicate the assigned T_g value accurately, a complete description of the system must also be given [adapted from Seyler (1994c)].

molecular mobility is the underlying cause (and as such, should be the focal point of investigation) and the glass transition is the effect. This focus on molecular mobility of a system, rather than on the glass transition effect, is also advocated by Fennema (1996) and is integrated into the views and discussion presented in this review.

3. *Measurement methods*

Several material properties exhibit a distinct change over the range of T_g. These properties can be classified into three major categories—thermodynamic quantities (i.e., enthalpy, heat capacity, volume, and thermal expansion coefficient), molecular dynamics quantities (i.e., rotational and translational mobility), and physicochemical properties (i.e., viscosity, viscoelastic proprieties, dielectric constant). Figure 34 schematically illustrates changes in selected material properties (free volume, thermal expansion coefficient, enthalpy, heat capacity, viscosity, and dielectric constant) as functions of temperature over the range of T_g. A number of analytical methods can be used to monitor these and other property changes and

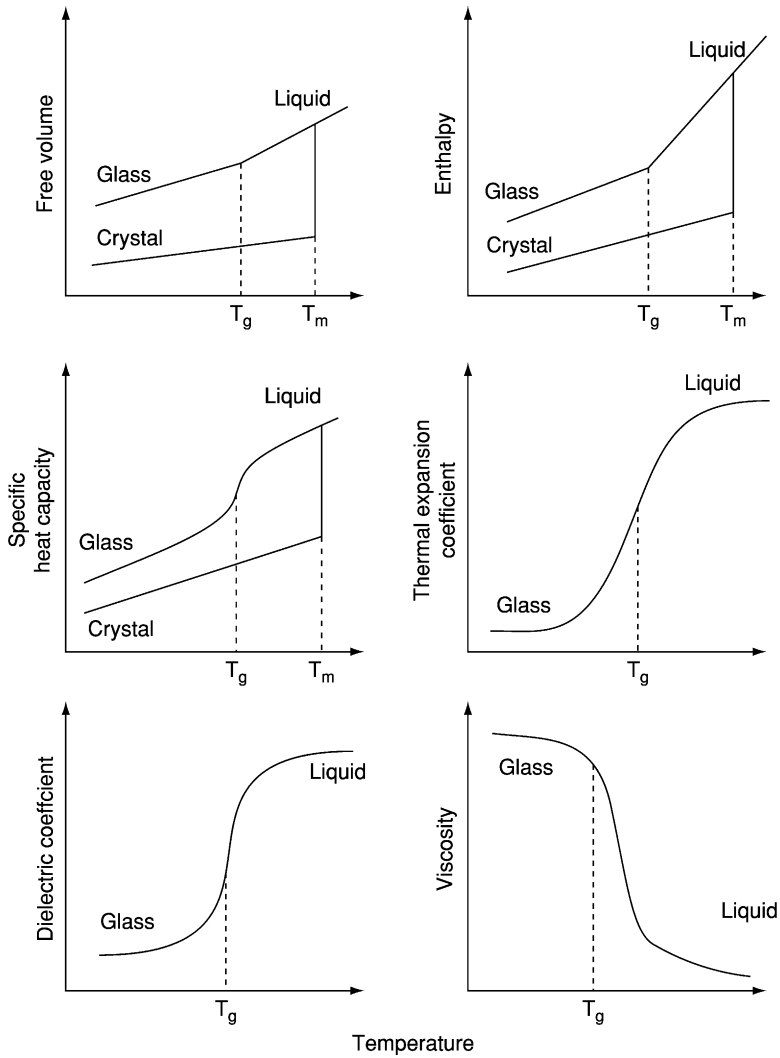

FIG. 34 Schematic illustrations of changes in selected material properties (free volume, thermal expansion coefficient, enthalpy, heat capacity, viscosity, and dielectric constant) as functions of temperature over the range of T_g.

thus identity the glass transition. The most common methods and their descriptions are given in Table VIII. Modulated DSC techniques have been introduced that may be helpful for observing the glass transition in systems with weak, broad, or overlapping transitions (De Meuter *et al.*,

TABLE VIII
;SELECTED ANALYTICAL METHODS USED TO OBSERVE T_g[a]

Analytical method	Description	ASTM designation and references
Differential scanning calorimetry (DSC)	Method involves continuously monitoring the difference in heat flow between a reference material (usually an empty pan) and a test material when they are heated or cooled at a controlled rate through the glass transition region of the test material and analyzing the resultant thermal curve to provide the glass transition temperature. The glass transition is manifested as a step change in specific heat capacity (ΔC_p), which occurs between the glassy (lower C_p) and the rubbery–liquid (higher C_p) states of the sample	ASTM E 1356–98 Wunderlich (1990)
Thermomechanical analysis (TMA)	Method uses thermomechanical analysis equipment to assign the change in dimension of a specimen observed when the material is subjected to a constant heating rate through its glass transition. This change in dimension associated with the change from vitreous solid to amorphous liquid is observed as movement of the sensing probe in direct contact with the specimen and is recorded as a function of temperature. The intersection of the extrapolation of the slope of the probe displacement curve before and after the transition is used to determine the glass transition temperature. In the TMA under tension method tensile mode is used	ASTM E 1545–00 ASTM E 1824–96 under tension Seyler (1994a); Wunderlich (1990)
Dynamic mechanical analysis (DMA)	A specimen of known geometry is placed in mechanical oscillation at either fixed or resonant frequency, and changes in viscoelastic response of the material are monitored as a function of temperature. The glass transition region is marked by a rapid decrease in the storage modulus and a rapid increase in the loss modulus. Glass transition of the test specimen is indicated by the extrapolated onset of the decrease in storage modulus, which marks the transition from a glassy to a rubbery solid	ASTM E 1640–99 Macinnes (1993); Seyler (1994a); Wunderlich (1990)

(*continued*)

TABLE VIII (*continued*)

Analytical method	Description	ASTM designation and references
Dielectric analysis (DEA)	Method involves placing a specimen between parallel plate capacitors and applying a sinusoidal voltage (frequencies ranging from 1 mHz to 1 MHz) to one of the plates to establish an electric field in the specimen. In response to this field, a specimen becomes electrically polarized and can conduct a small charge from one plate to the other. Through measurement of the resultant current, the dielectric constant and dielectric loss constant for a specimen can be measured. The sharp increases in both the dielectric constant and the dielectric loss constant during a temperature scan are correlated with the occurrence of T_g	Bidstrup and Day (1994); Roos (1995)
Nuclear magnetic resonance (NMR) spectroscopy	Method involves measuring the change in molecular mobility (rotational and translational mobility) experienced by nuclei associated with solid components (e.g., ^{1}H and ^{13}C). The temperature associated with an increase in solid component mobility is assigned as T_g	Ablett *et al.* (1993); Kou *et al.* (1999); Ruan and Chen (1998); Ruan *et al.* (1998, 1999)
Electron spin resonance (ESR) spectroscopy	Method involves measuring the change in rotational correlation time for a free radical probe (e.g., nitroxide spin probes) introduced into a sample being studied. The temperature associated with a decrease in the rotational correlation time of a spin probe is assigned as T_g	Hemminga *et al.* (1993); Roos (1996)

[a]Where possible, the ASTM test method description and designation have been included.

1999; Paeschke, 2002; Riga and Judovits, 2001). Additional methods are given in Rahman (1995), Roos (1995), and Slade and Levine (1995), and a discussion of some of the unsettled issues associated with various T_g methods is given in Levine (2002).

It is important to emphasize that the T_g of a given sample is not a unique value, but rather depends on the analytical method and protocol employed, as well as a complete description of the sample, its composition (e.g., moisture content), and its history (i.e., under what conditions was it made

and stored). Because each method "sees" a sample from its own perspective (i.e., property and level being probed), the T_g value observed by each method for a single sample may or may not be the same. For example, Ruan *et al.* (1998) reported T_g values for a DE-15 maltodextrin sample using DSC (reported as T_g) and ^{1}H NMR (T_{T1}—temperature assigned as marking the glass transition, using the longitudinal relaxation time, and T_{T2S}—temperature assigned as marking the glass transition, using the transverse relaxation time of the short-relaxing component). They found that T_{T2S} values were, on average, only 1.2 °C lower than DSC T_g values, whereas T_{T1} values were, on average, 11.2 °C lower than DSC T_g values. Additional examples comparing T_g values obtained using different methods for the same (or similar) samples are given in Schmidt (1999).

In addition to possible variations between methods, there may also be variations in T_g within a method, depending on the measurement protocol employed. For example, the DCS T_g midpoint for a quench-cooled (~100 K/min) maltose sample, heated at a scanning rate of 10 K/min, was 43.1 ± 0.21 °C, whereas for a maltose sample prepared using equal heating and cooling rates of 10 K/min the T_g was 41.2 ± 0.10 °C (Schmidt and Lammert, 1996). For the same samples, DSC T_g fictive temperatures were also calculated. T_g fictive for the quench-cooled sample was 41.0 ± 0.20 °C, whereas for the equal-rate sample, T_g fictive was 38.6 ± 0.06 °C.

Because of the possible differences in T_g obtained by different measurement methods, a question often arises as to what measurement method should be used? Since no one method yields an "absolute" or "true" T_g, any method performed correctly can yield a useful T_g value. What is important to remember is that the T_g obtained is dependent on the method used (i.e., reflects the experimental time scale of the method) and the system probed (recall Figure 33). Therefore, the measurement method should be selected according to the needs of an application.

By definition, the glass transition reflects changes experienced by the solid component(s) of a sample, as it transitions from an amorphous solid to a rubbery–liquid. Thus, the descriptions of the methods listed in Table VIII focus on changes experienced by solids in the glass transition region, and most often, what is measured is an average T_g for an entire system. What about the mobility experienced by the individual components that comprise a system, including water, relative to the glass transition for the entire system?

Recall that the glass transition for a given glass-forming solute–water blend (i.e., the glass transition for the entire system) is determined by the weight-average molecular weight ($\overline{M}w$) of the blend (Slade and Levine, 1991). In turn, as explained by Slade and Levine (2003), the relative mobility of an individual component in a multicomponent system is determined by

the molecular weight ($\overline{M}w$ or the number-average molecular weight [$\overline{M}n$], depending on which is appropriate to use) of that component, compared to $\overline{M}w$ of the system. For example, a molecule of higher molecular weight than that of the system (use $\overline{M}n$ in this case) would already be immobilized at the glass transition of the system, whereas a molecule of lower molecular weight (use $\overline{M}w$ in this case) than that of the system, such as water, would still be mobile at temperatures below the glass transition. A probe molecule of the same molecule weight (use $\overline{M}w$) as that of the system would be immobilized at T_g of the system. Thus, the molecular weight (and the configuration, in cases of equal or near-equal molecular weight) of a component determines its mobility relative to the glass transition of the system. A number of studies have shown that water retains a high degree of rotational and transitional mobility in glassy states relative to the glass transition of solid components (Ablett *et al*., 1993; Kou *et al*., 1999; Le Meste *et al*., 2002; Roudaut *et al*., 1999a; Tromp *et al*., 1997). This finding again emphasizes the importance of keeping in mind that results obtained depend on the viewpoint of the method and component being used to probe a system under study.

Differences in mobility of various components (e.g., starch, sucrose, water) within a food system (e.g., a cookie), as well as the inherent heterogeneity of many food systems (e.g., crust versus crumb of a cookie), suggest the need to measure more than an average T_g for a system. Ruan and Chen (1998) proposed the creation of a "T_g map" to capture the distribution of T_g values within a food system. Since conventional techniques used to measure T_g do not have the capacity at the present time to provide spatial information, Ruan and Chen (1998) suggested the use of MRI, as a function of temperature, to produce a "T_g map."

4. Distance and timescales involved in glass transition

The distance scale associated within the glass transition is related to the method used. For example, thermal and mechanical techniques provide macroscopic views of the glass transition, whereas spectroscopy techniques yield a molecular-level view. Thus, it is not surprising to find that molecular-level techniques, such as NMR, may result in lower T_g values compared to those obtained using a macroscopic technique, such as DSC. Both T_g values are correct, but not necessarily equal, given the different points of view the two methods are probing.

As discussed earlier, the amorphous state is a nonequilibrium state at temperatures below the equilibrium melting temperature of a material. Because of the nonequilibrium nature of the amorphous state, various properties of amorphous materials, such as the glass transition, are dependent on time and temperature (Slade and Levine, 1988, 1991; Roos, 1995, 2003). Therefore,

methods using different experimental timescales, such as frequency and cooling/heating rates, can result in different locations of the glass transition for the same material. In addition, various enthalpic relaxations may be associated with the observed glass transition, depending on the rates of glass formation and measurement [e.g., slow cooling followed by fast heating in a DSC experiment results in an endothermic peak in the heat capacity curve (Wunderlich, 1990)], as well as the process of physical aging that can occur in the glassy state (Roos, 2003). In the case of physical aging, an endothermic relaxation peak is observed during measurement of the glass transition by DSC. The size of the endothermic peak increases with aging time and has been shown to interfere with the accurate assignment of T_g (Richardson and Saville, 1975), especially when one uses standard instrumental software to obtain T_g. For example, Wungtanagorn and Schmidt (2001), studying the aging of glucose and fructose glasses, reported that T_g values obtained using the instrumental software increased as a function of aging time, whereas theoretically these T_g values should decrease with aging time. Factors responsible for this artificial increase in software-measured T_g values with aging time are discussed in detail in Wungtanagorn and Schmidt (2001).

5. *Usefulness of the glass transition concept for foods*

There is no doubt that the introduction and application of Slade and Levine's food polymer science approach to better understand processing and stability of food systems have been exceedingly stimulating and have led to a number of important scientific advances. On many fronts, the usefulness of the food polymer science approach has been widely demonstrated. However, use of the glass transition as the single ultimate index temperature of food stability, as it was first embraced, is said by some to be untenable (Chirife and Buera, 1996; Le Meste *et al*., 2002). Rather, the glass transition, as is the case with water activity, is more useful and applicable in some situations compared to others. This last statement is in no way meant to lessen the significance of the glass transition concept in foods, but rather reflects an increased focus on the importance of other independent factors, such as pH, temperature, and reactant and product concentrations (Roos, 2003).

The compilation of ideas about the usefulness of the glass transition concept in foods, presented in this section, was influenced by the following sources: Rahman (1995), Chirife and Buera (1996), Fennema (1996), Roos *et al*. (1996), Champion *et al*. (2000), Labuza *et al*. (2001), Le Meste *et al*. (2002), Bhandari and Howes (2000), Slade and Levine (2003), and Roos (2003). Because there are a number of reviews (including those just listed) that specifically address the usefulness of the glass transition in food processing and stability, only a brief summary is provided here.

a. Development of state diagrams, expanded state diagrams, and mobility and stability maps. As introduced earlier, state diagrams are very useful tools for describing relationships among the physical state of food materials, temperature, concentration, pressure, and time (Karel *et al.*, 1993; Roos, 1995; Slade and Levine, 1991). State diagrams can be expanded and plotted in a variety of creative ways to enhance their usefulness and to facilitate the understanding of complex series of events that can occur in the processing and storage of food systems. State diagrams have been augmented by adding paths associated with [see, e.g., Figure 17.13 in Levine and Slade (1993), Figures 4–6 and 8 in Strahm (1998), and Figure 2 in Zweifel *et al.* (2000)] or areas important to [see, e.g., Roos (1995)] various food processes and technologies, such as drying, baking, cooling, freezing, heating, hydration, and extrusion. Product types have been indicated on state diagrams of major components comprising those products [see, e.g., Figure 2.13 in Karel *et al.* (1993)]. Constant-relaxation time lines, as well as isoviscosity lines, have been plotted on state diagrams [see, e.g., Figure 3 in Parker and Ring (2001), Figures 5 and 6 in Roos (2002), and Figures 2.13 and 2.14 in Roos (1998)]. The relative locations of food quality-deteriorating events, such as crystallization, collapse, caking, and stickiness, have also been indicated on state diagrams [see, e.g., Figures 7.7 and 10.12 in Roos (1995)], illustrating stability in the glassy state and time-dependent changes in the rubbery state (Roos and Karel, 1991). Additional discussions of applications of state diagrams can be found in Roos and Karel (1991), Karel *et al.* (1993), Nelson and Labuza (1993), and Roos (1995).

More recently, Slade and Levine (2003) developed a combination glass transition-universal isotherm diagram (Figure 35) to illustrate the concept that multiple texture stabilization requires control of moisture content, sample RH, molecular T_g, and network T_g. The diagram contains portions of the glass curves for sorbitol (T_g sorbitol), for a nonnetworked biopolymer (T_g biopolymer), and for a permanent network (T_g permanent network) positioned relative to a "universal isotherm curve" as a means of showing, e.g., that molecular T_g controls water vapor migration, while network T_g controls bulk liquid water migration.

Using the time-dependent aspect of state diagrams, Roos (2003) illustrated the effects of temperature, water activity, or water content on relaxation times and relative rates of mechanical changes in amorphous systems (Figure 36). This diagram can be considered as a type of mobility map, where mobility increases (relaxation time decreases) as temperature and/or water content/activity increases. Le Meste *et al.* (2002) suggested the establishment of "mobility maps" for food materials showing characteristic relaxation times for different types of molecular motions as a function of temperature and water content.

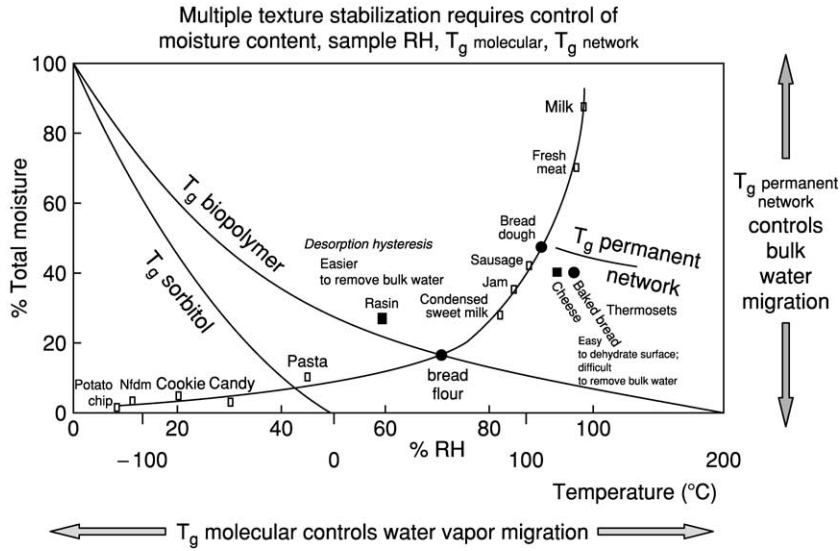

FIG. 35 Percentage relative humidities of common foods at room temperature and typical steady-state moisture contents plotted as a "universal sorption isotherm" with portions of three glass curves (relatively positioned) for sorbitol, for a nonnetworked biopolymer, and for a permanent network [reproduced with permission from Slade and Levine (2003)].

In addition to these state diagram-based maps, various stability (or quality) maps have been created to depict the stability of a system as influenced by the T_g or associated critical water activity value. For example, in Figure 12.4 of their paper, van den Berg *et al.* (1993) plotted a T_g curve as a function of %RH for safe storage of amorphous sucrose and labeled the temperature–%RH area below the curve as stable and the area above the curve as unstable. In another example, Roos *et al.* (1996) plotted relative rates of typical mechanical and deteriorative changes in foods as (1) a function of temperature and included T_g (see Figure 5A in Roos *et al.*, 1996) or (2) a function of water activity and included a critical water activity value (see Figure 5B in Roos *et al.*, 1996). The latter stability map is similar in concept to the original water activity stability map in Labuza *et al.* (1970) (illustrated previously in Figure 15), but instead of including a sorption isotherm, critical water activity is used as the point at which molecular mobility and rates of diffusion-controlled changes begin to increase. Figure 37 shows a stability map of the latter type, specifically for dairy powders containing amorphous lactose, developed by Roos (2003). Roos also developed schematic diagrams

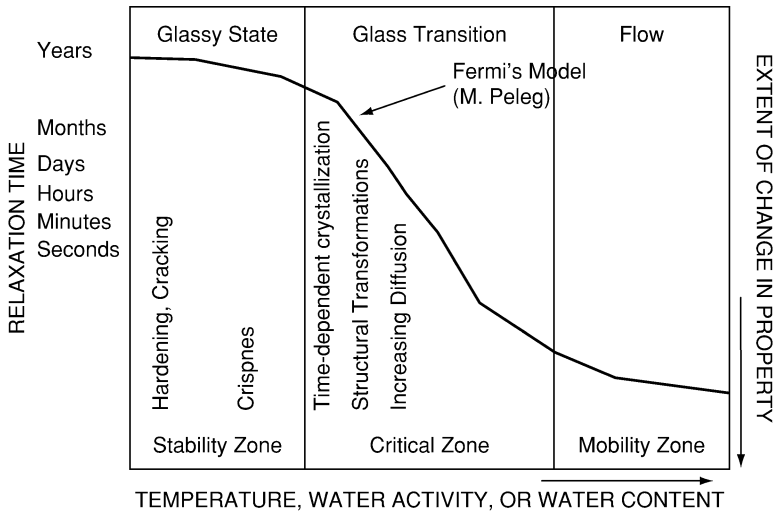

FIG. 36 Effects of temperature, water activity, or water content on relaxation times and relative rates of mechanical changes in amorphous materials [reproduced with permission from Roos (2003)]. M. Peleg reference is Peleg (1996).

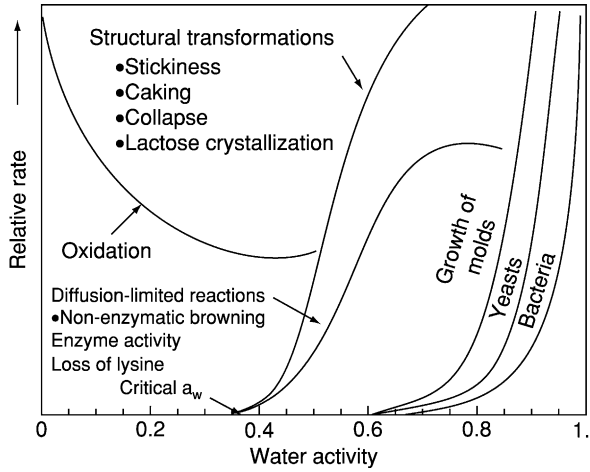

FIG. 37 Stability map for dairy powders containing amorphous lactose. The critical water activity (0.37 a_w) corresponds to the water activity of amorphous lactose with T_g of 24 °C (and a moisture content of 6.8 g water/100 g solids) [reproduced with permission from Roos (2003)].

illustrating the time dependence of crystallization as a function of water activity and moisture content in lactose (see Figure 23 in Roos, 1992) and in foods containing amorphous sugars and carbohydrates (see Figure 2.11 in Roos, 1998).

b. Selection of ingredients. Because, for a glass-forming solute–water blend, T_g is determined by the weight-average molecular weight ($\overline{M}w$) of that blend (Slade and Levine, 1988), T_g of a food matrix can be manipulated by the selection of ingredients incorporated into the blend. In general, low molecular weight components, such as simple sugars, have low T_g values, whereas high molecular weight components, such as starch and proteins, have high T_g values (Slade and Levine, 1988). For the interested reader, Nelson and Labuza (1993) give several examples relating state diagrams for processes and ingredients to the texture of various cereal foods.

c. Determination of product stability and shelf life. The location of T_g influences the stability of food systems. In very general terms, low-moisture food ingredients and systems are most stable when produced and held at temperatures below, rather than above, their T_g. Above T_g, food stability decreases as the temperature of a food increases above its T_g (defined in terms of $\Delta T = T - T_g$) (Slade and Levine, 1991). However, it has been found that use of T_g as a universal index temperature for food stability depends on the specific aspect of stability (e.g., chemical, biochemical, physical, and microbial growth and toxin production) under consideration (Roos, 1995). In other words, T_g is a better predicator of stability in some instances than in others.

The most well-established relationship between T_g and food stability involves the control and prediction of physical processes in amorphous food systems, such as stickiness, caking, collapse, loss of crispness, and crystallization of amorphous solids (Roos, 2003; Slade and Levine, 1991). The rapid changes in viscosity and modulus that occur above T_g govern many of the aforementioned changes in physical properties (Peleg, 1993). Despite the very successful use of T_g to predict the stability of physical properties in many amorphous food systems, exceptions are noted and discussed in detail by Le Meste *et al.* (2002). One example involves work on glassy breads (Le Meste *et al.*, 1996; Roudaut *et al.*, 1998, 1999a,b). Le Meste *et al.* (2002), summarizing results from those studies, reported that the water content at which a loss in sensory crispness occurred (~9% wb) was lower than the water content corresponding to T_g (~15% wb) at the experimental temperature (25 °C). Thus, this important textural change took place while the material was in a glassy state. The underlying microstructural events responsible for those results are not completely elucidated

yet. However, Roudaut *et al.* (1998) suggested that the loss of sensory crispness, sensory hardness, and other mechanical properties in the glassy solid matrix is related to a secondary physical transition, from brittle to ductile, which occurs at a temperature. T_β, below T_g. The possibility of this sub-T_g influence on texture was alluded to previously by Slade and Levine (1991) and is discussed in Slade and Levine (2003) and Roudaut *et al.* (2002).

As far as a relationship between T_g and chemical and biochemical (e.g., enzymatic) reactions rates, no direct relationship has been universally established. In general, reaction rates do increase as temperature increases; however, rates for a variety of reactions have been reported to be significant at temperatures below the T_g for various food matrices. Such reactions have included rates of Maillard browning (Bell *et al.*, 1998; Craig *et al.*, 2001; Schebor *et al.*, 1999), hydrolysis of sucrose by invertase (Chen *et al.*, 1999), peptide bond hydrolysis (Streefland *et al.*, 1998), aspartame degradation (Bell and Hageman, 1994), and hydrolytic deamidation of asparagines (Lai *et al.*, 1999a,b). Results from these and other studies strongly suggest that reaction rates seem to be affected by a number of additional and independent factors, such as pH, temperature, reactant and product concentration and solubility, oxidation–reduction potential, water content, water activity, phase separation, and local differences in water sorption and microstructure, and not merely by an average macroscopic T_g of a food matrix (Fennema, 1996; Lievonen and Roos, 2002a; Roos, 2003; Sherwin and Labuza, 2003). Lievonen and Roos (2002b) demonstrated the feasibility of determining reaction rates for food systems in sealed containers at several temperatures as a method for further investigating the relationship between glass transition and reaction kinetics.

Despite the current lack of clarity regarding the relationship between glass transition and chemical reaction kinetics, it is still quite feasible that chemical and biochemical reaction rates may be governed by mobility, i.e., the mobility that is most rate limiting to a particular reaction scheme (e.g., water mobility, reactant mobility, molecular-level matrix mobility, local or microregion mobility), but perhaps not simply by an average amorphous solid mobility as reflected by the T_g. Ludescher *et al.* (2001) recommend the use of luminescence spectroscopy to investigate how rates of specific chemical and physical processes important in amorphous solid foods are influenced by specific modes of molecular mobility, as well as by molecular structure.

The relationship between T_g and microbial stability is the least studied of all the stability areas. Based mainly on mold germination data, Slade and Levine (1991) postulated that glass transition parameters, specifically T_m/T_g ratio, T'_g and W'_g (related to C'_g defined previously in Figure 32), could be useful for predicting the microbial stability of concentrated and

intermediate-moisture foods. Kou *et al.* (1999), who studied stability in sucrose, starch, and sucrose/starch systems, reported conidia germination of *Aspergillus niger* in only those samples that had DSC midpoint T_g values below 20 °C (the experimental temperature) (see Figure 29), which included two instant dent starch samples (0.946 and 0.976 a_w), four sucrose samples (0.890 to 0.976 a_w), and four 1:1 sucrose/starch samples (0.890 to 0.976 a_w). They reported no conidia germination in samples that had T_g values above 20 °C because those samples were in a glassy state. However, according to a critical review by Chirife and Buera (1996), there seem to be a number of unanswered questions regarding the widespread tenability of the relationship between T_g and microbial stability of foods. As suggested by Le Meste *et al.* (2002), additional research involving different types of microorganisms and substrates, including measurement of microbial growth and metabolic activity, not just spore germination, is needed to further investigate this relationship.

d. Influences on product behavior during processing. T_g is an important food matrix property of value in many food processing operations, such as drying, extrusion cooking, puffing, and flaking (Bhandari and Howes, 2000; Le Meste *et al.*, 2002; Lillford, 2003; Roos, 1995). The selection of appropriate processing parameters to produce and maintain foods of optimum quality and stability (at reasonable costs) in these unit operations is strongly influenced by the glass transition behavior of a product during processing and storage. For example, to avoid quality problems, such as collapse during freeze-drying, two temperature limits are essential. First, a material should be frozen to below the onset temperature of ice melting (T'_m in Figure 32) or, more practically, to below T'_g to ensure sample solidity and avoid viscous flow of an amorphous, freeze-concentrated solute matrix. Second, the temperature of a material, throughout both primary (sublimation of ice under vacuum) and secondary (removal of unfrozen water from a product) drying processes, should be maintained below the T_g curve of the material to keep the material from existing in a rubber–liquid state, which would result in structural collapse and loss of porosity and very poor rehydration properties (Craig *et al.*, 1999; Khalloufi and Ratti, 2003; Roos, 1995; Slade and Levine, 1991; van den Berg *et al.* 1993). Detailed explanations regarding the influence of glass transition behavior on a variety of other processing operations can be found in Slade and Levine (1991), Levine and Slade (1993), Roos (1995), Strahm (1998), Bhandari and Howes (2000), Zweifel *et al.* (2000), Roos (2002), and Vautaz (2002).

The introduction of Slade and Levine's food polymer science approach has mobilized (no pun intended!) a large number of researchers to pursue the question of how the glass transition concept applies to the processing and

stability of specific food systems. Although much progress has been made, still more needs to be accomplished. As with any process of inquiry, there is a good deal of constructive debate that remains to be resolved [e.g., see Chirife and Buera (1994, 1995, 1996); Labuza *et al*. (2001); Le Meste *et al*. (2002); Peleg (1996 and 1997); Slade and Levine (1991)].

6. *Measurement of glass transition temperature in foods*

As discussed earlier, the usefulness of the food polymer science approach to the study of water dynamics in foods has been widely demonstrated by numerous researchers studying both model and real food systems. Along with the success of the approach, there still exist a number of areas of concern that need to be mentioned.

Despite years of investigation, there remains an active controversy as to exactly what T_g is and is not. There are a number of theories associated with the nature of T_g, such as free volume and statistical mechanical theories, but as of yet there is no universally agreed-upon explanation for the phenomenon (Craig *et al*., 1999; Hancock and Zografi, 1997). The good news is that focused and complementary experimental efforts, numerical simulations, and analytical theory are helping to fill in some of the missing pieces (Stillinger, 1995).

As pointed out previously, T_g is not a single or unique value, even for a well-defined sample; rather, it occurs over a temperature range and is dependent on the measurement method used and the system involved (recall Figure 33). In addition, it is quite possible that complex, multiphase food systems possess more than one T_g. The complexity inherent in many food systems sometimes makes it difficult to observe a T_g value at all (Labuza *et al*., 2001; Vittadini *et al*., 2002).

The food polymer science approach is being applied successfully in the food industry for understanding, improving, and developing food processes and products. However, to date, the glass transition generally remains more of a research and development tool than a routine quality assurance measure of food processability and stability.

7. *Relationship between glass transition temperature and* a_w

Because both T_g and water activity are functions of water content, the two parameters can be correlated to each other. This can be done in two main ways, as presented by Roos (1995). The first is to measure T_g of samples humidified to known water activity values (i.e., using saturated salt solutions) and then plot T_g values as a function of water activity (e.g., see Figure 6.2A in Roos, 1995). Over the entire a_w range, a sigmoid-shaped curve was

observed (Roos, 1995). Another approach for correlating existing isotherm and glass transition data was presented by Slade and Levine (1991). Sorption isotherm data at different temperatures are transformed to a series of iso-RVP contours (i.e., combinations of moisture content and temperature that yield the same values of observed RVP) that are then plotted on a state diagram (a water/glass dynamics map as they called it) for the same (or a similar) material. For example, Slade and Levine (1991) converted literature sorption data for apple pectin at four temperatures (25, 40, 60, and 80 °C) to a series of iso-RVP contours and plotted them as a function of weight percentage solids on a state diagram (T_g as a function of weight percent solids) for hemicellulose (see Figure 26 in Slade and Levine, 1991).

The second way is to add a sorption isotherm obtained at a temperature of interest (usually ambient temperature) to a state diagram. Such a modified state diagram, as suggested by Roos (1995, 2003), can be developed by modeling water plasticization data using the Gordon–Taylor equation and modeling sorption isotherm data using the Guggenheim–Anderson–De Boer (GAB) equation (both equations can be found in Roos, 1995). In this approach, the moisture content associated with the T_g equal to the temperature at which an isotherm was obtained is identified (referred to as critical mc) and is then used to locate a critical water activity value. This approach is illustrated, for instant dent starch, in Figure 38 using starch isotherm data (obtained at 20 °C) and starch DSC midpoint T_g data from Kou *et al.* (1999). The critical moisture content was 21.8% (wet basis), which corresponds to a critical water activity value of 0.92. It is important to note that the critical moisture content and water activity values obtained may vary slightly depending on the specific equations selected to model the water plasticization and sorption isotherm data. For example, using the same Gordon–Taylor determined critical moisture content value (22% wet basis) for the instant dent starch discussed in Figure 38, an a_w value of 0.936 was obtained using the Smith (1947) equation to fit the sorption isotherm data (Kou *et al.* 1999) compared to the 0.92 a_w value obtained using the GAB equation.

IV. EMERGING PICTURE OF FOOD SYSTEM MOBILITY: SUMMARY AND FUTURE DIRECTIONS

Throughout this review, the concept of mobility has been highlighted as a key parameter for understanding and predicting the processability and stability of food systems. Mobility is the common denominator of the three methods examined in this review—water activity, nuclear magnetic resonance, and glass transition. An emerging aspect of the picture for food

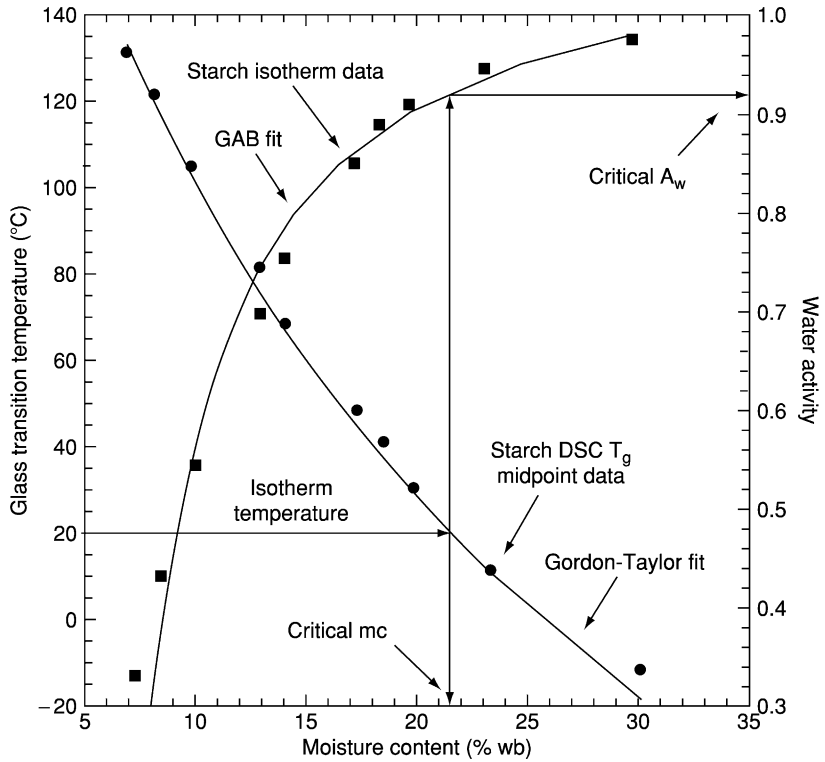

FIG. 38 Graph of a modified state diagram for instant dent starch, which includes both DSC T_g midpoint data plotted as a function of moisture content (% wb) and sorption isotherm data obtained at 20 °C. DSC T_g midpoint data were fit to the Gordon–Talyor equation, and sorption isotherm data were fit to the GAB equation. The moisture content associated with the T_g at 20 °C is called the critical mc and is equal to 21.8% (wb), and the corresponding critical water activity value is 0.92.

system mobility is that food systems do not possess one type of mobility, but many—depending on the species (i.e., water or a specific solid component), distance (molecular through macroscopic), and timescales (picoseconds through centuries) being probed. Thus, a single measure of mobility (or a single approach) is unlikely to provide us with the comprehensive and complete picture we seek so that we can solve the myriad of processing and stability problems that exist. In the past, researchers focused on water activity and water mobility as the "answers" to food stability. More recently, the focus has switched to solids mobility. However, what is being recognized is that a combined approach, which probes both water and solids mobility

(at various distance and time scales) and their individual and combined relationships to food stability, is most desirable.

However, even water and solids mobility are not completely sufficient, as there are still other factors that need to be taken into account and investigated, on a case-by-case basis, such as chemical properties, pH, oxidation–reduction potential, and temperature (Fennema, 1996). Development and application of complementary techniques are needed, such as those presented in this review, as well as others [e.g., optical luminescence (Ludescher *et al.*, 2001)], to continue to develop a full and complete picture of the time-dependent changes taking place in food systems during processing and storage. Much progress has been made in the study of the physicochemical properties of foods, recently termed the material food science field by Karel (1999), but as always there is still much more that needs investigating.

ACKNOWLEDGMENTS

I am grateful for the cohort of colleagues, students, and friends spread all over the globe who share my passion for investigating the complex nature of water and solids in edible things. Special appreciation is extended to Martin Chaplin, Professor of Applied Science and Head of the Food Research Centre, South Bank University, London, for the many e-mail discussions we had regarding the properties of water. A special thanks is also extended to Harry Levine, who spent a great deal of time and effort reviewing and editing a draft copy of this manuscript. I appreciate and could not do what I do without the love and support of my wonderful family, Art, Robbie, and Annie Schmidt, as well as my friends Mevanee and Phill Parmer. The artwork assistance of Carl Burton from the Visualization, Media, and Imaging Laboratory, Beckman Institute for Advanced Science and Technology, is also gratefully acknowledged.

GLOSSARY

Chemical shift Electrons of the atoms and molecules surrounding a nucleus interact with B_0 and induce an additional local field at the position of the nucleus being probed. The effect of this local magnetic field is to reduce the magnitude of the external magnetic field experienced by local nuclei. This results in a shift in the resonance frequency of nuclei. Chemical shifts are measured in parts per million (ppm).

Eutectic point (T_e) A single point on a temperature–concentration phase (or state) diagram for a binary solution (e.g., water and sugars or salts) where the solution can exist in equilibrium with both crystalline solute and crystalline solvent. Under equilibrium conditions, cooling at T_e results in simultaneous crystallization of solvent and solute in constant proportion and at constant temperature until maximum solidification has occurred (based on Fennema, 1996).

Hurdle technology Involves manipulating various growth-controlling parameters in a manner such that growth of microorganisms will not occur; each parameter serves as a "hurdle" to microbial growth (based on Fennema, 1996).

Hydrological cycle The cyclic transfer of water vapor from the Earth's surface via evapotranspiration into the atmosphere, from the atmosphere via precipitation back to earth, and through runoff into streams, rivers, and lakes, and ultimately into the oceans (U.S. Geological Survey, 2003).

Latent heat The quantity of heat that must be added or removed from a substance to change its phase without changing its temperature. The units of latent heat are commonly reported as cal/g.

Nuclear Overhauser effect Occurs as a result of cross-relaxation between dipolar-coupled spins resulting from spin–spin interactions through space.

Phase diagram Summarizes the pressure and temperature conditions at which each phase of a homogeneous material is most stable.

Sensible heat The quantity of heat that must be added or removed from a substance to change its temperature. The units of sensible heat are commonly reported as cal/g °C.

Spin–spin coupling (also called scalar or "J" coupling) Splitting of NMR resonance signals by neighboring magnetic nuclei. The coupling is a magnetic interaction that occurs through the electrons of chemical bonds connecting two spins.

REFERENCES

Ablett, S., Darke, A.H., Izzard, M.J., and Lillford, P.J. 1993. Studies of the glass transition in maltooligomers. *In* "The Glassy State in Foods" (J.M.V. Blanshard and P.J. Lillford, eds), pp. 189–206. Nottingham Univ. Press, Loughborough, Leicestershire.

Angell, C.A. 1983. Supercooled water. *Annu. Rev. Phys. Chem.* **34**, 593–630.

Angell, C.A. 2001. Water: What we know and what we don't. *In* "Water Science for Food, Health, Agriculture and Environment" ISOPOW 8 (Z. Berk, R.B. Leslie, P.J. Lillford, and S. Mizrahi, eds), pp. 1–30. Technomic Publishing, Lancaster, PA.

Arabosse, P., Rodier, E., Ferrasse, J.H., Chavez, S., and Lecomte, D. 2003. Comparison between static and dynamic methods for sorption isotherm measurements. *Drying Technol.* **21**, 479–497.

ASTM E 1142-97, ASTM Book of Standards 2002. "Standard Terminology Relating to Thermophysical Properties". ASTM International, Conshohocken, PA.

ASTM E 1356-98, ASTM Book of Standards 2002. "Standard Test Method for Assignment of the Glass Transition Temperature by Differential Scanning Calorimetry or Differential Thermal Analysis". ASTM International, Conshohocken, PA.

ASTM E 1545-00, ASTM Book of Standards 2002. "Standard Test Method for Assignment of the Glass Transition Temperature by Thermomechanical Analysis". ASTM International, Conshohocken, PA.

ASTM E 1640-99, ASTM Book of Standards 2002. "Standard Test Method for Assignment of the Glass Transition Temperature by Dynamic Mechanical Analysis". ASTM International, Conshohocken, PA.

ASTM E 1824-96, ASTM Book of Standards 2002. "Standard Test Method for Assignment of the Glass Transition Temperature Using Thermomechanical Analysis under Tension". ASTM International, Conshohocken, PA.

Audu, T.O.K., Loncin, M., and Weisser, H. 1978. Sorption isotherms of sugars. *Lebensm. Wiss. Technol.* **11**, 31–34.

Avogadro, A. 1811. Essay on a Manner of Determining the Relative Masses of the Elementary Molecules of Bodies, and the Proportions in Which They Enter into These Compounds. *J. Physi.* **73**, 58–76. [Alembic Club Reprint No. 4] Translated paper available online at http://webserver.lemoyne.edu/faculty/giunta/avogadro.html.

Bair, H.E. 1994. Glass transition measurements by DSC. *In* "Assignment of the Glass Transition" (R.J. Seyler, ed.), pp. 50–74. American Society for Testing and Materials, Philadelphia, PA.

Balcom, B.J., MacGregor, R.P., Beyea, S.D., Green, D.P., Armstrong, R.L., and Bremmer, T.W. 1996. Single point ramped imaging with T1 enhancement (SPRITE). *J. Magn. Reson.* **A123**, 131–134.

Ball, P. 2001. "Life's Matrix: A Biography of Water". University of California Press, Berkeley, CA.

Bell, L.N., Bell, H.M., and Glass, T.E. 2002. Water mobility in glassy and rubbery solids as determined by oxygen-17 nuclear magnetic resonance: Impact on chemical stability. *Lebensm. Wiss. Technol.* **35**, 108–113.

Bell, L.N. and Hageman, M.J. 1994. Differentiating between the effects of water activity and glass transition dependent mobility on a solid state chemical reaction: Aspartame degradation. *J. Agric. Food Chem.* **42**, 2398–2401.

Bell, L.N. and Labuza, T. P. 2000. "Moisture Sorption: Practical Aspects of Isotherm Measurement and Use". 2nd Ed. American Association of Cereal Chemists, St. Paul, MN.

Bell, L.N., Touma, D.E., White, K.I., and Chen, Y.H. 1998. Glycine loss and Maillard browning as related to the glass transition in a model food system. *J. Food Sci.* **63**, 625–628.

Belton, P.S. 1990. Can nuclear magnetic resonance give useful information about the state of water in foodstuffs? *Comments Agric. Food Chem.* **2**, 179–209.

Belton, P.S. 1994. Introduction: An overview of spectroscopic methods. *In* "Spectroscopic Techniques for Food Analysis" (R.H. Wilson, ed.), pp. 1–11. VCH Publishers, New York.

Belton, P.S. 1995. NMR in context. *In* "Annual Reports on NMR Spectroscopy" (G.A. Webb, P.S. Belton, and M.J. McCarthy, eds), Vol. 31, pp. 1–18. Academic Press, New York.

Belton, P.S., Colquhoun, I.J., and Hills, B.P. 1993. Applications of NMR to food science. *In* "Annual Reports on NMR Spectroscopy" (G.A. Webb, ed.), Vol. 26, pp. 1–45. Academic Press, New York.

Belton, P.S., Delgadillo, I., Gil, A.M., and Webb, G.A. (eds) 1995. "Magnetic Resonance in Food Science". Royal Society of Chemistry, Cambridge, UK.

Belton, P.S., Hills, B.P., and Webb, G.A. (eds) 1999. "Advances in Magnetic Resonance in Food Science". Royal Society of Chemistry, Cambridge, UK.

Belton, P.S. and Wang, Y. 2001. Fast field cycling NMR: Applications to foods. *In* "Magnetic Resonance in Food Science: A View to the Future" (G.A. Webb, P.S. Belton, A.M. Gil, and I. Delgadillo, eds), pp. 145–156. Royal Society of Chemistry, Cambridge, UK.

Berzelius, J.J. 1814. Essay on the Cause of Chemical Proportions, and on Some Circumstances Relating to Them: Together with a Short and Easy Method of Expressing Them. *Ann. Philos.* **3**, 51–293–106, 244–255, 353–364 [from Henry M. Leicester & Herbert S. Klickstein, eds, A Source Book in Chemistry, 1400–1900 (Cambridge, MA: Harvard, 1952)]. Translated paper available online at http://webserver.lemoyne.edu/ faculty/giunta/berzelius.html.

Bhandari, B.R. and Howes, T. 2000. Glass transition in processing and stability of food. *Food Aust.* **52**, 579–585.

Bidstrup, S.A. and Day, D.R. 1994. Assignment of the glass transition temperature using dielectric analysis: A review. *In* "Assignment of the Glass Transition" (R.J. Seyler, ed.), pp. 108–119. American Society for Testing and Materials, Philadelphia, PA.

Blanshard, J.M.V. and Lillford, P.J. (eds) 1993. "The Glassy State in Foods". Nottingham Univ. Press, Loughborough, Leicestershire.

Campbell, I.D. and Dwek, R.A. 1984. "Biological Spectroscopy". Benjamin/Cummings, Menlo Park, CA.

Champion, D., Le Meste, M., and Simatos, D. 2000. Towards an improved understanding of glass transition and relaxations in foods: Molecular mobility in the glass transition range. *Trends Food Sci. Technol.* **11**, 41–55.

Chaplin, M. 1999. A proposal for the structuring of water. *Biophys. Chem.* **83**, 211–221.

Chaplin, M. 2001. Water: Its importance to life. *Biochem. Mol. Educat.* **29**, 54–59.

Chaplin, M. 2004. Water structure and behavior. http://www.sbu.ac.uk/water/ January 8, 2004.

Charley, H. and Weaver, C. 1998. "Foods: A Scientific Approach". 3rd Ed. Merrill, Columbus, OH.

Chen, A., Wu, D., and Johnson, C.S.J. 1995. Determination of molecular weight distributions for polymers by diffusion-ordered NMR. *J. Am. Chem. Soc.* **117**, 7965–7970.

Chen, Y.H., Aull, J.L., and Bell, L.N. 1999. Invertase storage stability and sucrose hydrolysis in solids as affected by water activity and glass transition. *J. Agric. Food Chem.* **47**, 504–509.

Chirife, J. 1994. Specific solute effects with specific reference to *Staphylococcus aureus*. *J. Food Engin.* **22**, 409–419.

Chirife, J. and Buera, M.P. 1994. Water activity, glass transition and microbial stability in concentrated and semimoist food systems. *J. Food Sci.* **59**, 921–927.

Chirife, J. and Buera, M.P. 1995. A critical review of the effect of some nonequilibrium situations and glass transitions on water activity values of foods in the microbiological growth range. *J. Food Engin.* **25**, 531–552.

Chirife, J. and Buera, M.B. 1996. Water activity, water glass dynamics, and the control of microbiological growth in foods. *Crit. Rev. Food Sci. Nutr.* **36**, 465–513.

Choi, S.-G. and Kerr, W.L. 2003a. ^{1}H NMR studies of molecular mobility in wheat starch. *Food Res. Int.* **36**, 341–348.

Choi, S.-G. and Kerr, W.L. 2003b. Effect of chemical modification of wheat starch on molecular mobility as studied by pulsed H-1 NMR. *Lebensm. Wiss. Technol. Food Sci. Technol.* **36**, 105–112.

Christian, J.H.B. and Scott, W.J. 1953. Water relations of Salmonellae at 30 °C. *Aust. J. Biol. Sci.* **6**, 565–573.

Chudek, J.A. and Hunter, G. 2002. Stray field (STRAFI) and single point (SPI) magnetic resonance imaging. *In* "Annual Reports on NMR Spectroscopy" (G.A. Webb, ed.), Vol. 45, pp. 152–187. Academic Press, New York.

Claridge, T.D.W. 1999. "High-Resolution NMR Techniques in Organic Chemistry". Pergamon, New York.

Coleridge, S.T. 1798. The Rime of the Ancient Mariner.

Colquhoun, I.J. and Goodfellow, B.J. 1994. Nuclear magnetic resonance spectroscopy. *In* "Spectroscopic Techniques for Food Analysis" (R.H. Wilson, ed.), pp. 87–145. VCH Publishers, New York.

Conway, B.E. 1981. "Ionic Hydration in Chemistry and Biophysics". Elsevier, New York.

Cornillon, P. and Salim, L.C. 2000. Charaterization of water mobility and distribution in low- and intermediate-moisture food systems. *Magn. Reson. Imag.* **18**, 335–341.

Craig, D.Q.M., Royall, P.G., Kett, V.L., and Hopton, M.L. 1999. The relevance of the amorphous state to pharmaceutical dosage forms: Glassy drugs and freeze dried systems. *Int. J. Pharm.* **179**, 179–207.

Craig, I.D., Parker, R., Rigby, N.M., Cairns, P., and Ring, S.G. 2001. Maillard reaction kinetics in model preservation systems in the vicinity of the glass transition: Experiment and theory. *J. Agric. Food Chem.* **49**, 4706–4712.

De Meuter, P., Rahier, H., and Van Mele, B. 1999. The use of modulated temperature differential scanning calorimetry for the characterization of food systems. *Int. J. Pharm.* **192**, 77–84.

Duce, S.L. and Hall, L.D. 1995. Visualisation of the hydration of food by nuclear magnetic resonance imaging. *J. Food Engin.* **26**, 251–257.

Duarte, I.F., Godejohann, M., Braumann, U., Spraul, M., and Gil, A.M. 2003. Application of NMR spectroscopy and LC-NMR/MS to the identification of carbohydrates in beer. *J. Food Chem.* **51**, 4847–4852.

Eads, T.M. 1995. Wide-line and high-resolution 1H NMR of food materials. *In* "Annual Reports on NMR Spectroscopy" (G.A. Webb, P.S. Belton, and M.J. McCarthy, eds), Vol. 31, pp. 143–156. Academic Press, New York.

Eads, T.M. 1998. Magnetic resonance. *In* "Food Analysis" (S.S. Nielsen, ed.), 2nd Ed. pp. 455–481. Aspen, Gaithersburg, MD.

Eads, T.M. 1999. Principles for nuclear magnetic resonance analysis of intact food materials. *In* "Spectral Methods in Food Analysis" (M.M. Mossoba, ed.), pp. 1–88. Dekker, New York.

Eads, T.M. and Axelson, D.E. 1995. Nuclear cross relaxation spectroscopy and single point imaging measurements of solids and solidity in foods. *In* "Magnetic Resonance in Food Science" (P.S. Belton, I. Delgadillo, A.M. Gil, and G.A. Webb, eds), pp. 230–242. Royal Society of Chemistry, Cambridge, UK.

Eisenberg, D. and Crothers, D. 1979. "Physical Chemistry with Applications to the Life Sciences". Benjamin/Cummings, Menlo Park, CA.

Ernst, R.R., Bodenhausen, G., and Wokaun, A. 1987. "Principles of Nuclear Magnetic Resonance in One and Two Dimensions". Oxford Univ. Press, New York.

Errington, J.R. and Debenedetti, P.G. 2001. Relationship between structural order and the anomalies of liquid water. *Nature* **409**, 318–321.

Fennema, O. 1996. Water and ice. *In* "Food Chemistry" (O. Fennema, ed.). Dekker, New York.

Finney, J.L. 2001. The water molecule and its interactions: The interaction between theory, modeling and experiment. *J. Mol. Liquids* **90**, 303–312.

Finney, J.L., Bowron, D.T., Soper, A.K., Loerting, T., Mayer, E., and Hallbrucker, A. 2002. Structure of a new dense amorphous ice. *Phys. Rev. Lett.* **89**, 205503.

Franks, F. 1982. Water activity as a measure of biological viability and quality control. *Cereal Foods World* **27**, 403–407.

Franks, F. 1984. "Water". Royal Society of Chemistry, Burlington House, London.

Franks, F. 1991. Water activity: A credible measure of food safety and quality? *Trends Food Sci. Technol.* **2**, 68–72.

Franks, F. 2000. "Water: A Matrix of Life". Royal Society of Chemistry, Cambridge, UK.

Franks, F., Asquith, M.H., Hammond, C.C., Skaer, H.B., and Echlin, P. 1977. Polymeric cryoprotectants in the preservation of biological ultrastructure. *J. Microsc.* **110**, 223–238.

Gil, A.M., Belton, P.S., and Hills, B.P. 1996. Applications of NMR to food science. *In* "Annual Reports on NMR Spectroscopy" (G.A. Webb, ed.), Vol. 32, pp. 1–43. Academic Press, New York.

Glasel, J.A. 1972. Nuclear magnetic resonance studies on water and ice. *In* "Water: A Comprehensive Treatise" (F. Franks, ed.), Vol. 1, pp. 215–254. Plenum Press, New York.

Goff, H.D. 1998. Foods Under the Microscope—Ice cream structure. http://www.foodsci.uoguelph.ca/dairyedu/icmilos2.html 1998.

Goff, H.D. and Sahagian, M.E. 1996. Glass transitions in aqueous carbohydrate solutions and their relevance to frozen food stability. *Thermochim. Acta* **280**, 449–464.

Gonera, A. and Cornillion, P. 2002. Gelatinization of starch/gum/sugar systems studied by using DSC, NMR, and CSLM. *Starch/Starke* **54**, 508–516.

Grant, D.M. and Harris, R.K. 2002. "Encyclopedia of Nuclear Magnetic Resonance", Vol. 9. Wiley, New York.

Green, J.M. and Peterson, A. 1992. "The History of Chemistry: Woodrow Wilson Summer Institute". http://www.woodrow.org/teachers/chemistry/institutes/1992/Gay-Lussac.html January 12, 2004.

Greenspan, L. 1977. Humidity fixed points of binary saturated aqueous solutions. *J. Res. Natl. Bur. Stand. Sect. A.* **81**, 89–102.

Gribnau, M.C.M. 1992. Determination of solid/liquid ratios of fats and oils by low-resolution pulsed NMR. *Trends Food Sci. Technol.* **3**, 186–190.

Guillot, B. 2002. A reappraisal of what we have learnt during three decades of computer simulations on water. *J. Mol. Liquids* **101**, 219–260.

Halle, B. and Karlstrom, G. 1983a. Prototropic charge migration in water. 1. Rate constants in light and heavy water and in salt solutions from oxygen-17 spin relaxation. *J. Chem. Soc. Faraday Trans. II* **79**, 1031–1046.

Halle, B. and Karlstrom, G. 1983b. Prototropic charge migration in water. 2. Interpretation of nuclear magnetic resonance and conductivity data in terms of model mechanisms. *J. Chem. Soc. Faraday Trans. II* **79**, 1047–1073.

Hancock, B.C. and Zografi, G. 1997. Characteristics and significance of the amorphous state in pharmaceutical systems. *J. Pharm. Sci.* **86**, 1–12.

Harris, R.K. 2001. Recent advances in solid-state NMR. *In* "Magnetic Resonance in Food Science: A View to the Future" (G.A. Webb, P.S. Belton, A.M. Gil, and I. Delgadillo, eds), pp. 3–16. Royal Society of Chemistry, Cambridge, UK.

Hartel, R.W. 1998. Phase transitions in ice cream. *In* "Phase/State Transitions in Foods" (M.A. Rao and R.W. Hartel, eds), pp. 327–368. Dekker, New York.

Hemminga, M., Roozen, M.J.G.W., and Walstra, P. 1993. Molecular motions and the glassy state. *In* "The Glassy State in Foods" (J.M.V. Blanshard and P.J. Lillford, eds), pp. 157–171. Nottingham Univ. Press, Loughborough, Leicestershire.

Hills, B. 1995. Food processing: An MRI perspective. *Trends Food Sci. Technol.* **6**, 111–117.

Hills, B. 1998. "Magnetic Resonance Imaging in Food Science". Wiley, New York.

Hills, B.P. 1999. NMR studies of water mobility in foods. *In* "Water Management in the Design and Distribution of Quality Foods" ISOPOW 7 (Y.H. Roos, R.B. Leslie, and P.J. Lillford, eds). Technomic Publishing, Lancaster, PA.

Hills, B.P. and Pardoe, K. 1995. Proton and deuterium NMR studies of the glass transition in a 10% water-maltose solution. *J. Mol. Liquids* **62**, 229–237.

Hills, B.P. and Manning, C.E. 1998. NMR oxygen-17 studies of water dynamics in heterogeneous gel and particulate systems. *J. Mol. Liquids* **75**, 61–76.

Hills, B.P., Manning, C.E., and Godward, J. 1999. A multistate theory of water relations in biopolymer systems. *In* "Advances in Magnetic Resonance in Food Science" (P.S. Belton, B.P. Hill, and G.A. Webb, eds), pp. 45–62. Royal Society of Chemistry, Cambridge, UK.

Hills, B.P., Manning, C.E., and Ridge, Y. 1996a. New theory of water activity in heterogeneous systems. *J. Chem. Soc., Faraday Trans.* **92**, 979–983.

Hills, B.P., Ridge, C.E., and Brocklehurst, T. 1996b. NMR water relaxation, water activity, and bacterial survival in porous media. *J. Sci. Food Agric.* **71**, 185–194.

Hills, B.P., Tang, H., and Belton, P. 1998. NMR oxygen-17 studies of the state of water in a saturated sucrose solution. *J. Mol. Liquids* **75**, 45–59.

Hills, B.P., Wang, Y.L., and Tang, H.R. 2001. Molecular dynamics in concentrated sugar solutions and glasses: An NMR field cycling study. *Mol. Phy.* **99**, 1679–1687.

Hsu, C.L., Heldman, D.R., Taylor, T.A., and Kramer, H.L. 2003. Influence of cooling rate on glass transition temperature of sucrose solutions and rice starch gel. *J. Food Sci.* **68**, 1970–1975.

International Association for the Properties of Water and SteamGuidelines for the use of fundamental physical constants and basic constants of water. 2002. Revision of September 2001 guidelines, Gaitherburg, MA. Available online at http://www.iapws.org.

Javenkoski, J.S. 2001. "Instructional Visualization of Aqueous Phase Transitions in Food Systems". Ph.D. Thesis, University of Illinois at Urbana-Champaign, IL.

Jones, L. and Atkins, P. 2000. "Chemistry: Molecules, Matter, and Change". Freeman, New York.

Kalichevsky, M.T., Knorr, D., and Lillford, P.J. 1995. Potential food applications of high-pressure effects in ice-water transitions. *Trends Food Sci. Technol.* **6**, 253–259.

Kapsalis, J.G. 1987. Influence of hysteresis and temperature on moisture sorption isotherms. *In* "Water Activity: Theory and Application to Foods" (L.B. Rockland and L.R. Beuchat, eds), pp. 173–213. Dekker, New York.

Karel, M. 1999. Food research tasks at the beginning of the new millennium: A personal vision. *In* "Water Management in the Design and Distribution of Quality Foods" ISOPOW 7 (Y.H. Roos, R.B. Leslie, and P.J. Lillford, eds). Technomic Publishing, Lancaster, PA.

Karel, M., Buera, M.P., and Roos, Y. 1993. Effects of glass transitions on processing and storage. *In* "The Glassy State in Foods" (J.M.V. Blanshard and P.J. Lillford, eds), pp. 13–34. Nottingham Univ. Press, Loughborough, Leicestershire.

Kemp, W. 1986. "NMR in Chemistry: A Multinuclear Introduction". MacMillan Education, London.

Kern, C.W. and Karplus, M. 1972. The water molecule. *In* "Water: A Comprehensive Treatise" (F. Franks, ed.), Vol. 1, pp. 21–91. Plenum Press, New York.

Khalloufi, S. and Ratti, C. 2003. Quality deterioration of freeze-dried foods as explained by their glass transition temperature and internal structure. *J. Food Sci.* **68**, 892–903.

Kivelson, D. and Tarjus, G. 2001. H_2O below 277 K: A novel picture. *J. Phys. Chem.* **B 105**, 6620–6627.

Knorr, D., Schlueter, O., and Heinz, V. 1998. Impact of high hydrostatic pressure on phase transitions of foods. *Food Technol.* **52**, 43–45.

Kou, Y., Molitor, P.F., and Schmidt, S.J. 1999. Mobility and stability characterizing of model food systems using NMR, DSC, and conidia germination techniques. *J. Food Sci.* **64**, 950–959.

Labuza, T.P. 1984. "Moisture Sorption: Practical Aspects of Isotherm Measurement and Use". 1st Ed. American Association of Cereal Chemists, Inc., St. Paul, MN.

Labuza, T.P., Tannenbaum, S.R., and Karel, M. 1970. Water content and stability of low moisture and intermediate moisture foods. *Food Technol.* **24**, 543–550.

Labuza, T.P. *et al.* 2001. The Water in Foods Panel ISOPOW VIII September 16–21. Zichron Yaakov, Israel. What do we know and what do we agree on? http://courses.che.umn.edu/02fscn4342-1s/Readings_Folder/ISOPOW8_WaterInFood_ Panel.pdf January 12, 2004.

Lai, M.C., Hageman, M.J., Schowen, R.L., Borchardt, R.T., and Topp, E.M. 1999a. Chemical stability of peptides in polymers. 1. Effect of water on peptide deamidation in poly(vinyl alcohol) and poly(vinyl pyrrolidone) matrixes. *J. Pharm. Sci.* **88**, 1073–1080.

Lai, M.C., Hageman, M.J., Schowen, R.L., Borchardt, R.T., Laiard, B.B., and Topp, E.M. 1999b. Chemical stability of peptides in polymers. 2. Discriminating between solvent and plasticizing effects of water on peptide demidation in poly(vinyl pyrrolidone). *J. Pharm. Sci.* **88**, 1081–1089.

Laing, M. 1987. No rabbit ears on water. *J. Chem. Educ.* **64**, 124–128.

Lang, K.W., McCune, T.D., and Steinberg, M.P. 1981. A proximity equilibration cell for rapid determination of sorption isotherms. *J. Food Sci.* **46**, 936–938.

Leistner, L. 1987. Shelf-stable products and intermediate moisture foods based on meat. *In* "Water Activity: Theory and Applications to Foods" (L.B. Rockland and L.R. Beuchat, eds), pp. 295–327. Dekker, New York.

Le Meste, M., Champion, D., Roudaut, G., Blond, G., and Simatos, D. 2002. Glass transition and food technology: A critical appraisal. *J. Food Sci.* **67**, 2444–2458.

Le Meste, M., Roudaut, G., and Davidou, S. 1996. Thermomechanical properties of glassy cereal foods. *J. Thermal Anal.* **47**, 1361–1376.

Lee, S., Cornillion, P., and Kim, Y.R. 2002. Spatial investigation of the non-frozen water distribution in frozen foods using NMR SPRITE. *J. Food Sci.* **67**, 2251–2255.

Levine, H. 2002. Introduction: Progress in amorphous food and pharmaceutical systems. *In* "Amorphous Food and Pharmaceutical Systems" (H. Levine, ed.). Royal Society of Chemistry, Cambridge, UK.

Levine, H. and Slade, L. 1993. The glassy state in applications for the food industry with emphasis on cookie and cracker production. *In* "The Glassy State in Foods" (J.M.V. Blanshard and P.J. Lillford, eds), pp. 333–373. Nottingham Univ. Press, Loughborough, Leicestershire.

Lewen, K.S., Paeschke, T., Reid, J., Molitor, P., and Schmidt, S.J. 2003. Analysis of the retrogradation of low starch concentration gels using differential scanning calorimetry, rheology, and nuclear magnetic resonance spectroscopy. *J. Agric. Food Chem.* **51**, 2348–2358.

Lewicki, P.P. and Pomaranska-Lazuka, W. 2003. Errors in static desiccator method of water sorption isotherms estimation. *Int. J. Food Prop.* **6**, 557–563.

Lewis, G.N. and Randall, M. 1923. "Thermodynamics and the Free Energy of Chemical Substances". McGraw-Hill, New York.

Li, S., Dickerson, L.C., and Chinachoti, P. 1998. Mobility of "unfreezable" and "freezable" water in waxy corn starch by ^{2}H and ^{1}H and NMR. *J. Agric. Food Chem.* **46**, 62–71.

Lide, D.R. 2002–2003. "CRC Handbook of Chemistry and Physics". 83rd Ed. CRC Press, Boca Raton, FL.

Lievonen, S.M. and Roos, Y.H. 2002a. Nonenzymatic browning in amorphous food models: Effect of glass transition and water. *J. Food Sci.* **67**, 2100–2106.

Lievonen, S.M. and Roos, Y.H. 2002b. Water sorption of food models for studies of glass transition and reaction kinetics. *J. Food Sci.* **67**, 1758–1766.

Lillford, P. 2003. Status and needs in drying technology for the food and pharmaceutical industry. *Food Sci. Technol. Int.* **9**, 145–149.

Lindsay, R.C. 1996. Flavors. *In* "Food Chemistry" (O.R. Fennema, ed.), 3rd Ed. pp. 723–765. Dekker, New York.

Locker, T. 1997. "Water Dance". Harcourt, Orlando, FL.

Luck, W.A.P. 1981. Structures of water in aqueous systems. *In* "Water Activity: Influences on Food Quality" (L.B. Rockland and G.F. Stewart, eds), pp. 407–434. Academic Press, New York.

Ludescher, R.D., Shah, N.K., McCaul, C.P., and Simon, K.V. 2001. Beyond Tg: Optical luminescence measurements of molecular mobility in amorphous solid foods. *Food Hydrocolloids* **15**, 331–339.

Ludwig, R. 2001. Water: From cluster to the bulk. *Angewandte Chem. Int. Ed.* **40**, 1808–1827.

MacInnes, W.M. 1993. Dynamic mechanical thermal analysis of sucrose solutions. *In* "The Glassy State in Foods" (J.M.V. Blanshard and P.J. Lillford, eds), pp. 223–248. Nottingham Univ. Press, Loughborough, Leicestershire.

MacKenzie, A.P. 1977. Non-equilibrium freezing behavior of aqueous systems. *Phil. Trans. R. Soc. Lond B.* **278**, 167–189.

Makower, B. and Dye, W.B. 1956. Equilibrium moisture content and crystallization of amorphous sucrose and glucose. *J. Agric. Food Chem.* **4**, 72–77.

Mariette, F., Topgaard, D., Jonsson, B., and Soderman, O. 2002. 1H NMR diffusometry study of water in casein dispersions and gels. *J. Agric. Food Chem.* **50**, 4295–4302.

Martin, R.B. 1988. Localized and spectroscopic orbitals: Squirrel ears on water. *J. Chem. Educ.* **65**, 668–670.

Mason, B.J. 1957. "The Physics of Clouds". Clarendon, Oxford.

Mathlouthi, M. and Roge, B. 2003. Water vapour sorption isotherms and the caking of food powders. *Food Chem.* **82**, 61–71.

Matveev, Y.I. and Ablett, S. 2002. Calculation of the Cg′ and Tg′ intersection point in the state diagram of frozen solutions. *Food Hydrocolloids* **16**, 419–422.

McCarthy, K.L., Gonzalez, J.J., and McCarthy, M.J. 2002. Changes in moisture distribution in lasagna pasta post cooking. *J. Food Sci.* **67**, 1785–1789.

McCarthy, M.J. 1994. "Magnetic Resonance Imaging in Foods". Chapman and Hall, New York.

Metais, A. and Mariette, F. 2003. Determination of water self-diffusion coefficient in complex food products by low field h-1 PFG-NMR: Comparison between the standard spin-echo sequence and the T-1-weighted spin-echo sequence. *J. Magn. Reson.* **165**, 265–275.

Mishima, O. and Stanley, H.E. 1998. The relationship between liquid, supercooled and glassy water. *Nature* **396**, 329–335.

Modig, K., Pfrommer, B.G., and Halle, B. 2003. Temperature-dependent hydrogen-bond geometry in liquid water. *Phys. Rev. Lett.* **90**, 075502.

Morris, G.A. 2002a. Special Issue: NMR and diffusion. *Magn. Reson. Chem.* **40**, S1–S152.

Morris, G.A. 2002b. Diffusion-ordered spectroscopy. *In* "Encyclopedia of NMR" (M. Grant and R.K. Harris, eds), Vol. 9D, pp. 35–44. Wiley, New York.

Morris, K.F. and Johnson, C.S., Jr. 1993. Resolution of discrete and continuous molecular size distribution by means of diffusion-ordered 2D NMR spectroscopy. *J. Am. Chem. Soc.* **115**, 4291–4299.

Nelson, K.A. and Labuza, T.P. 1993. Glass transition theory and the texture of cereal foods. *In* "The Glassy State in Foods" (J.M.V. Blanshard and P.J. Lillford, eds), pp. 513–517. Nottingham Univ. Press, Loughborough, Leicestershire.

Netz, P.A., Starr, F., Barbosa, M.C., and Stanley, H.E. 2002. Translational and rotational diffusion in stretched water. *J. Mol. Liquids* **101**, 159–168.

Noack, F., Becker, St., and Struppe, J. 1997. Applications of field-cycling NMR. *In* "Annual Reports on NMR Spectroscopy" (G.A. Webb, ed.), Vol. 33, pp. 1–35. Academic Press, New York.

Norrish, R.S. 1966. An equation for the activity coefficients and equilibrium relative humidities of water in confectionery syrups. *J. Food Technol.* **1**, 25–39.

O'Brien, J. 1992. Application of nuclear magnetic resonance techniques in food research. *Trends Food Sci. Technol.* **3**, 177–249.

O'Grady, P. 2001. The Internet Encyclopedia of Philosophy, Thales of Miletus. http://www.utm.edu/research/iep/t/thales.html January 12, 2004.

Okos, M.R., Narsimhan, G., and Singh, R.K. 1992. "Food dehydration". *In* "Handbook of Food Engineering" (R. Heldman and D.B. Lund, eds), pp. 437–562. Dekker, New York.

Olson, B.F. 1999. "Analysis of the Diffusion Coefficients in Gelatinizated Starch-Water Systems over Time Using Diffusion-Ordered Spectroscopy". Masters Thesis, University of Illinois, Urbana-Champaign, IL.

Paeschke, T.M. 2002. "The Effect of Starch Microstructure on the Glass Transition, Gelatinization, and the Elevation of the Gelatinization Temperature by Saccharides". Ph.D. Thesis, University of Illinois at Urbana-Champaign.

Parker, R. and Ring, S.G. 2001. Aspects of the physical chemistry of starch. *J. Cereal Sci.* **34**, 1–17.

Peleg, M. 1993. Mapping the stiffness-temperature-moisture relationship of solid biomaterials at and around their glass transition. *Rheol. Acta* **32**, 575–580.

Peleg, M. 1996. On modeling changes in food and biosolids at and around their glass transition temperature range. *Crit. Rev. Food Sci. Nutr.* **36**, 49–67.

Peleg, M.A. 1997. Dissenting view on glass transition summary. *Food Technol.* **51**, 30–31.
Pelta, M.D., Morris, G.A., Stchedroff, M.J., and Hammond, S.J. 2002. A one-shot sequence for high-resolution diffusion-ordered spectroscopy. *Magn. Reson. Chem.* **40**, S147–S152.
Poole, P.H., Sciortino, F., Essmann, U., and Stanley, H.E. 1992. Phase behavior of metastable water. *Nature* **360**, 324–328.
Price, W.S. 1996. Gradient NMR. *In* "Annual Reports on NMR Spectroscopy" (G.A. Webb, ed.), Vol. 32, pp. 52–142. Academic Press, New York.
Price, W.S. 1997. Pulsed-field gradient nuclear magnetic resonance as a tool for studying translational diffusion. P 1. Basic theory. *Concepts Magn. Reson.* **9**, 299–336.
Price, W.S. 1998a. Pulsed-field gradient nuclear magnetic resonance as a tool for studying translational diffusion. II. Experimental aspects. Basic theory. *Concepts in Magn. Reson.* **10**, 197–237.
Price, W.S. 1998b. NMR imaging. *In* "Annual Reports on NMR Spectroscopy" (G.A. Webb, ed.), Vol. 34, pp. 140–216. Academic Press, New York.
Rahman, S. 1995. "Food Properties Handbook". CRC Press, Boca Raton, FL.
Richardson, S.J. 1989. Contribution of proton exchange to the oxygen-17 nuclear magnetic resonance transverse relaxation rate in water and starch-water systems. *Cereal Chem.* **66**, 244–246.
Richardson, M.J. and Saville, N.G. 1975. Derivation of accurate glass transition temperatures by differential scanning calorimetry. *Polymer* **16**, 753–757.
Richardson, S.J., Baianu, I.C., and Steinberg, M.P. 1987. Mobility of water in corn starch powders by nuclear resonance. *Starch* **39**(6), 198.
Riga, A.T. and Judovits, L. 2001. "Material Characterization by Dynamic and Modulated Thermal Analytical Techniques". American Society for Testing Materials, West Conshohocken, PA.
Rockland, L.B. 1987. Introduction. *In* "Water Activity: Theory and Application to Foods" (L.B. Rockland and L.B. Beuchat, eds), p. vii. Dekker, New York.
Roos, Y. and Karel, M. 1991. Applying state diagrams to food processing and development. *Food Technol.* **45**, 66–71 and 107.
Roos, Y.H. 1992. Phase transitions and transformations in food systems. *In* "Handbook of Food Engineering (D.R. Heldman and D.B. Lund, eds), pp. 145–197. Dekker, New York.
Roos, Y.H. 1995. "Phase Transitions in Foods". Academic Press, New York.
Roos, Y.H. 1998. Role of water in phase-transition phenomena in foods. *In* "Phase/State Transitions in Foods" (M.A. Rao and R.W. Hartel, eds), pp. 57–93. Dekker, New York.
Roos, Y.H. 2002. Importance of glass transition and water activity to spray drying and stability of dairy powders. *Lait* **82**, 475–484.
Roos, Y.H. 2003. Thermal analysis, state transitions and food quality. *J. Thermal Anal. Calorimetry* **71**, 197–203.
Roos, Y.H., Karel, M., and Kokini, J.L. 1996. Glass transitions in low moisture and frozen foods: Effects on shelf life and quality. *Food Technol.* **50**, 95–108.
Ross, K.D. 1975. Estimation of water activity in intermediate moisture foods. *Food Technol.* **29**, 26, 28, 30, 32, and 34.
Roudaut, G., Dacremont, C., and Le Meste, M. 1998. Influence of water on the crispness of cereal foods: Acoustic, mechanical, and sensory studies. *J. Texture Stud.* **29**, 199–213.
Roudaut, G., Dacremont, C., Valles Pamies, B., Colas, B., and Le Meste, M. 2002. Crispness: A critical review on sensory and material science approaches. *Trends Food Sci. Technol.* **13**, 217–227.
Roudaut, G., Maglione, M., van Dusschoten, D., and Le Meste, M. 1999a. Molecular mobility in glassy bread: A multispectroscopy approach. *Cereal Chem.* **76**, 70–77.
Roudaut, G., Maglione, M., and Le Meste, M. 1999b. Relaxations below glass transition temperature in bread and its components. *Cereal Chem.* **76**, 78–81.
Ruan, R.R. and Chen, P.L. 1998. "Water in Foods and Biological Materials: A Nuclear Magnetic Resonance Approach". Technomic Publishing, Lancaster, PA.

Ruan, R.R., Long, Z., Song, A., and Chen, P.L. 1998. Determination of the glass transition temperature of food polymers using low field NMR. *Lebensm. Wiss. Technol.* **31**, 516–521.

Ruan, R., Long, Z., Chen, P., Huang, V., Almaer, S., and Taub, I. 1999. Pulsed NMR study of the glass transition in maltodextrin. *J. Food Sci.* **64**, 6–9.

Ruscic, B., Wagner, A.F., Harding, L.B., Asher, R.L., Feller, D., Dixon, D.A., Peterson, K.A., Song, Y., Qian, Q.M., Ng, C.Y., Liu, J.B., and Chen, W.W. 2002. On the enthalpy of formation of hydroxyl radical and gas-phase bond dissociation energies of water and hydroxyl. *J. Phys. Chem. A.* **106**, 2727–2747.

Sastry, S., Debenedetti, P., Sciortino, F., and Stanley, H.E. 1996. Singularity-free interpretation of the thermodynamics of supercooled water. *Phys. Rev.* **E53**, 6144–6154.

Savage, H. 1986. Water structure in crystalline solids: Ices to proteins. *In* "Water Science Reviews 2: Crystalline Hydrates" (F. Franks, ed.), pp. 67–148. Cambridge Univ. Press, Cambridge, UK.

Schebor, C., Buera, M.P., Karel, M., and Chirife, J. 1999. Color formation due to nonenzymatic browning in amorphous, glassy, anhydrous, model systems. *Food Chem.* **65**, 427–432.

Schmidt, S.J. 1991. Determination of moisture content by pulsed nuclear magnetic resonance spectroscopy. *In* "Water Relationships in Foods" (H. Levine and L. Slade, eds), pp. 599–613. Plenum Press, New York.

Schmidt, S.J. 1999. Probing the physical and sensory properties of food systems using NMR spectroscopy. *In* "Advances in Magnetic Resonance in Food Science" (P.S. Belton, B.P. Hills, and G.A. Webb, eds), pp. 79–94. Royal Society of Chemistry, Cambridge, UK.

Schmidt, S.J. and Lammert, A.M. 1996. Physical aging of maltose glasses. *J. Food Sci.* **61**, 870–875.

Schmidt, S.J., Sun, X., and Litchfield, J.B. 1996. Applications of magnetic resonance imaging in food science. *Crit. Rev. Food Sci. Nutr.* **36**, 357–385.

Scott, W.J. 1953. Water relations of *Staphylococcus aureus* at 30 °C. *Aust. J. Biol. Sci.* **6**, 549–564.

Scott, W.J. 1957. Water relations of food spoilage microorganisms. *Adv. Food Res.* **7**, 83–127.

Seyler, R.J. (ed.) 1994a. "Assignment of the Glass Transition", STP 1249. American Society for Testing and Materials, Philadelphia, PA.

Seyler, R.J. 1994b. Opening discussion. *In* "Assignment of the Glass Transition", STP 1249 (R.J. Seyler, ed.), pp. 13–16. American Society for Testing and Materials, Philadelphia, PA.

Seyler, R.J. 1994c. Closing discussion: Highlights and the challenges that remain. *In* "Assignment of the Glass Transition", STP 1249 (R.J. Seyler, ed.), pp. 302–304. American Society for Testing and Materials, Philadelphia, PA.

Shaw, R.W., Brill, T.B., Clifford, A.A., Eckert, C.A., and Franck, E.U. 1991. Supercritical water: A medium for Chemistry. *C&EN* **23**, 26–39.

Sherwin, C.P. and Labuza, T.P. 2003. Role of moisture in maillard browning reaction rate in intermediate moisture foods: Comparing solvent phase and matrix properties. *J. Food Sci.* **68**, 588–594.

Sherwin, C.P., Labuza, T.P., McCormick, A., and Chen, B. 2002. Cross-polarization/magic angle spinning NMR to study glucose mobility in a model intermediate-moisture foods system. *J. Agric. Food Chem.* **50**, 7677–7683.

Shi, X.D., Brenner, M.P., and Nagel, S.R. 1994. A cascade of structure in a drop falling from a faucet. *Science* **265**, 219–222.

Slade, L. and Levine, H. 1985. Intermediate moisture systems; concentrated and supersaturated solutions; pastes and dispersions; water as plasticizer; the mystique of "bound" water; thermodynamics versus kinetics (Number 24). Presented at Faraday Division, Royal Society of Chemistry Discussion Conference – Water Activity: A Credible Measure of Technological Performance and Physiological Viability? Cambridge, July 1–3.

Slade, L. and Levine, H. 1988. Non-equilibrium behavior of small carbohydrate-water systems. *Pure App. Chem.* **60**, 1841–1864.

Slade, L. and Levine, H. 1991. Beyond water activity: Recent advances based on an alternative approach to the assessment of food quality and safety. *Crit. Rev. Food Sci. Nutr.* **30**, 115–360.

Slade, L. and Levine, H. 1995. Glass transitions and water-food structure interactions. *Adv. Food Nutr. Res.* **38**, 103–269.

Slade, L. and Levine, H. 1998. Selected aspects of glass transition phenomena in baked goods. *In* "Phase/State Transitions in Foods" (M.A. Rao and R.W. Hartel, eds), pp. 87–93. Dekker, New York.

Slade, L. and Levine, H. 2002. Progress in food processing and storage, based on amorphous product technology. *In* "Amorphous Food and Pharmaceutical Systems" (H. Levine, ed.), pp. 139–144. Royal Society of Chemistry, Cambridge, UK.

Slade, L. and Levine, H. 2003. Food polymer science approach to studies on freshness and shelf life. *In* "Freshness and Shelf Life of Foods" (K.R. Cadwallader and H. Weenen, eds), pp. 214–222. ACS Symposium Series 836, American Chemical Society, Washington, DC.

Smith, S.E. 1947. The sorption of water by high polymers. *J. Amer. Chem. Soc.* **69**, 646–651.

Sobolev, A.P., Segre, A., and Lamanna, R. 2003. Proton high-field NMR study of tomato juice. *Magn. Reson. Chem.* **41**, 237–245.

Sorland, G.H. and Aksnes, D. 2002. Artifacts and pitfalls in diffusion measurements by NMR. *Magn. Reson. Chem.* **40**, S139–S146.

Speedy, R.J. 1982. Stability-limit conjecture: An interpretation of the properties of water. *J. Phys. Chem.* **86**, 982–991.

Sperling, L.H. 1986. "Introduction to Physical Polymer Science". Wiley, New York.

Spraul, M.S., Braumann, U., Godejohann, M., and Hofmann, M. 2001. Hyphenated methods in NMR. *In* "Magnetic Resonance in Food Science: A View to the Future" (G.A. Webb, P.S. Belton, A.M. Gil, and I. Delgadillo, eds), pp. 54–66. Royal Society of Chemistry, Cambridge, UK.

Stanley, H.E., Budyrev, S.V., Mishima, O., Sadr-Lahijany, M.R., Scala, A., and Starr, F.W. 2000. Unsolved mysteries of water in its liquid and glassy phases. *J. Phys. Condens. Matter* **12**, A403–A412.

Stillinger, F.H. 1980. Water revisited. *Science* **209**, 451–457.

Stillinger, F.H. 1995. A topographic view of supercooled liquids and glass formation. *Science* **267**, 1935–1939.

Strahm, B. 1998. Fundamentals of polymer science as an applied extrusion tool. *Cereal Foods World* **43**, 621–625.

Streefland, L., Auffret, A.D., and Franks, F. 1998. Bond cleavage reactions in solid carbohydrate solutions. *Pharm Res.* **15**, 843–849.

Stryer, L. 1995. "Biochemistry". Freeman, New York.

Sun, X. and Schmidt, S.J. 1995. Probing water relations in foods using magnetic resonance techniques. *In* "Annual Reports on NMR Spectroscopy" (G.A. Webb, P.S. Belton, and M.J. McCarthy, eds), Vol. 31, pp. 239–273. Academic Press, New York.

Suresh, S.J. and Naik, V.M. 2000. Hydrogen bond thermodynamic properties of water from dielectric constant data. *J. Chem. Phys.* **113**, 9727–9732.

Tang, H.R., Godward, J., and Hills, B. 2000. The distribution of water in native starch granules: A multinuclear NMR study. *Carbohydr. Polym.* **43**, 375–387.

Tang, H. and Hills, B. 2001. Starch granules: A multinuclear magnetic resonance study. *In* "Magnetic Resonance in Food Science: A View to the Future" (G.A. Webb, P.S. Belton, A.M. Gil, and I. Delgadillo, eds). Royal Society of Chemistry, Cambridge, UK.

Tasker, R.F., Bucat, R.B., Sleet, R.J., and Chia, W. 1996a. Research into practice: Improving students' imagery in chemistry. http://vischem.cadre.com.au/assets/pdf/Water_Video_Evaln.pdf 1996a.

Tasker, R.F., Chia, W., Bucat, R.B., and Sleet, R.J. 1996b. The VisChem Project: Visualising chemistry with media. *Chem. Aust.* **63**, 395–397.

Teoh, H.M., Schmidt, S.J., Day, G.A., and Faller, J.F. 2001. Investigation of cornmeal components using dynamic vapor sorption and differential scanning calorimetry. *J. Food Sci.* **66**, 434–440.

Tromp, R.H., Parker, R., and Ring, S.G. 1997. Water diffusion in glasses of carbohydrates. *Carbohydr. Res.* **303**, 199–205.

U.S. Geological Survey 2003. Water science glossary of terms. http://ga.water.usgs.gov/edu/dictionary.html#H May 28, 2004.

van den Berg, C. 1981. "Vapour Sorption Equilibria and Other Water-Starch Interactions: A Physicochemical Approach". Ph.D. Thesis, Agricultural University Wageningen, The Netherlands.

van den Berg, C. 1986. Water activity. *In* "Concentration and Drying of Foods" (D. MacCarthy, ed.), pp. 11–36. Elsevier Applied Science, New York.

van den Berg, C. and Bruin, S. 1981. Water activity and its estimation in food systems: Theoretical aspects. *In* "Water Activity: Influences on Food Quality" (L.B. Rockland and G.F. Stewart, eds). Academic Press, New York.

van den Berg, C., Franks, F., and Echlin, P. 1993. The ultrastructure and stability of amorphous sugars. *In* "The Glassy State in Foods" (J.M.V. Blanshard and P.J. Lillford, eds), pp. 249–267. Nottingham Univ. Press, Loughborough, Leicestershire.

van den Dries, I.J., Besseling, N.A.M., van Dusschoten, D., Hemminga, M.A., and van der Linden, E. 2000a. Relation between a transition in molecular mobility and collapse phenomena in glucose-water systems. *J. Phys. Chem. B.* **104**, 9260–9266.

van den Dries, I.J., van Dusschoten, D., and Hemminga, M.A. 1998. Mobility in maltose-water glasses studied with 1H NMR. *J. Phys. Chem. B.* **102**, 10483–10489.

van den Dries, I.J., van Dusschoten, D., Hemminga, M.A., and van der Linden, E. 2000b. Effects of water content and molecular weight on spin probe and water mobility in malto-oligomer glasses. *J. Phys. Chem. B.* **104**, 10126–10132.

van Duynhoven, J.P.M., Goudappel, G.J.W., van Dalen, G., van Bruggen, P.C., Blonk, J.C.G., and Eijkelenboom, A.P.A.M. 2002. Scope of droplet size measurements in food emulsions by pulsed field gradient NMR at low field. *Magn. Reson. Chem.* **40**, S51–S59.

Vautaz, G. 2002. The phase diagram of milk: A new tool for optimizing the drying process. *Lait* **82**, 485–500.

Vittadini, E., Dickinson, L.C., and Chinachoti, P. 2002. NMR water mobility in xanthan and locust bean gum mixtures: Possible explanation of microbial response. *Carbohydr. Polym.* **49**, 261–269.

Wachner, A.M. and Jeffrey, K.R. 1999. A two-dimensional deuterium nuclear magnetic resonance study of molecular reorientation in sugar/water glasses. *J. Chem. Phys.* **111**, 10611–10616.

Wagner, W. and Pruss, A. 1993. International equations for the saturation properties of ordinary water substance: Revised according to the international temperature scale of 1990. *J. Phys. Chem. Ref. Data* **22**, 783–787.

Wagner, W., Saul, A., and Pruss, A. 1994. International equations for the pressure along the melting and along the sublimation curve of ordinary water substance. *J. Phys. Chem. Ref. Data* **23**, 515–527.

Wallqvist, A. and Mountain, R.D. 1999. Molecular models of water: Derivation and description. *Rev. Comput. Chem.* **13**, 183–247.

Walstra, P. 2003. "Physical Chemistry of Foods". Dekker, New York.

Weast, R.C. 1975/1976. "Handbook of Chemistry and Physics". CRC Press, Boca Raton, FL.

Webb, G.A., Belton, P.S., Gil, A.M., and Delgadillo, I. 2001. "Magnetic Resonance in Food Science: A View to the Future". Royal Society of Chemistry, Cambridge, UK.

Webb, G.A., Belton, P.S., and McCarthy, M.J. 1995. "Annual Reports on NMR Spectroscopy". Academic Press, New York.

White, G.W. and Cakebread, S.H. 1966. The glassy state in certain sugar-containing food products. *J. Food Technol.* **1**, 73–82.

Wick, W. 1997. "A Drop of Water". Scholastic Press, New York.

Wiederhold, P.R. 1997. "Water Vapor Measurement: Methods and Instrumentation". Dekker, New York.

Wiggins, P.M. 1995. High and low density water in gels. *Progr. Polymer Sci.* **20**, 1121–1163.

Witcombe, C. and Hwang, S. 2004. H_2O – The Mystery, Art, and Science of Water. http://witcombe.sbc.edu/water/index.html 2004.

Wolf, W., Spiess, W.E.L., and Jung, G. 1985. Standardization of isotherm measurements (COST-PROJECT 90 and 90 BIS). *In* "Properties of Water in Foods" (D. Simatos and J.L. Multon, eds), pp. 661–679. Martinus Nijhoff, Dordrecht, The Netherlands.

Wunderlich, B. 1990. "Thermal Analysis". Academic Press, New York.

Wunderlich, B. 1994. The nature of the glass transition and its determination by thermal analysis. *In* "Assignment of the Glass Transition" (R.J. Seyler, ed.), pp. 17–31. American Society for Testing and Materials, Philadelphia, PA.

Wungtanagorn, R. and Schmidt, S.J. 2001. Thermodynamic properties and kinetics of the physical aging of amorphous glucose, fructose, and their mixture. *J. Therm. Anal. Calorim.* **65**, 9–35.

Ziegler, G.R., MacMillian, B., and Balcom, B.J. 2003. Moisture migration in starch molding operations as observed by magnetic resonance imaging. *Food Res. Int.* **36**, 331–340.

Zimmerman, J.R. and Brittin, W.E. 1957. Nuclear magnetic resonance studies in multiple phase systems: Lifetime of a water molecule in an absorbing phase on silica gel. *J. Phys. Chem.* **61**, 1328–1333.

Zweifel, C., Conde-Petit, B., and Escher, F. 2000. Thermal modifications of starch during high-temperature drying of pasta. *Cereal Chem.* **77**, 645–651.